P. Starič, E. Margan:

# Wideband Amplifiers

## Part 4:

# Cascading Amplifier Stages, Selection of Poles

*For every circuit design there is an equivalent and opposite redesign!*
A generalization of Newton's Law by
Derek F. Bowers, Analog Devices

## To Calculate Or Not To Calculate — That Is Not A Question

In the fourth part of this book we discuss some basic system integration procedures and derive, based on two different optimization criteria, the two system families of poles, which we have already used extensively in previous parts: the Butterworth system family, i.e., the systems with a maximally flat amplitude response, and the Bessel system family, i.e., the systems with a maximally flat envelope delay.

Once we derive the relations from which the system poles are calculated, we shall present the resulting poles in table form, in the same way as is traditionally done in the literature (but, more often than not, without the corresponding derivation procedures).

Some readers might ask why on earth in the computer era do we bother to write tables full of numbers, which very probably no one will ever refer to? The answer is that many amplifier designers are ‘analog by vocation’, they use the computer only when they must and they like to do lots of paperwork before they finally sit by the breadboard. For them, without those tables a book like this would be incomplete (even if many of them first sit by the breadboard with the soldering iron in one hand and a ’scope probe in the other, and do the paperwork later!).

Anyway, for the younger generations we provide the necessary computer routines in Part 6.

The principles developed in this part will be used in Part 5, where some more sophisticated amplifier building blocks are discussed.

**Contents:**

**List of Figures:**

**List of Tables:**

(blank page)

# 4.0 Introduction

In a majority of cases the desired *gain* × *bandwidth* product is not achievable with a single transistor amplifier stage. Therefore more stages must be connected in cascade. But to do it correctly we must find the answer to several questions:

- Should all stages be equal or different?
- What is the optimal pole pattern for obtaining a desired response?
- Is it important which pole (pair) is assigned to which stage?
- Is it better to use many simple (first- and second-order) stages or is it worth the trouble to try more complex (third-, fourth- or higher order) stages?
- What is the optimum single stage gain to achieve the greatest possible gain × bandwidth product for a given number of stages?
- Is it possible to construct an ideal multi-stage amplifier with either a maximally flat amplitude (MFA) response or a maximally flat envelope delay (MFED), and if not, how close to the ideal response can we come?

These are the main questions which we shall try to answer in this part.

In Sec. 4.1 we discuss a cascade of identical DC coupled amplifier stages, with loads consisting of a parallel connection of a resistance and a (stray) capacitance. There we derive the formula for the calculation of an optimum number of amplifying stages to obtain the required gain with the smallest rise time possible for the complete amplifier.

Next we derive the expression for the optimum gain of an individual amplifying stage of a multi-stage amplifier in order to achieve the smallest possible rise time. We also discuss the effect of AC coupling between particular stages by means of a simple $RC$ network.

Butterworth poles, which are needed to achieve an MFA response, are derived next. This leads to the discussion of the (im)possibility to design an ideal MFA amplifier.

Then we derive the Bessel poles which provide the MFED response. Since they are derived from the condition for a unit envelope delay, the upper cut off frequency increases with the number of poles. Therefore we also present the derivation of two different pole normalizations: to equal cut off frequency and to equal stop band asymptote. We discuss the (im)possibility of designing an amplifier with the frequency response approaching an ideal Gaussian curve. Further we discuss the interpolation between the Bessel and the Butterworth poles.

Finally, we explain the merit of using staggered Bessel poles versus repeated second-order Bessel pole pairs.

Wherever practical, we calculate and plot the frequency, phase, group delay and step response to allow a quick comparison of different concepts.

(blank page)

## 4.1 A Cascade of Identical, DC Coupled, *RC* Loaded Stages

A multi-stage amplifier with DC coupled, $RC$ loaded stages is shown in Fig. 4.1.1. All stages are assumed to be identical. Junction field effect transistors (JFETs) are being used as active devices, since we want to focus on essential design problems; with bipolar junction transistors (BJTs), we would have to consider the loading effect of a relatively complicated base input impedance [Ref. 4.1].

At each stage load the capacitance $C_k$ ($k = 1 \ldots n$) represents the sum of all the stray capacitances at the $k^{\text{th}}$ node, including $C_{\text{GS}}$ (the gate–source capacitance) and the $C_{\text{GD}}(1 + A_k)$ equivalent capacitance (where $C_{\text{GD}}$ is the gate–drain capacitance and $A_k$ is the voltage gain of the individual stage). By doing so we obtain a simple parallel $RC$ load in each stage. The input resistance of a JFET is many orders of magnitude higher than the loading resistor $R$, so we can neglect it. All loading resistors are of equal value, and so are the mutual conductances $g_{\text{m}}$ of all the JFETs; therefore all individual gains $A_k$ are equal as well. Consequently, all the half power frequencies $\omega_{\text{h}k}$ and all the rise times $\tau_{\text{r}k}$ of the individual stages are also equal. In order to simplify the circuit further, we have not drawn the bias voltages and the power supply (which must represent a short circuit for AC signals; obviously, a short for DC would not be very useful!).

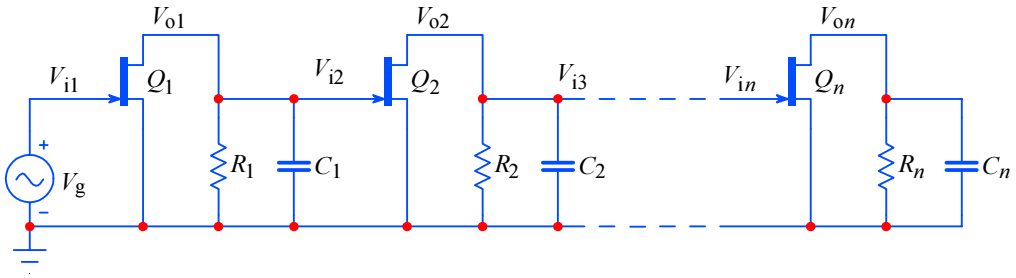


**Fig. 4.1.1**: A multi-stage amplifier as a cascade of identical, DC coupled, $RC$ loaded stages.

The voltage gain of an individual stage is:

$$A_k = g_{\text{m}}\, R\, \frac{1}{1 + j\omega RC} \tag{4.1.1}$$

with the magnitude:

$$|A_k| = \frac{g_{\text{m}}\, R}{\sqrt{1 + (\omega/\omega_{\text{h}})^2}} \tag{4.1.2}$$

where:

$g_{\text{m}}$ = mutual conductance of the JFET, [S] (siemens, [S] = $[1/\Omega]$);

$\omega_{\text{h}} = 1/RC$ = upper half power frequency of an individual stage, [rad/s].

### 4.1.1 Frequency Response and the Upper Half Power Frequency

We have $n$ equal stages with equal gains: $A_1 = A_2 = \cdots = A_n = A_k$. The gain of the complete amplifier is then:

$$A = A_1 \cdot A_2 \cdot A_3 \cdots A_n = A_k^n = \left[\frac{g_{\text{m}}\, R}{1 + j\,\omega\, RC}\right]^n \tag{4.1.3}$$

The magnitude is:

$$|A| = \left[ \frac{g_m R}{\sqrt{1 + (\omega/\omega_h)^2}} \right]^n \tag{4.1.4}$$

To be able to compare the bandwidth of the multi-stage amplifier for different number of stages, we must normalize the magnitude by dividing Eq. 4.1.4 by the system DC gain $A_0 = (g_m R)^n$. The plots are shown in Fig. 4.1.2. It is evident that the system bandwidth, $\omega_H$, shrinks with each additional amplifying stage.

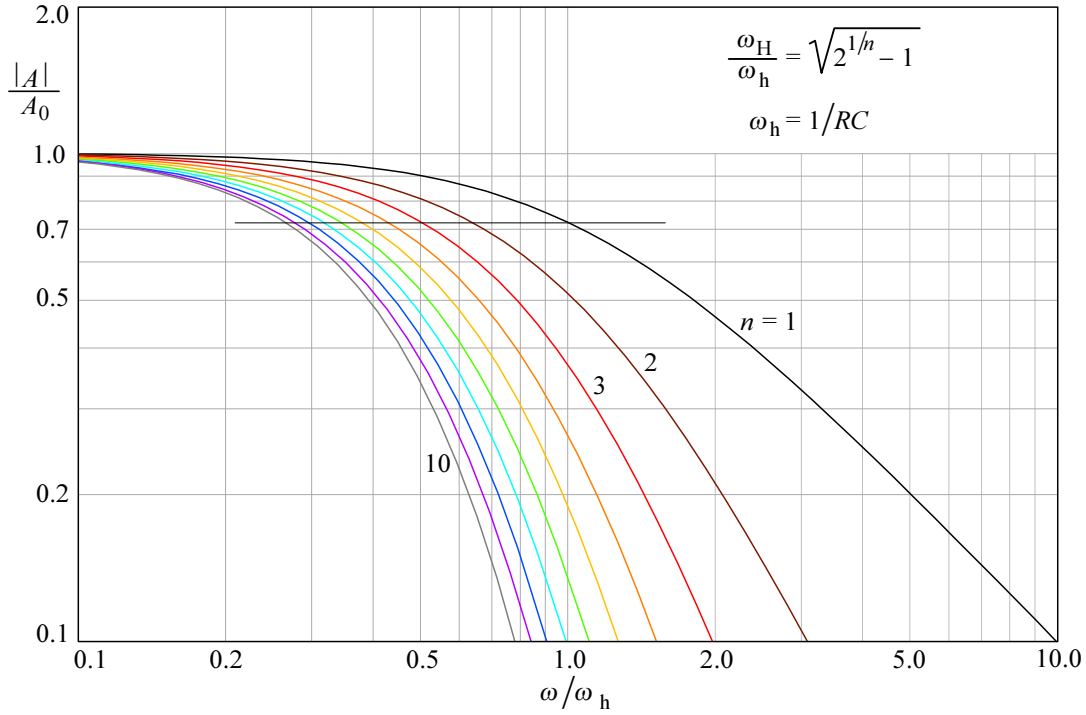


**Fig. 4.1.2**: Frequency response of an $n$-stage amplifier ($n = 1, 2, \ldots, 10$). To compare the bandwidth, the gain was normalized, i.e., divided by the system DC gain, $(g_m R)^n$. For each $n$, the bandwidth (the crossing of the $0.707$ level) shrinks by $\sqrt{2^{1/n} - 1}$ .

The upper half power frequency of the amplifier can be calculated by a simple relation:

$$\left[ \frac{1}{\sqrt{1 + (\omega_H/\omega_h)^2}} \right]^n = \frac{1}{\sqrt{2}} \tag{4.1.5}$$

By squaring we obtain:

$$\left[1 + (\omega_H/\omega_h)^2\right]^n = 2 \quad \Rightarrow \quad \left( \frac{\omega_H}{\omega_h} \right)^2 = 2^{1/n} - 1 \tag{4.1.6}$$

The upper half power frequency of the complete $n$-stage amplifier is:

$$\boxed{\omega_H = \omega_h \sqrt{2^{1/n} - 1}} \tag{4.1.7}$$

At high frequencies, the first stage response slope approaches the $-6\,\mathrm{dB/octave}$ asymptote ($-20\,\mathrm{dB/decade}$). The meaning of this slope is explained in Fig. 4.1.3. For the second stage the slope is twice as steep, and for the $n^{\mathrm{th}}$ stage it is $n$ times steeper.

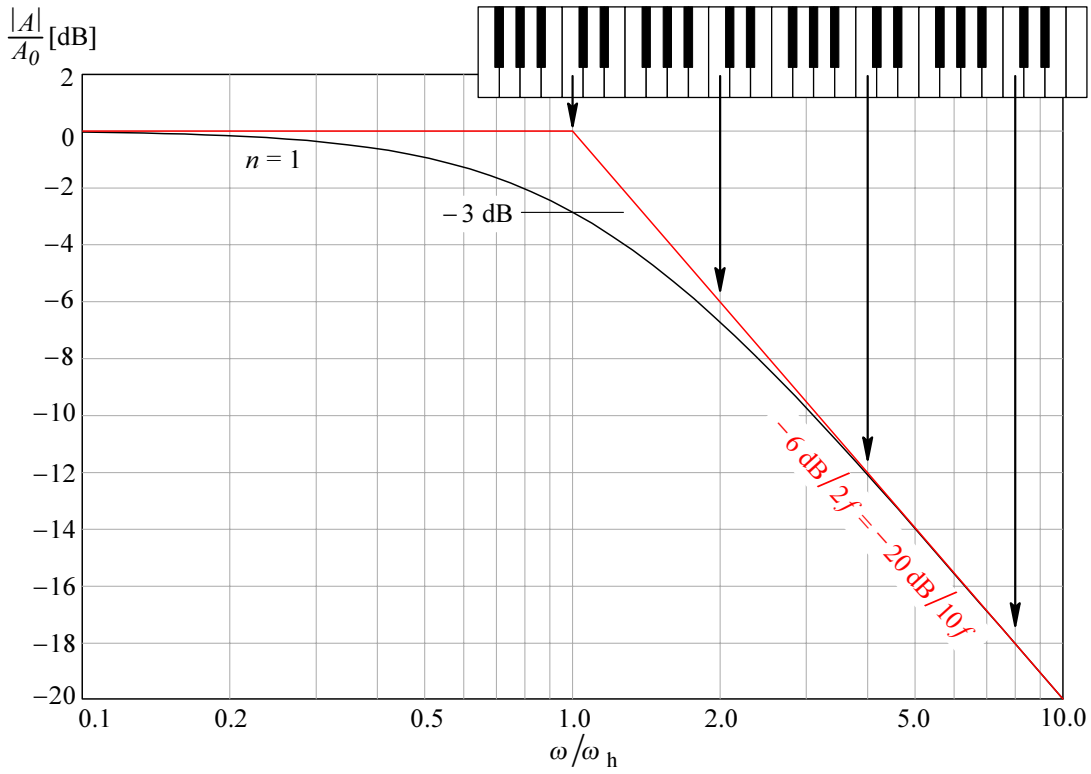


**Fig. 4.1.3**: The first-order system response and its asymptotes. Below the cut off, the asymptote is the level equal to the system gain at DC (normalized here to 0 dB). Above the cut off, the slope is $-6\,\mathrm{dB/octave}$ (an octave is a frequency span from $f$ to $2f$), which is also equal to $-20\,\mathrm{dB/decade}$ (a frequency decade is a span from $f$ to $10\,f$).

The values of $\omega_{\mathrm{H}}$ for $n = 1-10$ are reported in Table 4.1.1.

**Table 4.1.1**

| $n$ | 1 | 2 | 3 | 4 | 5 | 6 | 7 | 8 | 9 | 10 |
|---|---|---|---|---|---|---|---|---|---|---|
| $\omega_{\mathrm{H}}$ | 1.000 | 0.644 | 0.510 | 0.435 | 0.386 | 0.350 | 0.323 | 0.301 | 0.283 | 0.269 |

With ten equal stages connected in cascade the bandwidth is reduced to a poor $0.269\,\omega_{\mathrm{h}}$; such an amplifier is definitely not very efficient for wideband amplification.

Alternatively, in order to preserve the bandwidth a $n$-stage amplifier should have all its capacitors reduced by the same factor, $\sqrt{2^{1/n}-1}$. But in wideband amplifiers we already strive to work with stray capacitances only, so this approach is not a solution.

Nevertheless, the amplifier in Fig. 4.1.1 is the basis for more efficient amplifier configurations, which we shall discuss later.

### 4.1.2 Phase Response

Each individual stage of the amplifier in Fig. 4.1.1 has a frequency dependent phase angle:

$$\varphi_k = \arctan \frac{\Im\{F(j\omega)\}}{\Re\{F(j\omega)\}} = \arctan(-\omega/\omega_h) \tag{4.1.8}$$

where $F(j\omega)$ is taken from Eq. 4.1.1. For $n$ equal stages the total phase angle is simply $n$ times as much:

$$\boxed{\varphi_n = n \arctan(-\omega/\omega_h)} \tag{4.1.9}$$

The phase responses are plotted in Fig. 4.1.4. Note the high frequency asymptotic phase shift increasing by $\pi/2$ (or 90°) for each $n$. Also note the shift at $\omega = \omega_h$ being exactly $n\,\pi/4$, in spite of a reduced $\omega_h$ for each $n$.

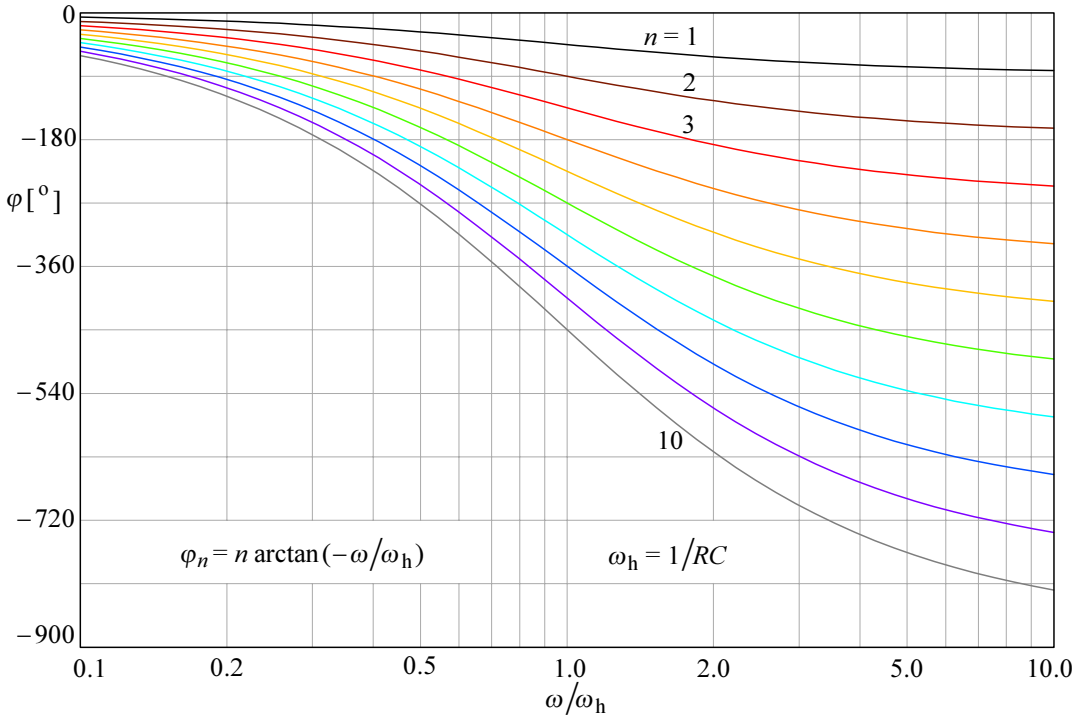


**Fig. 4.1.4:** Phase angle of the amplifier in Fig. 4.1.1, for $n$ = 1–10 amplifying stages.

### 4.1.3 Envelope Delay

For a single amplifying stage ($n = 1$) the envelope delay is the frequency derivative of the phase, $\tau_{en} = d\varphi_n/d\omega$ (where $\varphi_n$ is given by Eq. 4.1.9). The normalized single stage envelope delay is:

$$\tau_e\,\omega_h = \frac{-1}{1 + (\omega/\omega_h)^2} \tag{4.1.10}$$

and for $n$ equal stages:

$$\tau_{en}\,\omega_h = \frac{-n}{1+(\omega/\omega_h)^2} \tag{4.1.11}$$

Fig. 4.1.5 shows the frequency dependent envelope delay for $n = 1$–$10$. Note the delay at $\omega = \omega_h$ being exactly $1/2$ of the low frequency asymptotic value.

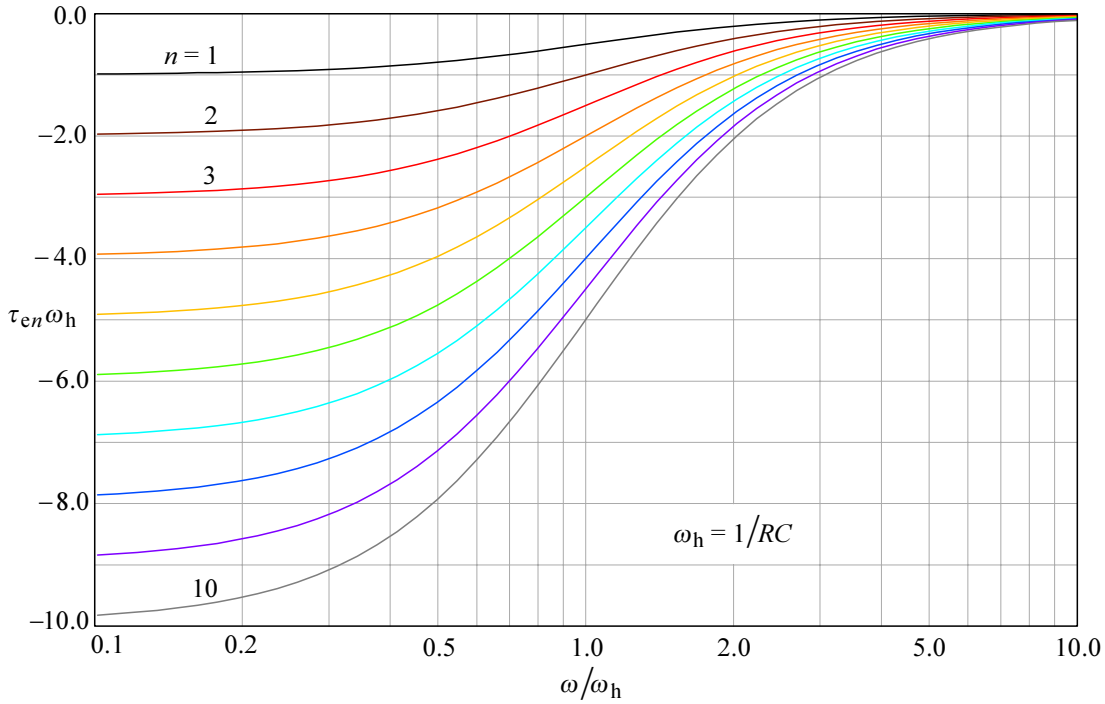


**Fig. 4.1.5**: Envelope delay of the amplifier in Fig. 4.1.1, for $n = 1$–$10$ amplifying stages. The delay at $\omega = \omega_h$ is $1/2$ of the low frequency asymptotic value. Note that if we were using $f/f_h$ for the abscissa, we would have to divide the $\tau_e$ scale by $2\pi$.

### 4.1.4 Step Response

To obtain the step response, the amplifier in Fig. 4.1.1 must be driven by the unit step function:

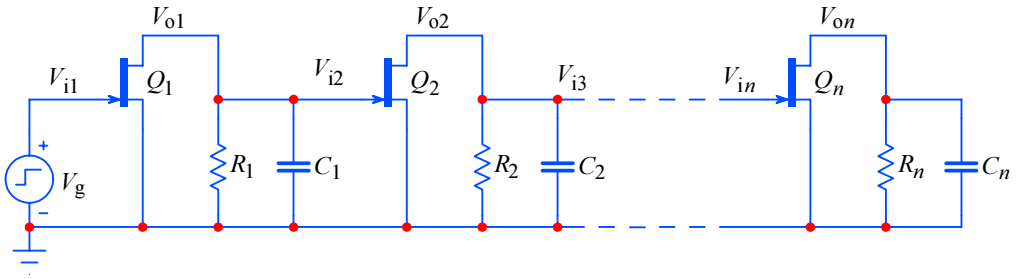


**Fig. 4.1.6**: Amplifier with $n$ equal DC coupled stages, excited by the unit step

We can derive the step response expression from Eq. 4.1.1 and Eq. 4.1.3. In order to simplify and generalize the expression we shall normalize the magnitude by dividing the transfer function by the DC gain, $g_m R$, and normalize the frequency by setting $\omega_h = 1/RC = 1$. Since we shall use the $\mathcal{L}^{-1}$ transform we shall replace the variable $j\omega$ by the complex variable $s = \sigma + j\omega$.

With all these changes we obtain:

$$F(s) = \frac{1}{(1+s)^n} \tag{4.1.12}$$

The amplifier input is excited by the unit step, therefore we must multiply the above formula by the unit step operator $1/s$:

$$G(s) = \frac{1}{s\,(1+s)^n} \tag{4.1.13}$$

The corresponding function in the time-domain is:

$$g(t) = \mathcal{L}^{-1}\{G(s)\} = \sum \text{res}\, \frac{\mathrm{e}^{s\,t}}{s\,(1+s)^n} \tag{41.14}$$

We have two residues. The first one does not depend of $n$:

$$\text{res}_0 = \lim_{s \to 0} s \left[ \frac{\mathrm{e}^{s\,t}}{s\,(1+s)^n} \right] = 1$$

whilst the second does:

$$\text{res}_1 = \lim_{s \to 1} \frac{1}{(n-1)!} \cdot \frac{d^{(n-1)}}{ds^{(n-1)}} \left[ (1+s)^n \, \frac{\mathrm{e}^{s\,t}}{s\,(1+s)^n} \right] =$$

$$= \lim_{s \to 1} \frac{1}{(n-1)!} \cdot \frac{d^{(n-1)}}{ds^{(n-1)}} \left( \frac{\mathrm{e}^{s\,t}}{s} \right) \tag{4.1.15}$$

Since $\text{res}_1$ depends on $n$, for $n = 1$ we obtain:

$$\text{res}_1\Big|_{n=1} = -\,\mathrm{e}^{-t} \tag{4.1.16}$$

for $n = 2$:

$$\text{res}_1\Big|_{n=2} = -\,\mathrm{e}^{-t}\,(1+t) \tag{4.1.17}$$

for $n = 3$:

$$\text{res}_1\Big|_{n=3} = -\,\mathrm{e}^{-t} \left( 1 + t + \frac{t^2}{2} \right) \tag{4.1.18}$$

… etc.

The general expression for the step response for any $n$ is:

$$\boxed{g_n(t) = \mathcal{L}^{-1}\big\{\mathrm{G}(s)\big\} = \text{res}_0 + \text{res}_1(n) = 1 - \mathrm{e}^{-t} \sum_{k=1}^{n} \frac{t^{k-1}}{(k-1)!}} \tag{4.1.19}$$

Here we must consider that $0! = 1$, by definition.

As an example, by inserting $n = 5$ into Eq. 4.1.19 we obtain:

$$g_5(t) = 1 - \mathrm{e}^{-t} \left( 1 + \frac{t}{1!} + \frac{t^2}{2!} + \frac{t^3}{3!} + \frac{t^4}{4!} \right) \tag{4.1.20}$$

The step response plots for $n = 1$–10, calculated by Eq. 4.1.19, are shown in Fig. 4.1.7. Note that there is **no overshoot** in any of the curves. Unfortunately, the efficiency of this kind of amplifier in the sense of the 'bandwidth per number of stages' is poor, since it has no peaking networks which would prevent the decrease of bandwidth with $n$.

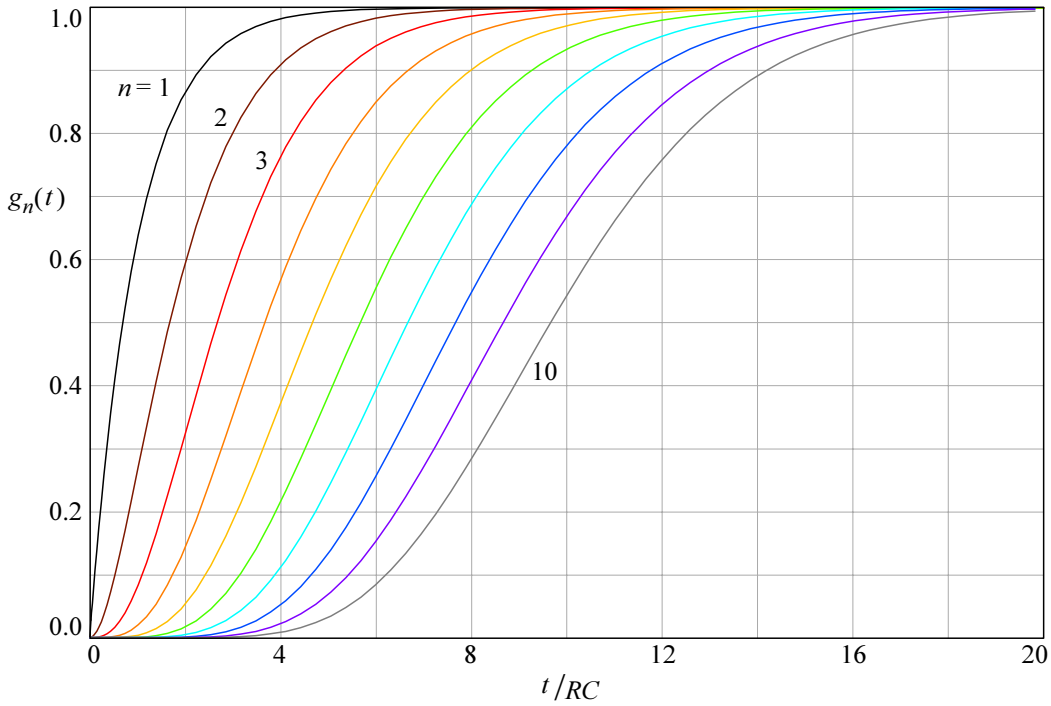


**Fig. 4.1.7:** Step response of the amplifier in Fig. 4.1.6, for $n = 1$–10 amplifying stages

### 4.1.5 Rise Time Calculation

In a multi-stage amplifier, where each particular stage has its respective rise time, $\tau_{r1}, \tau_{r2}, \ldots, \tau_{rn}$, we approximate the system's rise time [Ref. 4.2] as:

$$\tau_r \approx \sqrt{\tau_{r1}^2 + \tau_{r2}^2 + \tau_{r3}^2 + \cdots + \tau_{rn}^2} \tag{4.1.21}$$

In Part 2, Sec. 2.1.1, Eq. 2.1.1–4, we have calculated the rise time of an amplifier with a simple $RC$ load to be $\tau_{r1} = 2.20\,RC$. Since here we have $n$ equal stages the rise time of the complete amplifier is approximately:

$$\boxed{\tau_r \approx \tau_{r1}\sqrt{n} = 2.20\,RC\sqrt{n}} \tag{4.1.22}$$

Table 4.1.2 shows the actual rise time increasing with the number of stages. The numbers were calculated by using Eq. 4.1.19.

**Table 4.1.2**

| $n$ | 1 | 2 | 3 | 4 | 5 | 6 | 7 | 8 | 9 | 10 |
|---|---|---|---|---|---|---|---|---|---|---|
| $\tau_{rn}$ | 2.20 | 3.36 | 4.22 | 4.94 | 5.56 | 6.12 | 6.64 | 7.11 | 7.56 | 7.98 |
| $\tau_{rn}/\tau_{r1}$ | 1.00 | 1.53 | 1.92 | 2.25 | 2.53 | 1.79 | 3.02 | 3.24 | 3.44 | 3.63 |

### 4.1.6 Slew Rate Limit

The equations derived so far describe the small signal properties of an amplifier. If the signal amplitude is increased the maximum slope of the output signal $dV_o/dt$ becomes limited by the maximum current available to charge any capacitance present at the particular node. The amplifier stage which must handle the largest signal is the first to run into the slew rate limiting; usually it is the output stage.

To find the slew rate limit we drive the amplifier by a sinusoidal signal and increase the input amplitude until the output amplitude just begins to saturate; then we increase the frequency until we notice that the middle part of the sinusoidal waveform becomes distorted (changing linearly with time) and then decrease the frequency until the distortion just disappears. That frequency is equal to the *full power bandwidth* $\omega_{FP}$ (in *radians per second*, [rad/s]). Generally, an amplifier need not have the positive and negative slope equally steep; then it is the less steep slope to set the limit.

$$\frac{dV_o}{dt} = \frac{I_{omax}}{C} \tag{4.1.23}$$

For a sinusoidal input signal of angular frequency $\omega_{FP}$ and amplitude $V_{max}$, the slope varies with time as:

$$\frac{d(V_{max} \sin \omega_{FP} t)}{dt} = V_{max}\, \omega_{FP} \cos \omega_{FP} t \tag{4.1.24}$$

and it has a maximum at $\cos \omega_{FP} t = 1$ (which is at $t = 0$; see Fig. 4.1.8). Therefore:

$$\boxed{\textit{slew rate}: \quad SR = V_{max}\, \omega_{FP}} \tag{4.1.25}$$

The slew rate is usually expressed in *volts per microsecond* [V/µs]; for contemporary amplifiers a more appropriate figure would be *volts per nanosecond* [V/ns].

The time elapsed from the negative to the positive peak of the sinusoid with the amplitude $V_{max}$ and frequency $\omega_{FP}$ is equal to one half of the period, $T_{FP}/2$, of the full power bandwidth frequency, $f_{FP}$, in Hz:

$$\boxed{\frac{T_{FP}}{2} = \frac{\pi}{\omega_{FP}} = \frac{1}{2\, f_{FP}}} \tag{4.1.26}$$

If we increase the signal frequency beyond $f_{FP}$ the waveform will eventually be distorted into a linear ramp shape, with a reduced amplitude. If we imagine a ramp with the amplitude equal to that of the sine wave the slewing time can be found from:

$$SR = \frac{\Delta V}{\Delta t} = \frac{2\, V_{max}}{t_{slew}} \quad \Rightarrow \quad t_{slew} = \frac{2\, V_{max}}{V_{max}\, \omega_{FP}} = \frac{2}{\omega_{FP}} \tag{4.1.27}$$

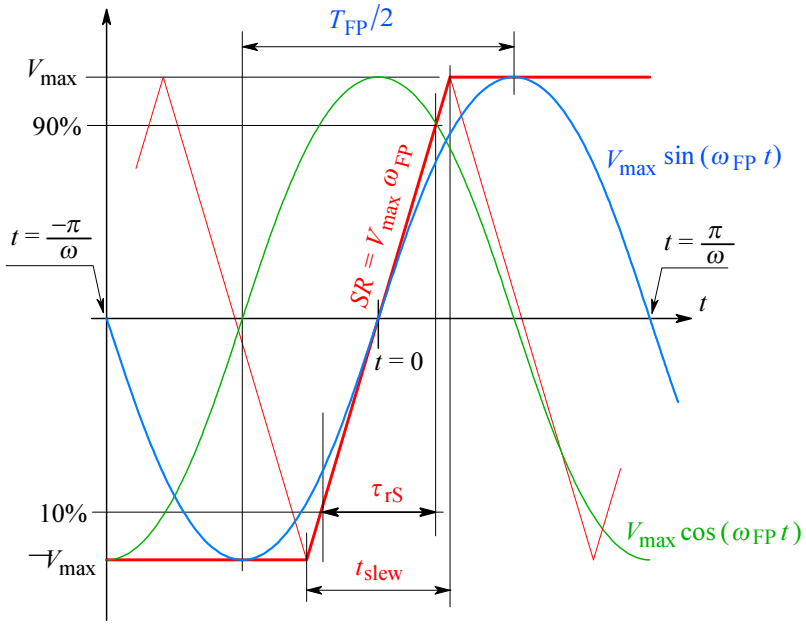


**Fig. 4.1.8**: Slew rate limiting: definitions of parameters.

All these calculations are valid for sinusoidal signals only, the slope of which decreases progressively and becomes zero at the peak voltage $\pm V_{max}$. These criteria can not be applied if the amplifier input is excited by a step pulse with the same output voltage range. In this case we, rather, speak of rise time. From 10 % to 90 % of $2V_{max}$, the output voltage rises by $0.8 \times 2V_{max}$. So the results of Eq. 4.1.27 must be multiplied by 0.8 to obtain:

$$\tau_{rS} = \frac{0.8 \times 2}{\omega_{FP}} = \frac{1.6}{2\,\pi\, f_{FP}} \approx \frac{0.2546}{f_{FP}} \tag{4.1.28}$$

Eq. 4.1.26 is generally used to characterize operational amplifiers, whilst for wideband and pulse amplifiers we prefer Eq. 4.1.28. It is very important to distinguish between the two definitions, since in most technical specifications they are tacitly assumed.

### 4.1.7 Optimum Single Stage Gain and Optimum Number of Stages

The first stage of the $n$-stage cascade amplifier of Fig. 4.1.6 has the voltage gain $A_1 = v_{o1}/v_{i1}$, the second stage gain is $A_2 = v_{o2}/v_{i2} = v_{o2}/v_{o1}$ and so on, up to $A_n = v_{on}/v_{in} = v_{on}/v_{o(n-1)}$ for the $n^{th}$ stage. Then the total gain is the product of individual stage gains:

$$A = \frac{v_{on}}{v_{i1}} = A_1 \cdot A_2 \cdots A_n \tag{4.1.29}$$

If all the amplifying stages are identical, we denote the gain of each stage as $A_k$, each loading resistor as $R$, and each loading capacitor as $C$. Then the total gain is:

$$A = (A_k)^n \tag{4.1.30}$$

The rise time of the complete multi-stage amplifier is approximated as the square root of the sum of the individual rise times squared (Eq. 4.1.21), but since the amplitude after each gain stage is different, we must normalize the rise times by multiplying each with its own gain factor $A_k$:

$$\tau_\mathrm{r} = \sqrt{\sum_{i=1}^{n} (A_k\,\tau_{\mathrm{r}k})^2} \tag{4.1.31}$$

We have assumed that all stages have identical gain $A_k$ and identical rise time $\tau_{\mathrm{r}k}$. Therefore:

$$\tau_\mathrm{r} = \sqrt{n\,(A_k\,\tau_{\mathrm{r}k})^2} = \sqrt{n}\;A_k\,\tau_{\mathrm{r}k} = \sqrt{n}\;A_k\,2.2\,RC \tag{4.1.32}$$

where $\tau_{\mathrm{r}k}$ is the rise time of an individual stage, as calculated in Part 2, Eq. 2.1.4. By considering Eq. 4.1.30, we obtain the following relation:

$$\boxed{\frac{\tau_\mathrm{r}}{\tau_{\mathrm{r}k}} = \sqrt{n}\;A^{1/n}} \tag{4.1.33}$$

We have plotted this relation in Fig. 4.1.9, using the system total gain $A$ as the parameter. Note that, in order to see the function $\tau_\mathrm{r}(n)$ better, we have assumed a continuous $n$; of course, we can not have, say, 4.63 stages — $n$ must be an integer.

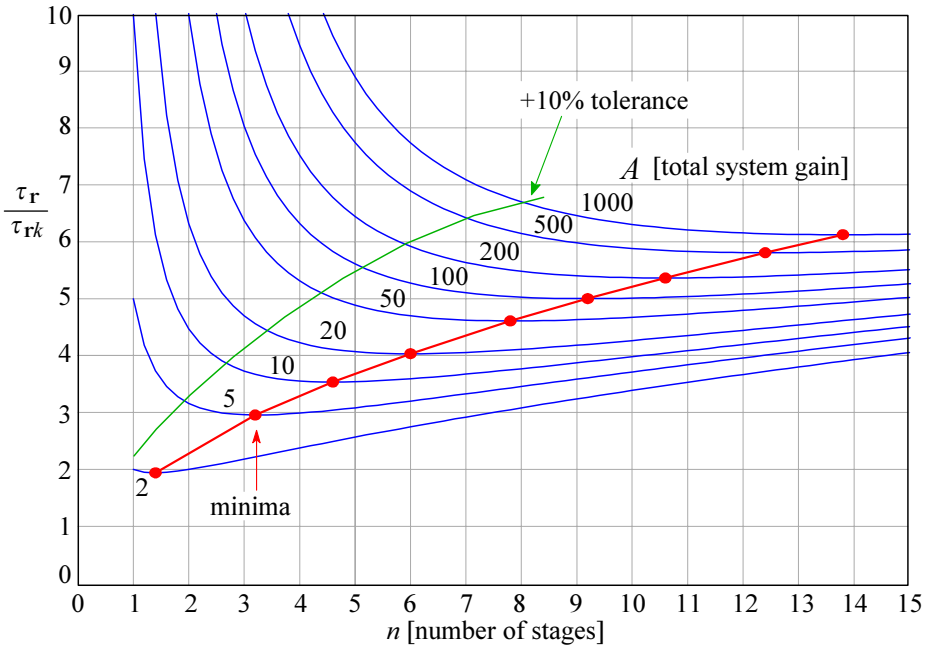


**Fig. 4.1.9:** Minimal relative rise time as a function of the number of stages $n$ and the total system gain $A$. Close to the minima the curves are relatively flat, so in practice we can trade off, say, a 10% increase in the system rise time and reduce the required number of stages accordingly; i.e., to achieve the gain of 100, only 5 stages could be used instead of 9, with a slight rise time increase.

From this diagram we can find the optimum number of the amplifying stages $n_\mathrm{opt}$ if the total system gain $A$ is known. These optima lie on the valleys of the curves and in the following discussion we will derive the necessary formulae.

The ratio $A/\tau_r$ characterizes the design efficiency of the amplifier. To design a multi-stage amplifier with the smallest possible rise time, we can differentiate $\tau_r$ from Eq. 4.1.33 with respect to $n$, and equate the result to zero to find the minimum:

$$\frac{\partial\,\tau_r}{\partial\,n} = \frac{\partial\left(\sqrt{n}\,A^{1/n}\,\tau_{rk}\right)}{\partial\,n} = 0 \tag{4.1.34}$$

The differentiation is solved as:

$$\frac{\tau_{rk}}{A}\left(\frac{1}{2\sqrt{n}}\,A^{1/n} - \sqrt{n}\,\frac{A^{1/n}}{n^2}\ln A\right) = 0 \tag{4.1.35}$$

Because neither $\tau_{rk}$ nor $A$ are zero we can equate the expression in parentheses to zero:

$$\frac{1}{2\sqrt{n}} - \frac{\sqrt{n}}{n^2}\ln A = 0 \tag{4.1.36}$$

By multiplying this by the $2\sqrt{n}$, we obtain an important intermediate result:

$$1 - \frac{2}{n}\ln A = 0 \quad \Rightarrow \quad n = 2\ln A \tag{4.1.37}$$

For a given total gain $A$ the optimum number of amplifying stages is approximately:

$$\boxed{1 \le n_{opt} \le \mathrm{int}(2\ln A)} \tag{4.1.38}$$

and since we can not have, say, 3.47 amplifying stages, we round the result to the nearest integer, the smallest obviously being 1.

On the basis of this simple relation we can draw the line *a* in Fig. 4.1.10 for a quick estimation of the number of amplifying stages necessary to obtain the smallest rise time if the total system gain $A$ is known. Again, the required number of amplifying stages can be reduced in practice, as indicated in Fig. 4.1.10 by the line *b*, without significantly increasing the rise time. Owing to reasons of economy, the most simple systems are often designed far from optimum, as indicated by the bars and the line *c*.

From Eq. 4.1.38 we can find the optimal gain value of the individual stage, independent of the actual number of stages in the system. For $n$ equal stages it is:

$$A_k = A^{1/n} = A^{1/(2\ln A)} \tag{4.1.39}$$

By taking a logarithm of this expression, we obtain:

$$\ln A_k = \frac{1}{2\ln A}\cdot\ln A = \frac{1}{2} \tag{4.1.40}$$

The optimal individual stage gain for the total minimal rise time is then:

$$\boxed{A_{k\mathrm{opt}} = \mathrm{e}^{1/2} = \sqrt{\mathrm{e}} \simeq 1.65} \tag{4.1.41}$$

Note that Eq. 4.1.41, as well as the approximations Eq. 4.1.33 and Eq. 4.1.38, can be applied also to amplifiers with peaking stages, although peaking stages are much more efficient in the gain-bandwidth product sense, as we shall see in Sec. 4.3 and 4.4.

This expression gives us the optimal value of the gain of the individual amplifying stage which minimizes the total rise time of a multi-stage amplifier. In practice we usually take a higher value, say, between 2 and 4, in order to decrease the cost and simplify the design. Eq. 4.1.41 can also be used for peaking stages.

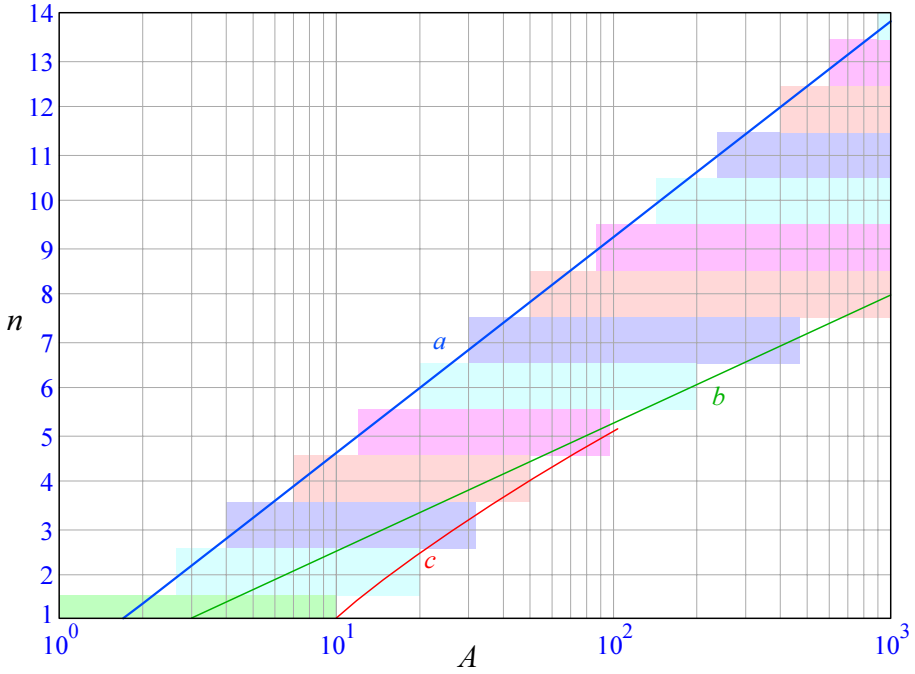


**Fig. 4.1.10:** The optimal number of stages, $n$, required to achieve the minimal rise time, given the total system gain $A$, as calculated by Eq. 4.1.38, is shown by line *a*. In practice, owing to economy reasons, we tend to use a lower number; the line *b* shows the same +10% rise time trade off as in Fig. 4.1.9. In low complexity systems we usually make even greater tradeoffs, as in *c*. The bars indicate the range of gain $A$ which can be achieved with a particular number of stages $n$ without departing much from the lowest rise time.

## 4.2 A Multi-stage Amplifier with Identical, AC Coupled Stages

In Fig. 4.1.1 all the amplifying stages were DC coupled. In times when the amplifiers were designed with electronic tubes the DC coupling was generally avoided to prevent drift owed to tube aging, unstable cathode heater voltages (changing of temperature), hum, and poor insulation between the heater and cathode. With the appearance of bipolar transistors and FETs only the temperature dependent drift remained on this nasty list. Because of it, many TV video and broadband RF amplifiers still use AC coupling between amplifying stages.

However, AC coupling introduces other undesirable properties, which in certain cases might not be acceptable. It is therefore interesting to investigate a multi-stage amplifier with equal stages, similar to that in Fig. 4.1.1, except that all the stages are AC coupled. In Fig. 4.2.1 we see a simplified circuit diagram of such an amplifier and here we are interested in its low-frequency performance.

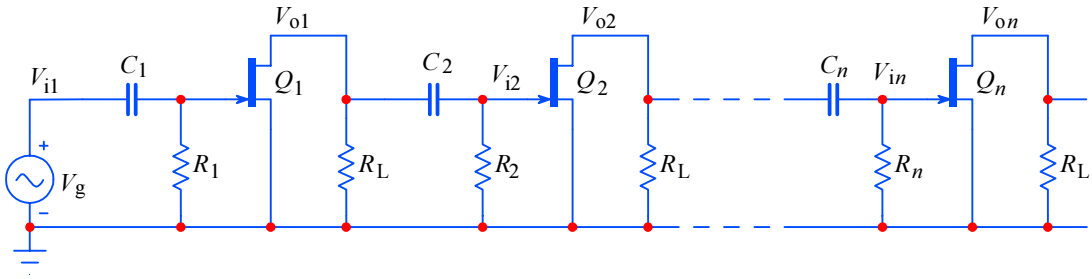


**Fig. 4.2.1:** Multi-stage amplifier with AC coupled stages. Again, to simplify the analysis, the power supply and the bias voltages are not shown.

Since we want to focus on essential problems only, here, too, we use FETs, instead of BJTs, in order to avoid the complicated expression for the base input impedance of each stage. Moreover, in a wideband amplifier we can assume $R_\mathrm{L} \ll R_n$, so we shall neglect the effect of $R_n$ on gain. On the other hand, $R_n$ and $C_n$ set the low frequency limit of each stage, which is $\omega_1 = 1/R_nC_n = 1/RC$, if all stages are identical. Usually, $\omega_1$ is many orders of magnitude below $\omega_\mathrm{h}$, so we can neglect the stray and input capacitances (both effectively in parallel to the loading resistors $R_\mathrm{L}$) as well. Thus, near $\omega_1$, the voltage gain of each stage is:

$$A_n = g_\mathrm{m} R_\mathrm{L} \frac{j\omega/\omega_1}{1 + j\omega/\omega_1} \tag{4.2.1}$$

and the magnitude is:

$$|A_n| = g_\mathrm{m} R_\mathrm{L} \frac{\omega/\omega_1}{\sqrt{1 + (\omega/\omega_1)^2}} \tag{4.2.2}$$

With all input time constants equal to $RC$ the system gain $A$ is $A_n$ to the $n^{\mathrm{th}}$ power:

$$A = \left[ g_\mathrm{m} R_\mathrm{L} \frac{j\omega/\omega_1}{1 + j\omega/\omega_1} \right]^n \tag{4.2.3}$$

with the magnitude:

$$|A| = \left[ g_\mathrm{m} R_\mathrm{L} \frac{\omega/\omega_1}{\sqrt{1 + (\omega/\omega_1)^2}} \right]^n \tag{4.2.4}$$

### 4.2.1 Frequency Response and Lower Half Power Frequency

In Fig. 4.2.2 we show the frequency response plots according to Eq. 4.2.4, normalized in amplitude by dividing it by $(g_m R_L)^n$.

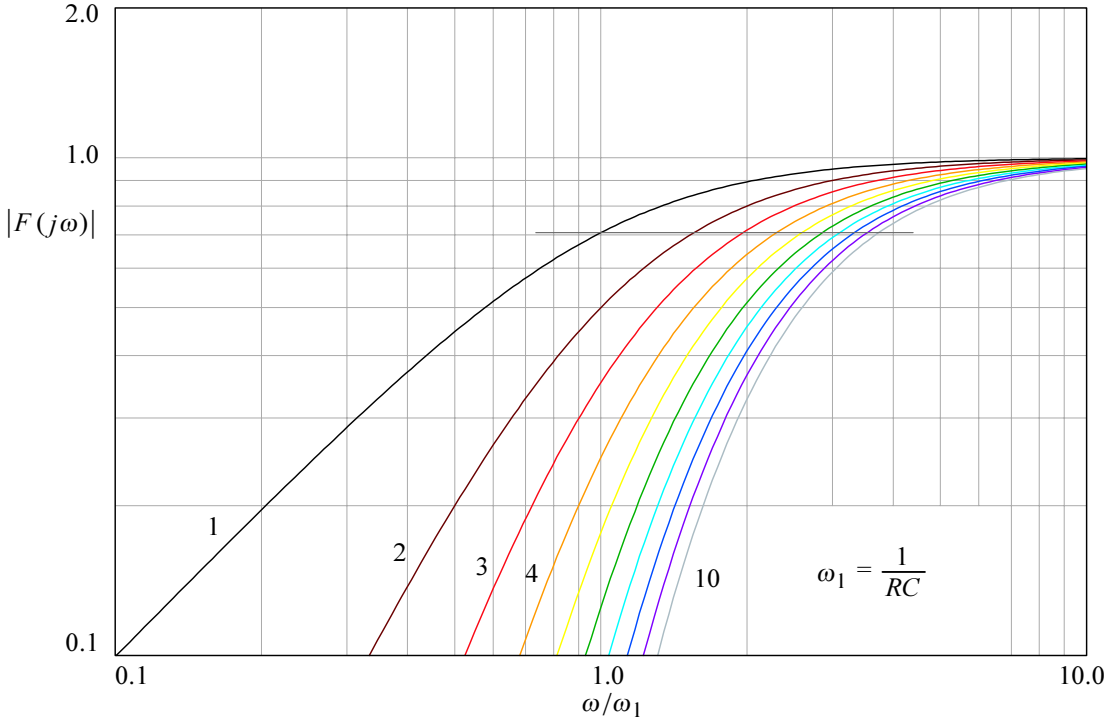


**Fig. 4.2.2:** Frequency response magnitude of the AC coupled amplifier for $n = 1$–$10$. The frequency scale is normalized to the lower cut off frequency $\omega_1$ of the single stage.

It is evident that the lower half power frequency $\omega_L$ of the complete amplifier increases with the number of stages. We can express $\omega_L$ as a function of $n$ from:

$$\left[\frac{\omega_L/\omega_1}{\sqrt{1+(\omega_L/\omega_1)^2}}\right]^n = \frac{1}{\sqrt{2}} \tag{4.2.5}$$

By eliminating the fractions:

$$[1+(\omega_L/\omega_1)^2]^n = 2\,(\omega_L/\omega_1)^{2n} \tag{4.2.6}$$

and taking the $n^{\text{th}}$ root:

$$1+(\omega_L/\omega_1)^2 = 2^{1/n}(\omega_L/\omega_1)^2 \tag{4.2.7}$$

and rearranging a little:

$$(\omega_L/\omega_1)^2\,(2^{1/2}-1) = 1 \tag{4.2.8}$$

we obtain the lower half power frequency of the complete multi-stage amplifier:

$$\boxed{\omega_L = \omega_1 \frac{1}{\sqrt{2^{1/n}-1}}} \tag{4.2.9}$$

We normalize this equation in frequency by setting $\omega_1 = 1/RC = 1$. The normalized values of the lower half power frequency for $n$ equal stages, $n = 1$–$10$, are shown in Table 4.2.1:

**Table 4.2.1**

| $n$ | 1 | 2 | 3 | 4 | 5 | 6 | 7 | 8 | 9 | 10 |
|---|---|---|---|---|---|---|---|---|---|---|
| $\omega_L/\omega_1$ | 1.000 | 1.554 | 1.961 | 2.299 | 2.593 | 2.858 | 3.100 | 3.334 | 3.534 | 3.733 |

### 4.2.2 Phase Response

The phase shift for a single stage is:

$$\varphi_i = \arctan(\omega_1/\omega) \tag{4.2.10}$$

The phase shift is positive and this means a phase advance. For $n$ stages the total phase advance is simply $n$ times as much:

$$\boxed{\varphi_n = n \arctan(\omega_1/\omega)} \tag{4.2.11}$$

The corresponding plots for $n = 1$–$10$ are shown in Fig. 4.2.3. Note the phase shift at $\omega = \omega_1$ being exactly $1/2$ the low frequency asymptotic value.

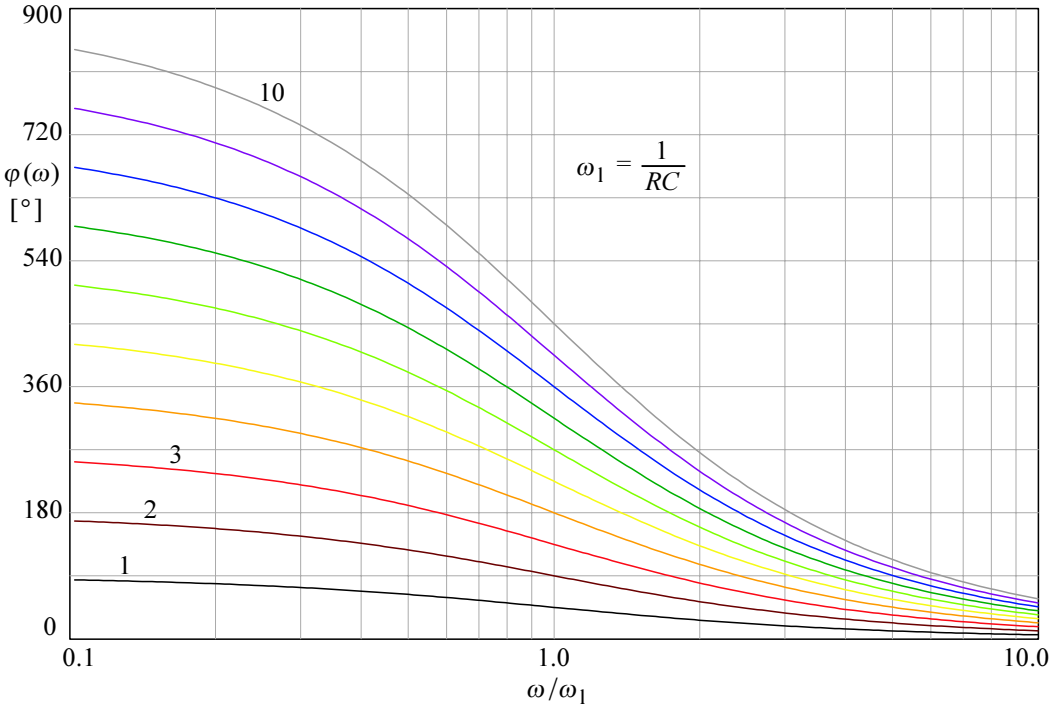


**Fig. 4.2.3:** Phase angle as a function of frequency for the AC coupled $n$-stage amplifier, $n = 1$–$10$. The frequency scale is normalized to the lower cutoff frequency of the single stage.

We will omit the calculation of envelope delay since in the low frequency region this aspect of amplifier performance is not very important.

### 4.2.3 Step Response

By replacing the sine wave generator in Fig. 4.2.1 with a unit step generator, we obtain the time domain step response of the AC coupled multi-stage amplifier. We want the plots to be normalized in amplitude, so we normalize Eq. 4.2.3 by dividing it by $(g_m R_L)^n$, the total amplifier gain at DC. We will use the $\mathcal{L}^{-1}$ transform, so we replace the normalized variable $j\omega/\omega_1$ by the complex variable $s = \sigma + j\omega$:

$$F_n(s) = \left(\frac{s}{1+s}\right)^n \tag{4.2.12}$$

The system's frequency response must be multiplied by the unit step operator $1/s$:

$$G_n(s) = \frac{1}{s}\left(\frac{s}{1+s}\right)^n \tag{4.2.13}$$

Now we apply the $\mathcal{L}^{-1}$ transformation and obtain the time domain step response:

$$g_n(t) = \mathcal{L}^{-1}\{G_n(s)\} = \operatorname{res} G_n(s)\,\mathrm{e}^{st} = \operatorname{res} \frac{s^{n-1}}{(1+s)^n}\,\mathrm{e}^{st} \tag{4.2.14}$$

Since we have here a single pole repeated $n$ times we have only a single residue, but — as we will see — it is composed of $n$ summands. A general expression for the residue for an arbitrary $n$ is:

$$g_n(t) = \lim_{s\to -1} \frac{1}{(n-1)!} \cdot \frac{d^{n-1}}{d\,s^{n-1}}\left[(1+s)^n \frac{s^{n-1}}{(1+s)^n}\,\mathrm{e}^{st}\right] \tag{4.2.15}$$

or, simplified:

$$g_n(t) = \frac{1}{(n-1)!} \cdot \frac{d^{n-1}}{d\,s^{n-1}}\left[s^{n-1}\,\mathrm{e}^{st}\right]\Big|_{s\to -1} \tag{4.2.16}$$

A few examples:

$$\begin{aligned}
n = 1 \quad &\Rightarrow \quad g_1(t) = \frac{1}{0!}\,\mathrm{e}^{-t} = \mathrm{e}^{-t} \\
n = 2 \quad &\Rightarrow \quad g_2(t) = \frac{1}{1!}\left(\mathrm{e}^{-t} - t\,\mathrm{e}^{-t}\right) = \mathrm{e}^{-t}(1-t) \\
n = 3 \quad &\Rightarrow \quad g_3(t) = \mathrm{e}^{-t}\left(1 - 2\,t + 0.5\,t^2\right) \\
n = 4 \quad &\Rightarrow \quad g_4(t) = \mathrm{e}^{-t}\left(1 - 3\,t + 1.5\,t^2 - 0.1667\,t^3\right) \\
n = 5 \quad &\Rightarrow \quad g_5(t) = \mathrm{e}^{-t}\left(1 - 4\,t + 3\,t^2 - 0.6667\,t^3 + 0.0417\,t^4\right)
\end{aligned} \tag{4.2.17}$$

The coefficients decrease rapidly with increasing number of stages $n$; e.g., the last summand for $n = 10$ is $-2.775 \cdot 10^{-6}\,t^9$.

The corresponding plots are drawn in Fig. 4.2.4. The plots for $n = 6$–$9$ are not shown, since it would be very difficult to distinguish the individual curves. We note that the $n^{\text{th}}$-order response intersects the abscissa $(n-1)$ times.

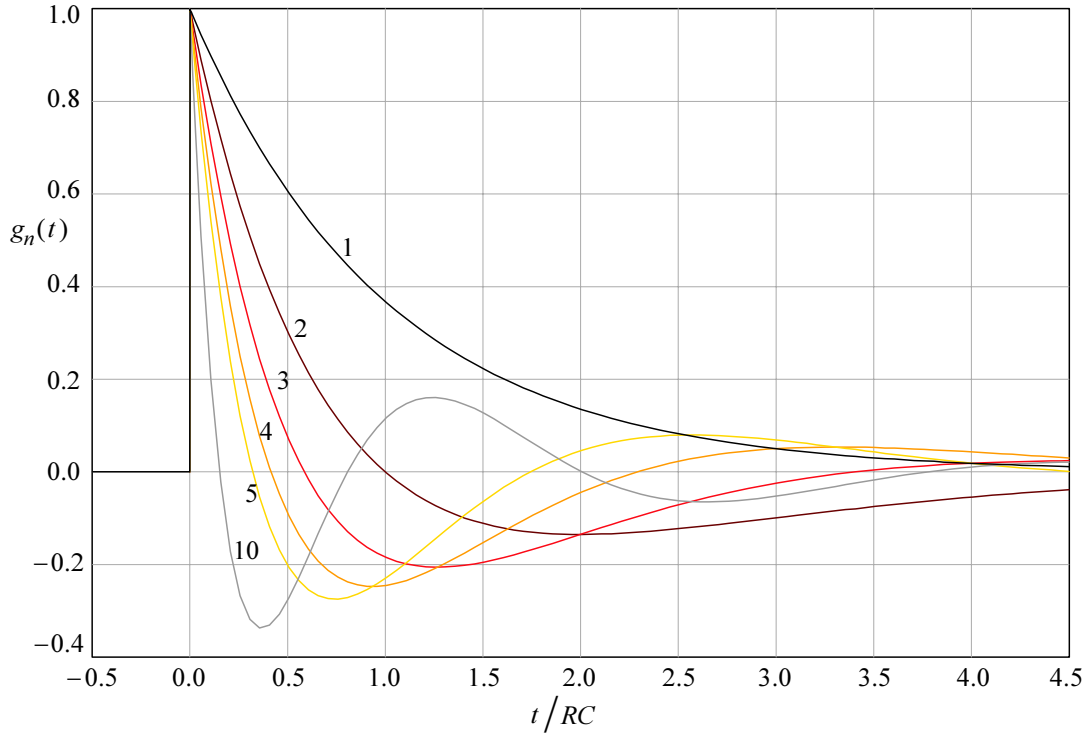


**Fig. 4.2.4:** Step response of the multi-stage AC coupled amplifier for $n = 1$–5 and $n = 10$.

For pulse amplification only the short starting portions of the curves come into consideration. An example for $n = 1$, 3, and 8 is shown in Fig. 4.2.5 for a pulse width $\Delta t = 0.1\,RC$.

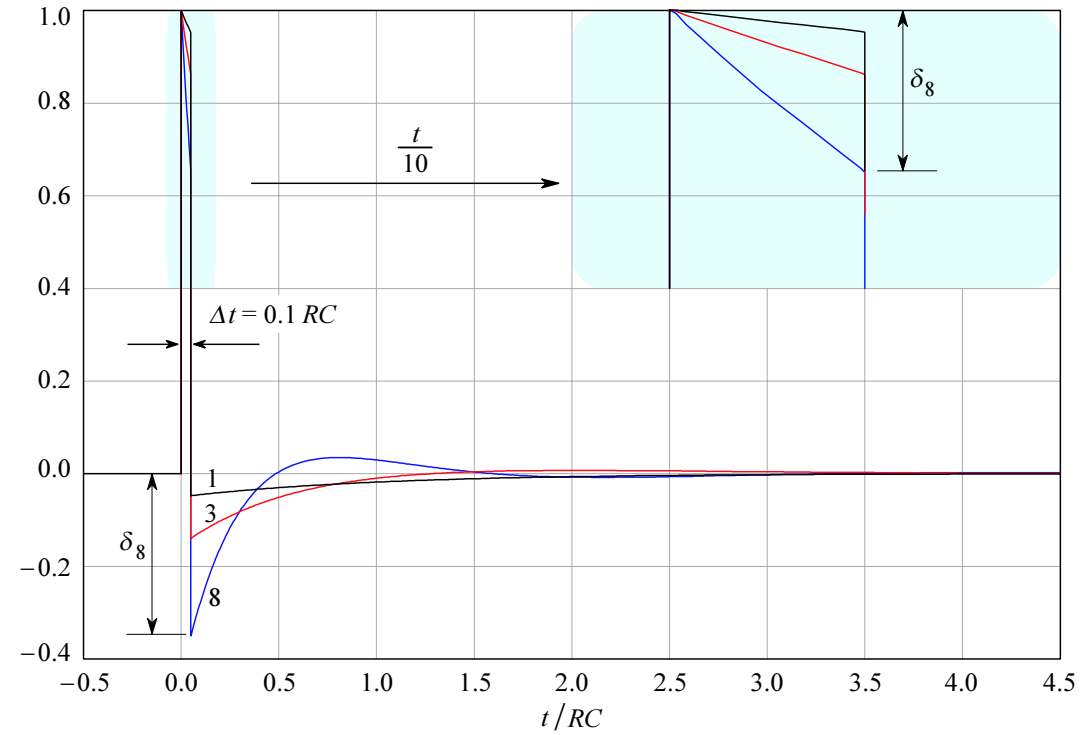


**Fig. 4.2.5:** Pulse response of the AC coupled multi-stage amplifier ($n = 1$, 3, and 8).

Note that the pulse in Fig. 4.2.5 sags, both on the leading and trailing edge, the sag increasing with the number of stages. We conclude that the AC coupled amplifier of Fig. 4.2.1 is not suitable for a faithful pulse amplification, except when the pulse duration is very short in comparison with the time constant $RC$ of a single amplifying stage (say, $\Delta t \leq 0.001\,RC$).

Another undesirable property of the AC coupled amplifier is that the output voltage makes $n-1$ damped oscillations when the pulse ends, no matter how short its duration is. This is especially annoying because the input voltage is by now already zero. The undesirable result is that the effective output DC level will depend on the pulse repetition rate.

Since today the DC amplification technique has reached a very high quality level, we can consider the AC coupled amplifier an inheritance from the era of electronic tubes and thus almost obsolete. However, we still use AC coupled amplifiers to avoid the drift in those cases where the deficiencies described are not important.

## 4.3 A Multi-stage Amplifier with Butterworth Poles (MFA)

In multi-stage amplifiers, like the one in Fig. 4.1.1, we can apply inductive peaking at each stage, see Fig. 4.3.7. As we have seen in Part 2, Sec. 2.9, where we discussed the shunt–series peaking circuit, the equations became very complicated because we had to consider the mutual influence of the shunt and series peaking circuit. If both circuits are separated by a buffer amplifier, the analysis is simplified. Basically, this was considered by *S. Butterworth* in his article *On the Theory of Filter Amplifiers* in the review *Experimental Wireless & the Wireless Engineer* in 1930 [Ref. 4.6]. When writing the article, which Butterworth wrote when he was serving in the British Navy, he obviously did not expect that his technique might also be applied to wideband amplifiers. In general his article became the basis for filter design for generations of engineers up to the present time.

The basic Butterworth equation, which, besides to filters, can also be applied to wideband amplifiers, either with a single or many stages, is:

$$F(\omega) = \frac{1}{1 + j\,(\omega/\omega_{\mathrm{H}})^{n}} \tag{4.3.1}$$

where $\omega_{\mathrm{H}}$ is the upper half power frequency of the (peaking) amplifier and $n$ is an integer, representing the number of stages. A network corresponding to this equation has a maximally flat amplitude response (MFA). The magnitude of $F(\omega)$ is:

$$\boxed{|F(\omega)| = \frac{1}{\sqrt{1 + (\omega/\omega_{\mathrm{H}})^{2\,n}}}} \tag{4.3.2}$$

The magnitude derivative, $d\big|F(\omega)\big|/d\omega$ is zero at $\omega = 0$:

$$\frac{d\big|F\,(\omega)\big|}{d\,\omega} = \frac{-\,n\,(\omega/\omega_{\mathrm{H}})^{2n-1}}{[1 + (\omega/\omega_{\mathrm{H}})^{2n}]^{3/2}} \cdot \frac{1}{\omega_{\mathrm{H}}} = 0 \Bigg|_{\omega\,=\,0} \tag{4.3.3}$$

and not just the first derivative, but all the $n - 1$ derivatives of an $n^{\mathrm{th}}$-order system are also zero at origin. This means that at very low frequencies ($\omega \ll \omega_{\mathrm{H}}$) the filter is essentially flat. The number of poles in Eq. 4.3.1 is equal to the parameter $n$ and the flatness of the frequency response in the passband also increases with $n$. The parameter $n$ is called the *system order*. To derive the expression for the poles we start with the denominator of Eq. 4.3.2, where the expression under the root can be simplified into:

$$1 + (\omega/\omega_{\mathrm{H}})^{2\,n} = 1 + s^{2\,n} \tag{4.3.4}$$

Whenever this expression is equal to zero, we have a pole, $F(j\omega) \rightarrow \pm\,\infty$. Thus:

$$1 + s^{2\,n} = 0 \qquad \text{or} \qquad s^{2\,n} = -1 \tag{4.3.5}$$

The roots of these equations are the poles of Eq. 4.3.1 and they can be calculated by the following general expression:

$$s = \sqrt[2n]{-1} \tag{4.3.6}$$

We solve this equation using *De Moivre*'s formula [Ref. 4.7]:

$$-1 = \cos(\pi + 2\pi q) + j\sin(\pi + 2\pi q) \tag{4.3.7}$$

where $q$ is either zero or a positive integer. Consequently the poles are:

$$\begin{aligned} s_q &= \sqrt[2n]{-1} = \sqrt[2n]{\cos(\pi + 2\,\pi\, q) + j\sin(\pi + 2\,\pi\, q)} \\ &= \cos\left(\pi\,\frac{1+2\,q}{2\,n}\right) + j\sin\left(\pi\,\frac{1+2\,q}{2\,n}\right) \end{aligned} \tag{4.3.8}$$

If we insert the value $0, 1, 2, \ldots, (2n-1)$ for $q$, we obtain $2n$ roots. The roots lie on a circle of radius $r = 1$, spaced by the angles $\pi/2n$. With this condition no pole is repeated and none of the poles lies on the imaginary axis. One half ( $= n$) of the poles lie in the left side of the $s$-plane; these are the poles of Eq. 4.3.1. The other half of the poles lie in the positive half of the $s$-plane and they can be associated with the complex conjugate of $F(j\omega)$; as shown in Fig. 4.3.1, owing to the Hurwitz stability requirement, they are not useful for our purpose.

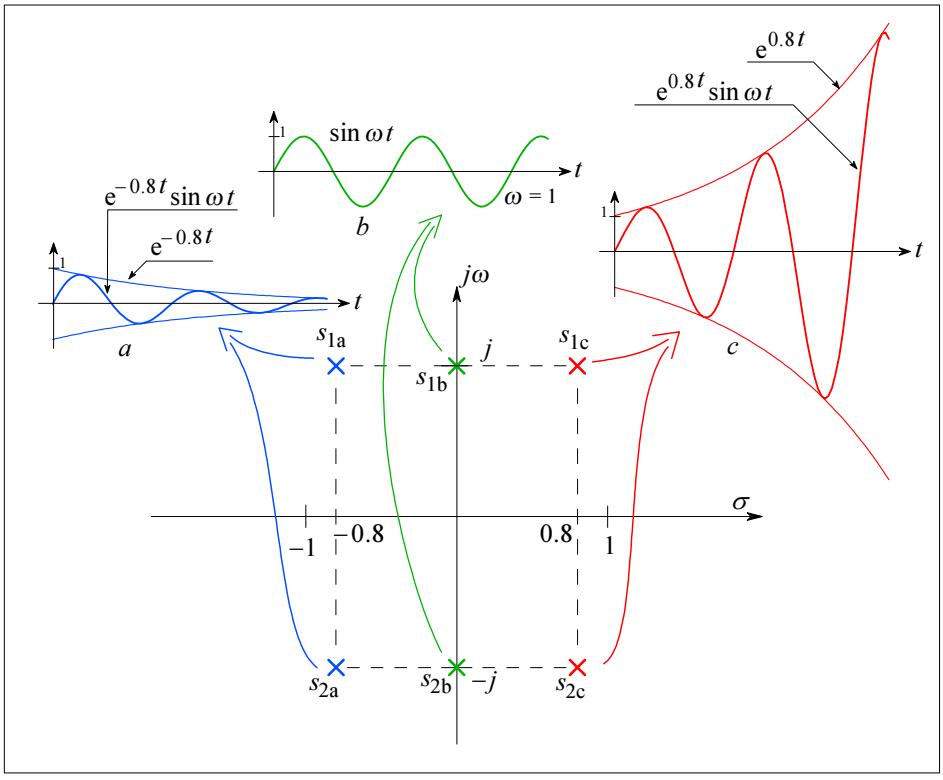


**Fig. 4.3.1:** Impulse response of three different complex conjugate pole pairs: The real part determines the system stability: $s_{1a}$ and $s_{2a}$ make the system unconditionally stable, since the negative exponent forces the response to decrease with time; $s_{1b}$ and $s_{2b}$ make the system conditionally stable, whilst $s_{1c}$ and $s_{2c}$ make it unstable.

This left- and right-half pole division is not arbitrary, but, as we have explained in Part 1, it reflects the direction of energy flow. If an unconditionally stable system is energized and then left alone, it will eventually dissipate all the energy into heath and RF radiation, so it is lost (from the system point of view) and therefore we agree to give it a negative sign. This is typical of a dominantly resistive systems. On the other hand, generators produce energy and we agree to give them a positive sign. In effect, generators can be treated as negative resistors. Inductances and capacitances can not dissipate energy, they can only store it in their associated electromagnetic fields (for a while). We therefore assign the resistive and generative action to the real axis, and the inductive and capacitive action to the imaginary axis.

For example, if we take a two–pole system with poles forming a complex conjugate pair, $s_1 = \sigma + j\omega$ and $s_2 = \sigma - j\omega$, the system impulse response function has the form:

$$f(t) = \mathrm{e}^{\sigma t} \sin \omega t \tag{4.3.9}$$

By referring to Fig. 4.3.1, let us first consider the poles $s_{1a} = -0.8 + j$ and $s_{2a} = -0.8 - j$, where $\omega = 1$. Their impulse function is a damped sinusoid:

$$f(t) = \mathrm{e}^{-0.8 t} \sin \omega t \tag{4.3.10}$$

This means that for any impulse disturbance the system reacts with a sinusoidal oscillation (governed by $\omega$), exponentially damped (by the rate set by $\sigma$). Such behavior is typical for an unconditionally stable system. But if we move the poles to the imaginary axis ($\sigma = 0$) so that $s_{1b} = j$ and $s_{2b} = -j$ (again, $\omega = 1$), then, since there is no damping ($\mathrm{e}^0 = 1$), an impulse excites the system into a continuous sine wave:

$$f(t) = \sin \omega t \tag{4.3.11}$$

If we push the poles further to the right side of the $s$ plane, so that $s_{1c} = 0.8 + j$ and $s_{2c} = 0.8 - j$, keeping $\omega = 1$, the slightest impulse disturbance, or even just the system's own noise, excites an exponentially rising sine wave:

$$f(t) = \mathrm{e}^{0.8 t} \sin \omega t \tag{4.3.12}$$

The poles on the imaginary axis are characteristic of a sine wave oscillator, in which we have the active components (amplifiers) set to make up for (and exactly match) any energy lost in resistive components. The poles on the right side of the $s$-plane also result in oscillations, but there the final amplitude is limited by the system power supply voltages. Because the active components provide much more energy than the system is capable of dissipating thermally, the top and bottom part of the waveform will be saturated, thus limiting the energy produced. Since we are interested in the design of amplifiers and not of oscillators, we shall not use the last two kinds of poles.

Let us return to the Butterworth poles. We want to find the general expression for $n$ poles on the left side of the $s$-plane. A general expression for a pole $s_q$, derived from Eq. 4.3.8 is:

$$s_q = \cos \theta_q + \sin \theta_q \tag{4.3.13}$$

where:

$$\theta_q = \pi \frac{1 + 2q}{2n} \tag{4.3.14}$$

The poles with the angle:

$$\frac{\pi}{2} < \theta_q < \frac{3\,\pi}{2} \tag{4.3.15}$$

lie in the left side of the $s$-plane. If we multiply Eq. 4.3.8 by $j$, we rotate it by $+\pi/2$, achieving the condition expressed in Eq. 4.3.15 for the first $n$ poles:

$$s_q = -\sin\pi\,\frac{1+2\,q}{2\,n} + j\cos\pi\,\frac{1+2\,q}{2\,n} \tag{4.3.16}$$

The parameter $q$ is an integer from $0, 1, \ldots, (n-1)$. We would prefer to have the poles starting with $1$ and ending with $n$. To do so, we introduce a new parameter $k = q + 1$ and consequently $q = k - 1$. With this, we arrive to the final expression for Butterworth poles:

$$\boxed{s_k = \sigma_k + j\,\omega_k = -\sin\pi\,\frac{2\,k-1}{2\,n} + j\cos\pi\,\frac{2\,k-1}{2\,n}} \tag{4.3.17}$$

where $k$ is an integer from $1$ to $n$. As shown in Fig. 4.3.2 (for $n = 1$–$5$), all these poles lie on a semicircle with the radius $r = 1$ in the left half of the $s$-plane:

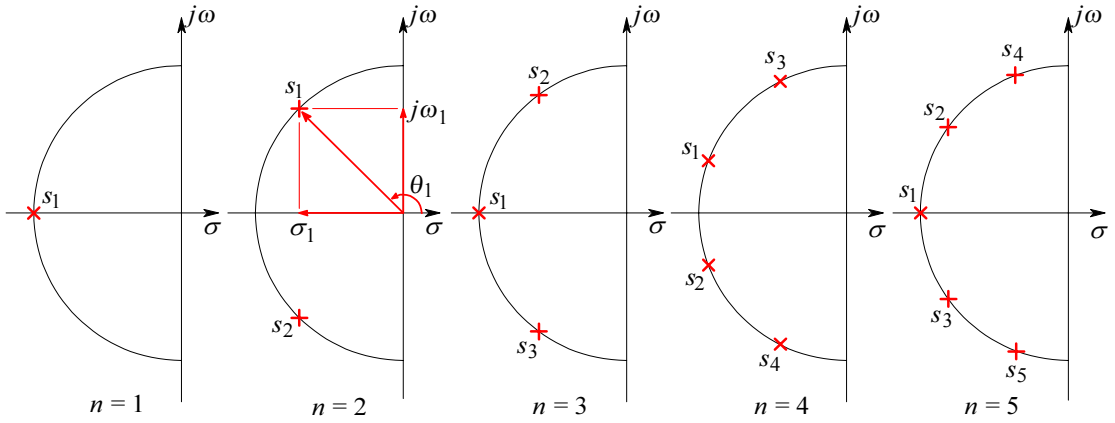


**Fig. 4.3.2:** Butterworth poles for the system order $n = 1$–$5$.

The numerical values of the poles for systems of order $n = 1$–$10$, together with the corresponding angle $\theta$, are listed in Table 4.3.1. Obviously, if $n$ is even the system has complex conjugate pole pairs only. If the $n$ is odd, one of the poles is real, and in the normalized presentation its value is $s_1 = -\omega/\omega_H = -1$. In the non-normalized form, the value of the real pole is equal to $-\omega_H$. Since this is the radius of the circle on which all the poles lie, we can calculate the upper half power frequency also from any pole (for Butterworth poles only!):

$$\boxed{\omega_H = |s_i| = \sqrt{\sigma_i^2 + \omega_i^2}} \tag{4.3.18}$$

or, when one of the poles ($s_1 = \sigma_1$) is real:

$$\boxed{\omega_H = -\sigma_1} \tag{4.3.19}$$

### 4.3.1 Frequency Response

The normalized frequency response magnitude plots, expressed by Eq. 4.3.2, with $\omega_H = 1$ and for $n = 1$–$10$, are drawn in Fig. 4.3.3. Evidently the passband's flatness increases with increasing $n$.

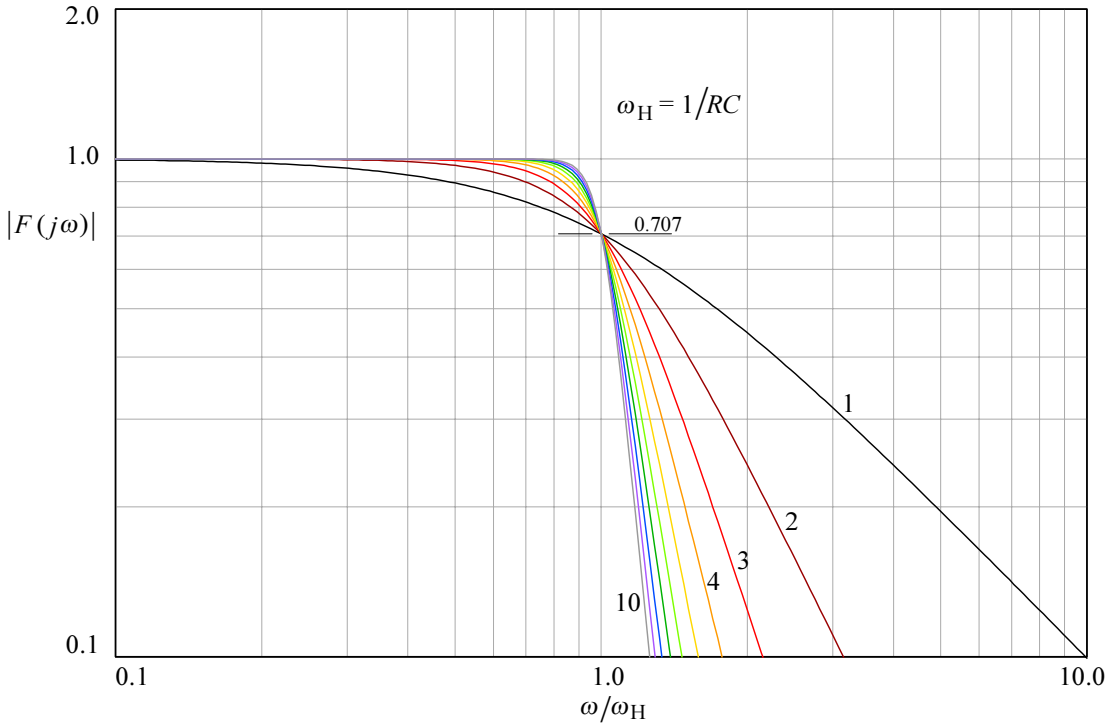


**Fig. 4.3.3:** Frequency response magnitude of $n^{th}$-order system with Butterworth poles, $n = 1$–$10$.

We can write the frequency response of an amplifier with Butterworth poles of order, say, $n = 5$, in three different ways. The general expression with poles is:

$$F_5(s) = \frac{(-1)^5\, s_1\, s_2\, s_3\, s_4\, s_5}{(s - s_1)(s - s_2)(s - s_3)(s - s_4)(s - s_5)} \tag{4.3.20}$$

with $s = j\omega/\omega_H$ and $s_i = \sigma_i + j\omega_i$ (the values of $\sigma_i$ and $\omega_i$ are listed in Table 4.3.1). By multiplying all the expressions in parentheses, we obtain:

$$F_5(s) = \frac{a_0}{s^5 + a_4\, s^4 + a_3\, s^3 + a_2\, s^2 + a_1\, s + a_0} \tag{4.3.21}$$

where:

$$\begin{aligned}
a_4 &= -s_1 - s_2 - s_3 - s_4 - s_5 \\
a_3 &= s_1\, s_2 + s_1\, s_3 + s_1\, s_4 + s_1\, s_5 + s_2\, s_3 + s_2\, s_4 + s_2\, s_5 + s_3\, s_4 + s_3\, s_5 + s_4 s_5 \\
a_2 &= -s_1\, s_2\, s_3 - s_1\, s_2\, s_4 - s_1\, s_2\, s_5 - s_2\, s_3\, s_4 - s_2\, s_3\, s_5 - s_3\, s_4\, s_5 \\
a_1 &= s_2\, s_3\, s_4\, s_5 + s_1\, s_3\, s_4\, s_5 + s_1\, s_2\, s_4\, s_5 + s_1\, s_2\, s_3\, s_5 + s_1\, s_2\, s_3\, s_4 \\
a_0 &= -s_1\, s_2\, s_3\, s_4\, s_5
\end{aligned} \tag{4.3.22}$$

If we use the normalized poles with the numerical values listed in Table 4.3.1 to calculate the coefficients $a_0 \ldots a_4$, we obtain:

$$F_5(s) = \frac{1}{s^5 + 3.2361\,s^4 + 5.2361\,s^3 + 5.2361\,s^2 + 3.2361\,s + 1} \tag{4.3.23}$$

For the magnitude only, by applying Eq. 4.3.2, we have:

$$|F_5(\omega)| = \frac{1}{\sqrt{1 + (\omega/\omega_\mathrm{H})^{10}}} \tag{4.3.24}$$

The reason why we took particular interest for the function with the normalized numerical values of the order $n = 5$ is that in Sec. 4.5 we shall compare it with the function having Bessel poles of the same order.

### 4.3.2 Phase response

The general expression for the phase angle is:

$$\varphi = \sum_{\mathrm{i}=1}^{n} \arctan \frac{\dfrac{\omega}{\omega_\mathrm{H}} + \omega_\mathrm{i}}{\sigma_\mathrm{i}} \tag{4.3.25}$$

For an odd number of poles the imaginary part of the middle pole $\omega_{n/2+1} = 0$. For the remaining poles or in the case of even $n$, we enter the complex conjugate pair components: $s_{\mathrm{i},n-\mathrm{i}+1} = \sigma_\mathrm{i} \pm j\,\omega_\mathrm{i}$. The phase response plots are drawn in Fig. 4.3.4. By comparing it with Fig. 4.1.4 we note that Butterworth poles result in a much steeper phase slope near the system's cut off frequency at $\omega = \omega_\mathrm{H}$ (which is even more evident in the envelope delay).

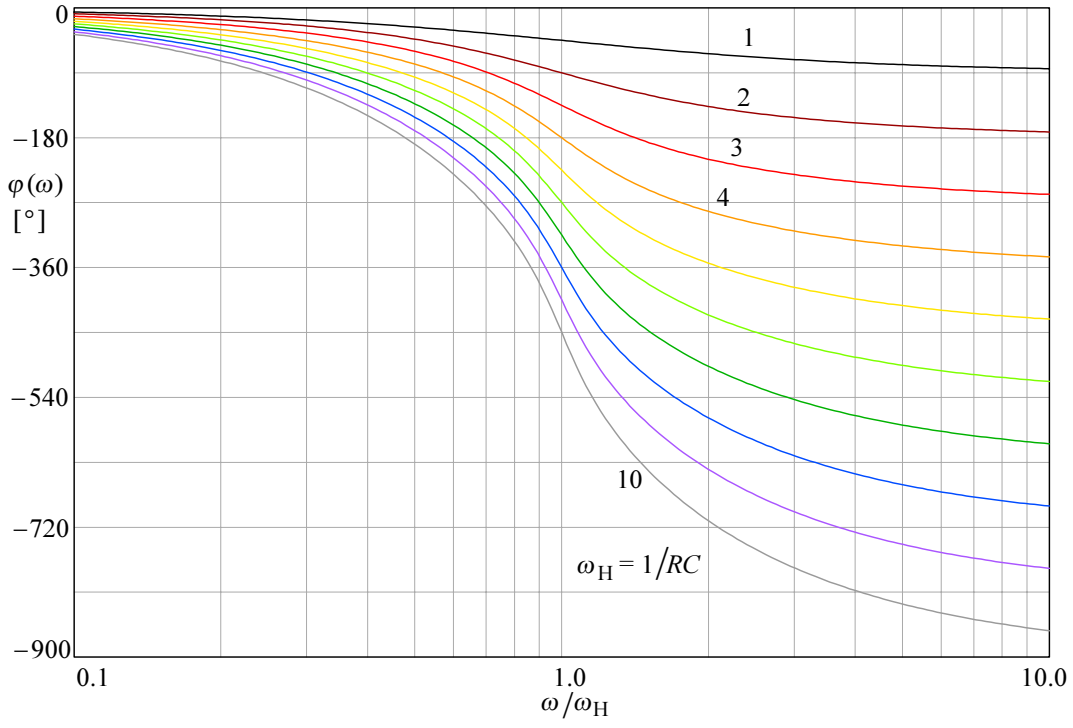


**Fig. 4.3.4:** Phase angle of $n^{\mathrm{th}}$-order system with Butterworth poles, $n = 1$–$10$.

### 4.3.3 Envelope Delay

We obtain the expressions for envelope delay by making a frequency derivative of Eq. 4.3.25:

$$\tau_e\,\omega_H = \sum_{i=1}^{n} \frac{\sigma_i}{\sigma_i^2 + \left(\frac{\omega}{\omega_H} + \omega_i\right)^2} \tag{4.3.26}$$

The envelope delay plots for $n = 1$–$10$ are shown in Fig. 4.3.5. Owing to the ever steeper phase shift, the curves for $n > 1$ dip around the system cut off frequency. Those frequencies are delayed more than the rest of the spectrum, thus revealing the system resonance on transients. Therefore we expect that amplifiers with Butterworth poles will exhibit an increasing amount of ringing in the step response, a property not acceptable in pulse amplification.

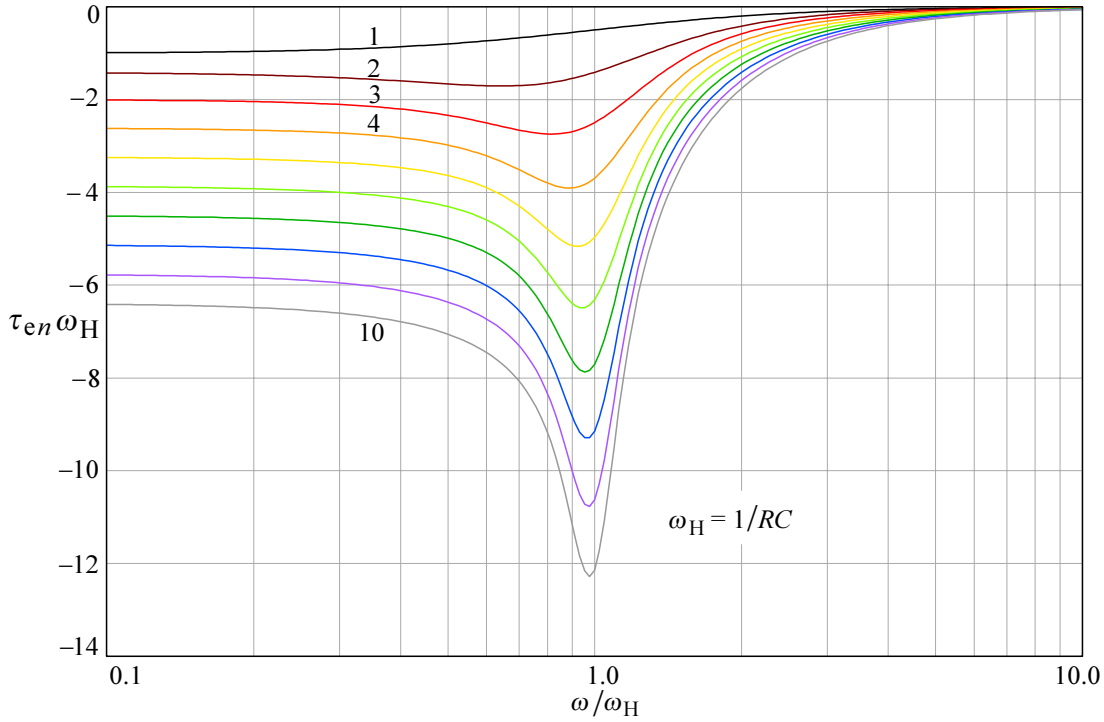


**Fig. 4.3.5:** Envelope delay of $n^{th}$-order system with Butterworth poles, $n = 1$–$10$.

### 4.3.4 Step Response

Since we have $n$ non-repeating poles we start with the frequency function in the form which is suitable for the $\mathcal{L}^{-1}$ transform:

$$F(s) = \frac{(-1)^n s_1 s_2 \cdots s_n}{(s - s_1)(s - s_2)\cdots(s - s_n)} \tag{4.3.27}$$

We multiply this by the unit step operator $1/s$ and obtain:

$$G(s) = \frac{(-1)^n s_1 s_2 \cdots s_n}{s\,(s - s_1)(s - s_2)\cdots(s - s_n)} \tag{4.3.28}$$

To obtain the step response in the time domain we use the $\mathcal{L}^{-1}$ transform:

$$g(t) = \mathcal{L}^{-1}\{G(s)\} = \sum_{i=1}^{n} \text{res}_i \frac{(-1)^n s_1 s_2 \cdots s_n \, e^{st}}{s\,(s-s_1)(s-s_2)\cdots(s-s_n)} \qquad (4.3.29)$$

It would take too much space to list the complete analytical calculation for systems with 1 to 10 poles. Some examples can be found in the Appendix 2.3 (one the disk). Here we shall use the computer routines, which we develop and discuss in detail in Part 6. The plots for $n = 1$–10 are shown in Fig. 4.3.6.

These plots confirm our expectation that amplifiers with Butterworth poles are not suitable for pulse amplification. The main advantage of Butterworth poles is the flat frequency response (MFA) in the passband (evident from the plots in Fig. 4.3.3). Therefore for measuring sinusoidal signals in a wide range of frequencies, e.g., in an electronic voltmeter, Butterworth poles offer the best solution.

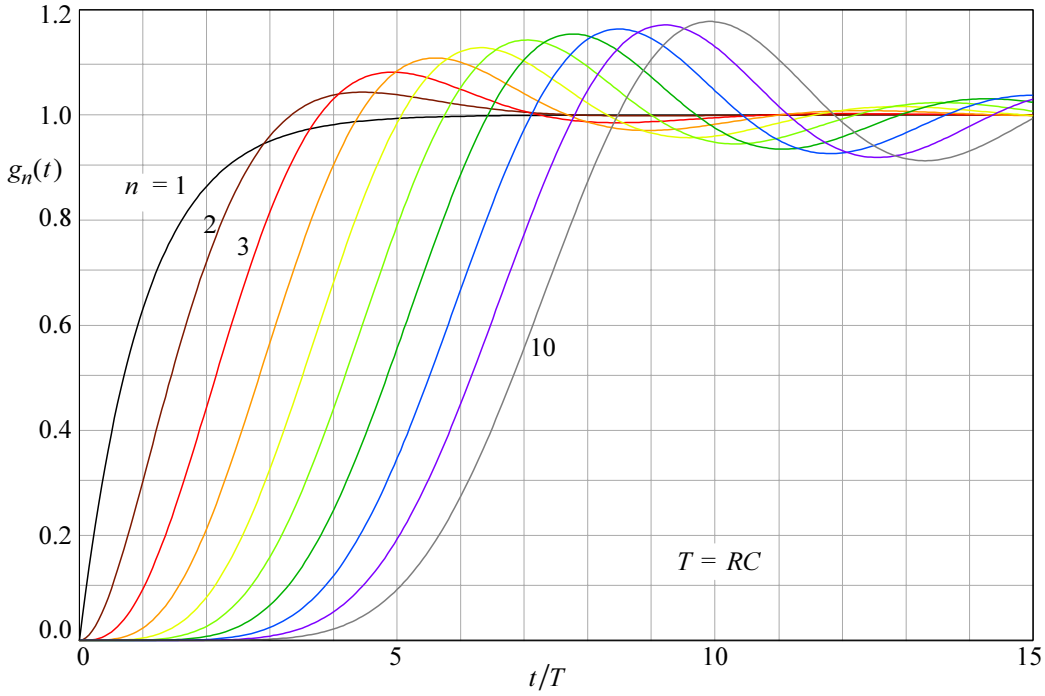


**Fig. 4.3.6:** Step response of $n^{\text{th}}$-order system with Butterworth poles, $n = 1$–10.

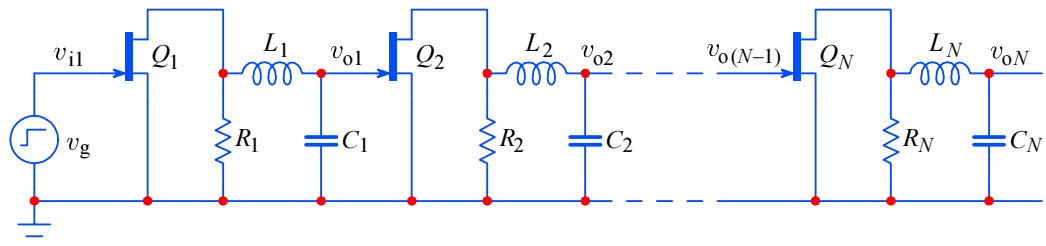


**Fig. 4.3.7:** An example of an amplifier with $N$ shunt peaking stages. Since each stage has one pair of complex conjugate poles the number of stages is equal to one half of the number of poles, $N = n/2$. For odd-order systems one stage (usually the first one) is of a single pole configuration ($L_1 = 0$), and $N = 1 + (n-1)/2$. Of course, instead of the shunt peaking, other peaking networks can be used.

**Table 4.3.1: Butterworth Poles**

| Order $n$ | $\sigma$ [rad/$s$] | $\omega$ [rad/$s$] | $\theta$ [°] |
|---|---|---|---|
| 1 | − 1.0000 | 0.0000 | 180 |
| 2 | − 0.7071 | ± 0.7071 | 180 ∓ 45.0000 |
| 3 | − 1.0000 | 0.0000 | 180 |
| | − 0.5000 | ± 0.8660 | 180 ∓ 60.0000 |
| 4 | − 0.9239 | ± 0.3827 | 180 ∓ 21.5000 |
| | − 0.3827 | ± 0.9239 | 180 ∓ 67.5000 |
| 5 | − 1.0000 | 0.0000 | 180 |
| | − 0.8090 | ± 0.5878 | 180 ∓ 36.0000 |
| | − 0.3090 | ± 0.9511 | 180 ∓ 72.0000 |
| 6 | − 0.9659 | ± 0.2588 | 180 ∓ 15.0000 |
| | − 0.7071 | ± 0.7071 | 180 ∓ 45.0000 |
| | − 0.2588 | ± 0.9659 | 180 ∓ 75.0000 |
| 7 | − 1.0000 | 0.0000 | 180 |
| | − 0.9010 | ± 0.4339 | 180 ∓ 25.7143 |
| | − 0.6235 | ± 0.7818 | 180 ∓ 51.4286 |
| | − 0.2225 | ± 0.9749 | 180 ∓ 77.1429 |
| 8 | − 0.9808 | ± 0.1951 | 180 ∓ 11.2500 |
| | − 0.8315 | ± 0.5556 | 180 ∓ 33.7500 |
| | − 0.5556 | ± 0.8315 | 180 ∓ 56.2500 |
| | − 0.1951 | ± 0.9808 | 180 ∓ 78.7500 |
| 9 | − 1.0000 | 0.0000 | 180 |
| | − 0.9397 | ± 0.3420 | 180 ∓ 20.0000 |
| | − 0.7660 | ± 0.6428 | 180 ∓ 40.0000 |
| | − 0.5000 | ± 0.8660 | 180 ∓ 60.0000 |
| | − 0.1736 | ± 0.9848 | 180 ∓ 80.0000 |
| 10 | − 0.9877 | ± 0.1564 | 180 ∓ 9.0000 |
| | − 0.8910 | ± 0.4540 | 180 ∓ 27.0000 |
| | − 0.7071 | ± 0.7071 | 180 ∓ 45.0000 |
| | − 0.4540 | ± 0.8910 | 180 ∓ 63.0000 |
| | − 0.1564 | ± 0.9877 | 180 ∓ 81.0000 |

Note: in this and all other tables we have arranged the poles in complex conjugate pairs, i.e., $s_{k,n-k+1} = \sigma_k \pm j\,\omega_k$, where $k = 1, 2, \ldots, n$. For $n$ odd the first pole is real.

### 4.3.5 Ideal MFA Filter; Paley–Wiener Criterion

The following discussion will be given in an abridged form, since a complete derivation would detract us too much from the discussion of amplifiers. We are interested in designing an amplifier with the ideal frequency response, maximally flat in the passband and zero outside, as in Fig. 4.3.8 (shown also for negative frequencies), expressed as:

$$A(\omega) = \begin{cases} 1\big|_{|\omega/\omega_H|<1} \\ 0\big|_{|\omega/\omega_H|>1} \end{cases} \tag{4.3.30}$$

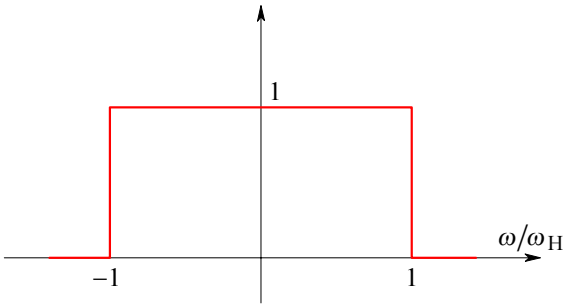


**Fig. 4.3.8:** Ideal MFA frequency response.

For the time being we assume that the function $A(\omega)$ is real, and consequently it has no phase shift. At the instant $t = 0$ we apply a unit step voltage to the input of the amplifier (multiply $A(s)$ by the unit step operator $1/s$). By applying the basic formula for the $\mathcal{L}^{-1}$ transform (Part 1, Eq. 1.4.4), the output function in the time domain is the integral of the $\sin(t)/t$ function [Ref. 4.2]:

$$\boxed{g(t) = \frac{1}{\pi}\int_{-\infty}^{t} \frac{\sin t}{t}\, dt} \tag{4.3.31}$$

The normalized plot of this integral is shown in Fig. 4.3.9. Here we have 50% of the signal amplitude at the instant $t = 0$. Also, there is some response for $t < 0$, before we applied any step voltage to the amplifier input, which is impossible. Any physically realizable amplifier would have some phase shift and an envelope delay, therefore the step response would be shifted rightwards from the origin. However, an infinite phase shift and delay would be needed in order to have no response for time $t < 0$.

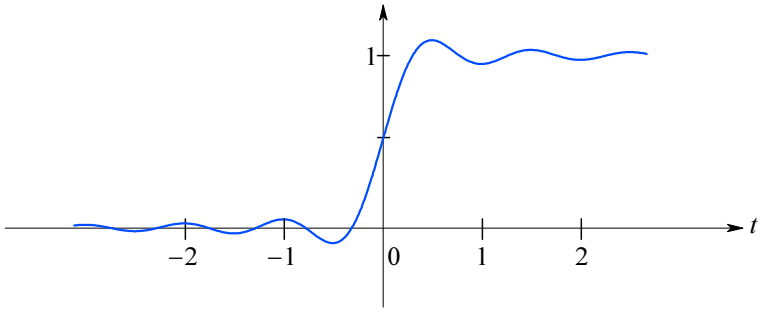


**Fig. 4.3.9:** Step response of a network having the ideal frequency response of Fig. 4.3.8.

What we would like to know is whether there is any phase response, linear or not, which the amplifier should have in order to suit Eq. 4.3.30 without any response for time $t < 0$. The answer is negative and it was proved by *R.E.A.C. Paley* and *N. Wiener*. Their criterion is given by an amplitude function [Ref. 4.2]:

$$\int_{-\infty}^{\infty} \frac{\left|\log A(\omega)\right|}{1+\omega^2}\, d\omega < \infty \tag{4.3.32}$$

Outside the range $-\omega_H < \omega < \omega_H$, $A(\omega) = 0$, as required by Eq. 4.3.30, but the magnitude in the numerator is infinite ($|\log 0| = \infty$); therefore the condition expressed by Eq. 4.3.32 is not met. Thus it is not possible to make an amplifier with a continuous infinite attenuation in a certain frequency band (it is, nevertheless, possible to have an infinite attenuation, but at **distinct** frequencies only). As we can derive from Eq. 4.3.32, the problem is not the steepness of the frequency response curve at $\omega_H$ in Fig. 4.3.8, but the requirement for an infinite attenuation everywhere outside the defined passband $-\omega_H < \omega < \omega_H$.

If we allow that outside the passband $A(\omega) = \epsilon$, no matter how small $\epsilon$ is, such a frequency response is possible to achieve. In this case the corresponding phase response must be [Ref. 4.2]:

$$\varphi(\omega) = \ln|\epsilon| \cdot \ln\left|\frac{1+\omega}{1-\omega}\right| \tag{4.3.33}$$

However, such an amplifier would still have a step response very similar to that in Fig. 4.3.9, except that it would be shifted rightwards and there would be no response for $t < 0$. This is because we have almost entirely (down to $\epsilon$) and suddenly cut the signal spectrum above $\omega_H$. The overshoot is approximately 9 %. We have met a similar situation in Part 1, Fig.1.2.7.a,b in connection with the square wave when we were discussing the *Gibbs*' phenomenon [Ref. 4.2].

Some readers may ask themselves why the step response overshoot of some systems with Butterworth poles in Fig. 4.3.6 exceeds 9%? The reason is the corresponding nonlinear phase response, resulting in a peak in the envelope delay, as shown in Fig. 4.3.5. This is a characteristic of not just the Butterworth poles, but also of any pole pattern, e.g., Chebyshev Type I and Elliptic (Cauer) systems, for which the magnitude and phase change more steeply near the cut off frequency.

We shall use Eq. 4.3.32 again when we shall discuss the possibility of obtaining the ideal Gaussian response of an amplifier.

(blank page)

## 4.4 Derivation of Bessel Poles for MFED Response

If we want to preserve the waveform shape, the amplifier must pass all frequency components with the same delay. From the requirement for a constant delay we can derive the system poles. The frequency response function having a constant delay $T$ [Ref. 4.8, 4.9] is of the form:

$$F(s) = \mathrm{e}^{-sT} \tag{4.4.1}$$

Let us normalize this expression by choosing a unit delay, $T = 1$. It is possible to approximate $\mathrm{e}^{-s}$ by a rational function, where the denominator is a polynomial and all its roots (the poles of $F(s)$) lie in the left half of the $s$-plane. In this case the denominator is a so called *Hurwitz polynomial* [Ref. 4.10]. The approximation then fulfills the constant delay condition expressed by Eq. 4.4.1 to a certain accuracy only up to a certain frequency. The higher the polynomial degree, the higher is the accuracy.

We can write $\mathrm{e}^{-s}$ also by using the hyperbolic sine and cosine functions:

$$F(s) = \frac{1}{\sinh s + \cosh s} = \frac{\dfrac{1}{\sinh s}}{1 + \dfrac{\cosh s}{\sinh s}} \tag{4.4.2}$$

Both hyperbolic functions can be expressed with their corresponding series:

$$\cosh s = 1 + \frac{s^2}{2!} + \frac{s^4}{4!} + \frac{s^6}{6!} + \frac{s^8}{8!} + \cdots \tag{4.4.3}$$

$$\sinh s = s + \frac{s^3}{3!} + \frac{s^5}{5!} + \frac{s^7}{7!} + \frac{s^9}{9!} + \cdots \tag{4.4.4}$$

With these suppositions and using ‘long division’ we obtain:

$$\frac{\sinh s}{\cosh s} = \frac{1}{s} + \cfrac{1}{\dfrac{3}{s} + \cfrac{1}{\dfrac{5}{s} + \cfrac{1}{\dfrac{7}{s} + \cfrac{1}{\dfrac{9}{s} + \cdots}}}} \tag{4.4.5}$$

With a successive multiplication we can simplify this continuous fraction into a simple rational function. By truncating the fraction at $9/s$ we obtain the following approximation:

$$\frac{\sinh s}{\cosh s} \approx \frac{15\,s^4 + 420\,s^2 + 945}{s^5 + 105\,s^3 + 945\,s} \tag{4.4.6}$$

Now we put this and Eq. 4.4.4 into Eq. 4.4.2 and perform the suggested division by $\sinh s$. A normalized expression, where $F(s) = 1$ if $s = 0$ is obtained by multiplying the numerator by 945. With these operations we obtain:

$$F(s) = \mathrm{e}^{-s} \approx \frac{945}{s^5 + 15\,s^4 + 105\,s^3 + 420\,s^2 + 945\,s + 945} \tag{4.4.7}$$

The poles of this equation are the roots of the denominator:

$$\begin{aligned} s_{1,2} &= -3.3520 \pm j\,1.7427 \\ s_{3,4} &= -2.3247 \pm j\,3.5710 \\ s_{5} &= -3.6467 \end{aligned}$$

A critical reader might ask why have we taken such a circuitous way to come to this result instead of deriving it straight from *McLaurin*'s series as:

$$\mathrm{e}^{-s} = \frac{1}{\mathrm{e}^{s}} \approx \frac{1}{1 + s + \frac{s^2}{2!} + \frac{s^3}{3!} + \frac{s^4}{4!} + \frac{s^5}{5!}} \tag{4.4.8}$$

In this case the roots are:

$$\begin{aligned} s_{1,2} &= -1.6496 \pm j\,1.6936 \\ s_{3,4} &= +0.2898 \pm j\,3.1283 \\ s_{5} &= -2.1806 \end{aligned}$$

and the roots $s_{3,4}$ lie in the **right half** of the $s$-plane. Therefore the denominator of Eq. 4.4.8 is not a Hurwitz polynomial [Ref. 4.10] (a closer investigation would reveal that the denominator is not a Hurwitz polynomial if its degree exceeds 4, but even for low order systems it can be shown that the McLaurin's series results in an envelope delay which is far from being maximally flat). Thus Eq. 4.4.8 describes an unstable system or an unrealizable transfer function.

Let us return to Eq. 4.4.7, which we express in a general form:

$$\boxed{F(s) = \frac{a_0}{s^n + a_{n-1}s^{n-1} + \cdots + a_2\,s^2 + a_1\,s + a_0}} \tag{4.4.9}$$

where the numerical values for the coefficients can be calculated by the equation:

$$\boxed{a_i = \frac{(2\,n - i)!}{2^{n-i}\,i!\,(n-i)!}} \tag{4.4.10}$$

We can express the ratio of hyperbolic functions also as:

$$\frac{\cosh s}{\sinh s} = \frac{J_{-1/2}\,(-j\,s)}{j\,J_{1/2}\,(j\,s)} \tag{4.4.11}$$

where $J_{-1/2}\,(-j\,s)$ and $j\,J_{1/2}\,(j\,s)$ are the spherical Bessel functions [Ref. 4.10, 4.11]. Therefore we name the polynomials having their coefficients expressed by Eq. 4.4.10 *Bessel polynomials*. Their roots are the poles of Eq. 4.4.9 and we call them *Bessel poles*. We have listed the values of Bessel poles for polynomials of order $n = 1$–$10$ in Table 4.4.1, along with the corresponding pole angles $\theta_i$.

We usually express Eq. 4.4.9 in another normalized form which is suitable for the $\mathcal{L}^{-1}$ transform:

$$F(s) = \frac{(-1)^n s_1\, s_2\, s_3 \cdots s_n}{(s - s_1)(s - s_2)(s - s_3) \cdots (s - s_n)} \tag{4.4.12}$$

where $s_1$, $s_2$, $s_3$, …, $s_n$ are the poles of the function $F(s)$.

In Sec. 4.3 we saw that Butterworth poles lie in the left half of the $s$-plane on an origin centered unit circle. Since the denominator of Eq. 4.4.12 is also a Hurwitz polynomial [Ref. 4.10], all the poles of this equation must also lie in the left half of the $s$-plane. This is evident from Fig. 4.4.1, where the Bessel poles of the order $n = 1$–$10$ are drawn. However, Bessel poles lie on ellipses (not on circles). The characteristics of this family of ellipses is that they all have the near focus at the origin of the complex plane and the other focus on the positive real axis.

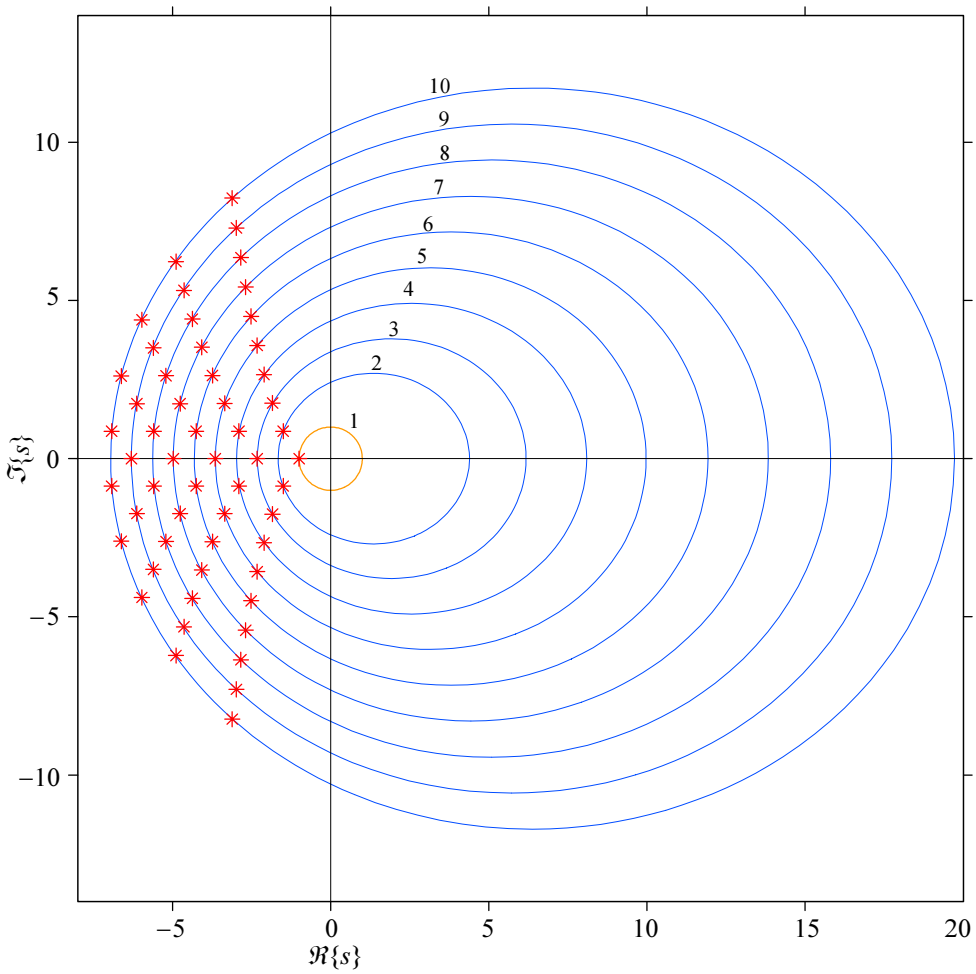


**Fig. 4.4.1:** Bessel poles for order $n = 1$–$10$. Bessel poles lie on a family of ellipses with one focus at the origin of the complex plane and the other focus on the positive real axis. The first-order pole is the same as for the Butterworth system and lies on the unit circle.

To implement these poles in a practical amplifier, the same circuit of Fig. 4.3.7, which we have used for Butterworth poles, can also be used for Bessel poles. Here too, instead of the shunt peaking shown, other, more efficient peaking networks can be used.

### 4.4.1 Frequency Response

A general normalized expression for the frequency response is the magnitude (absolute value) of Eq. 4.4.12:

$$\left|F(s)\right| = \left| \frac{s_1\, s_2\, s_3 \cdots s_n}{(s-s_1)(s-s_2)(s-s_3)\cdots(s-s_n)} \right|_{s\,=\,j\omega/\omega_\mathrm{h}} \tag{4.4.13}$$

where $\omega_\mathrm{h} = 1/RC$ is the non-peaking stage cut off frequency. If we put the numerical values for poles $s_\mathrm{i} = \sigma_\mathrm{i} \pm j\omega_\mathrm{i}$ and $s = j\omega/\omega_\mathrm{h}$ as suggested, then this formula obtains a form similar to Part 2, Eq. 2.6.10 (where we had 4 poles only).

The magnitude plots for $n = 1$–$10$ are shown in Fig. 4.4.2. By comparing this figure with Fig. 4.3.3, where the frequency response curves for Butterworth poles are displayed, we note an important difference: for Butterworth poles the upper half power frequency is always 1, regardless of the number of poles. In contrast, for Bessel poles the upper half power frequency increases with $n$.

The reason for the difference is that the derivation of $n$ Butterworth poles was based on $\sqrt[2n]{-1}$ (for magnitude), whilst the Bessel poles were derived from the condition for a unit envelope delay. This difference prevents any direct comparison of the bandwidth extension and the rise time improvement between both kinds of poles. To be able to compare the two types of systems on a fair basis we must normalize the Bessel poles to the first-order cut off frequency. We do this by recursively multiplying the poles by a correction factor and calculate the cut off frequency, until a satisfactory approximation is reached (see Sec. 4.4.6). Also, a special set of Bessel poles is derived in Sec. 4.5, allowing us to interpolate between Bessel and Butterworth poles. The BESTAP algorithm (in Part 6) calculates the Bessel poles in any of the three options.

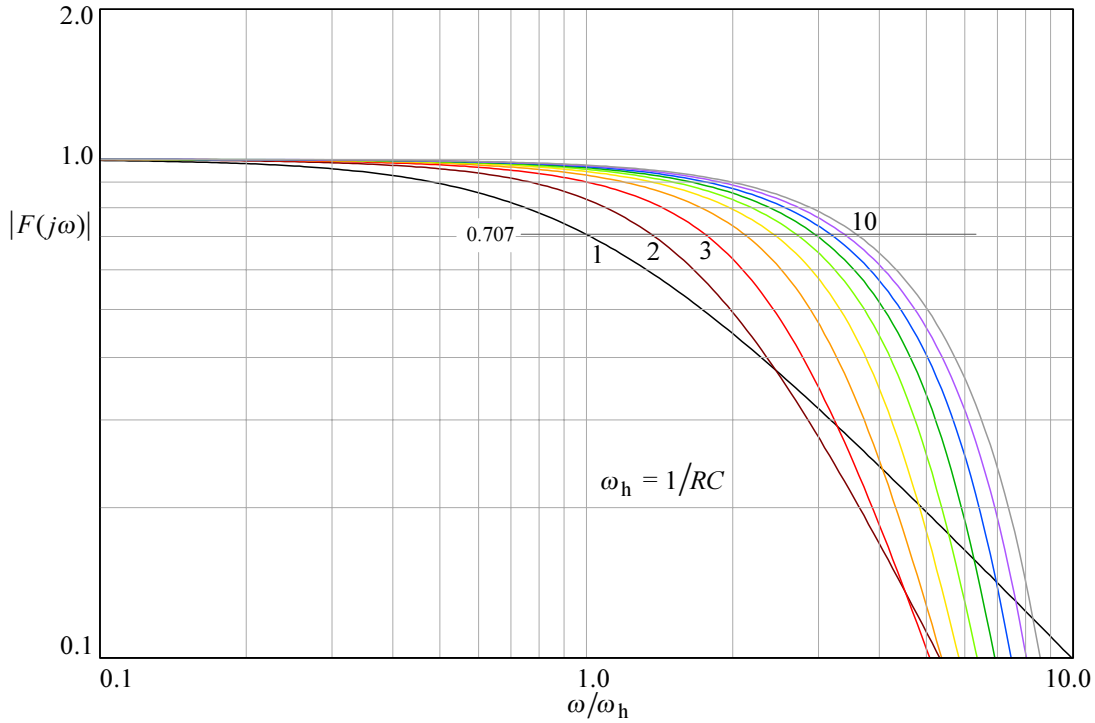


**Fig. 4.4.2:** Frequency-response magnitude of systems with Bessel poles for order $n = 1\ldots10$.

### 4.4.2 Upper Half Power Frequency

To find the cut off frequency and the bandwidth improvement offered by the Bessel poles an inversion formula should be developed from Eq. 4.4.13. This inversion formula would be different for each $n$, so there would not be a general solution. Instead, we shall use a computer program (see Part 6) to calculate the complete frequency response magnitude and find the cut off frequency from it. Calculated in this way, the bandwidth improvement factors $\eta_b = \omega_H/\omega_h$ for Bessel poles of the order $n = 1$–$10$ are listed in the following table:

**Table 4.4.1:** Relative Bandwidth Improvement with Bessel Poles

| $n$ | 1 | 2 | 3 | 4 | 5 | 6 | 7 | 8 | 9 | 10 |
|---|---|---|---|---|---|---|---|---|---|---|
| $\eta_b$ | 1.00 | 1.36 | 1.75 | 2.12 | 2.42 | 2.70 | 2.95 | 3.18 | 3.39 | 3.59 |

However, some special circuits can have a bandwidth improvement different from the one shown in the table for a corresponding order; e.g., T-coil circuits improve the bandwidth for $n = 2$ by exactly twice as much. We shall discuss this in Part 5, where we shall analyze a two-stage amplifier with 7 staggered Bessel poles, having one three-pole T-coil and one four-pole L+T circuit and obtain a total bandwidth improvement $\eta_b = 3.55$ for the complete amplifier.

### 4.4.3 Phase Response

The calculation is similar to the phase response for Butterworth poles; however there we had the normalized upper half power frequency $\omega_H = 1$, whilst for Bessel poles $\omega_H$ increases with the order $n$, so here we must use $\omega_h = 1/RC$ as the reference, where $RC$ is the time constant of the non-peaking amplifier. Then for the phase response we simply repeat Eq. 4.3.25 and write $\omega_h$ (instead of $\omega_H$):

$$\varphi(\omega) = \sum_{i=1}^{n} \arctan \frac{\dfrac{\omega}{\omega_h} + \omega_i}{\sigma_i} \tag{4.4.14}$$

Fig. 4.4.3 shows the phase plots of Eq. 4.4.14 for Bessel poles for the order $n = 1$–$10$ (owing to the cutoff frequency increasing with order $n$, the frequency scale had to be extended to see the asymptotic values at high frequencies).

So far we have used a logarithmic frequency scale for our phase response plots. However, by using a linear frequency scale, as in Fig. 4.4.4, the plots show that the phase response for Bessel poles is linear up to a certain frequency [Ref. 4.10], which increases with an increased order $n$.

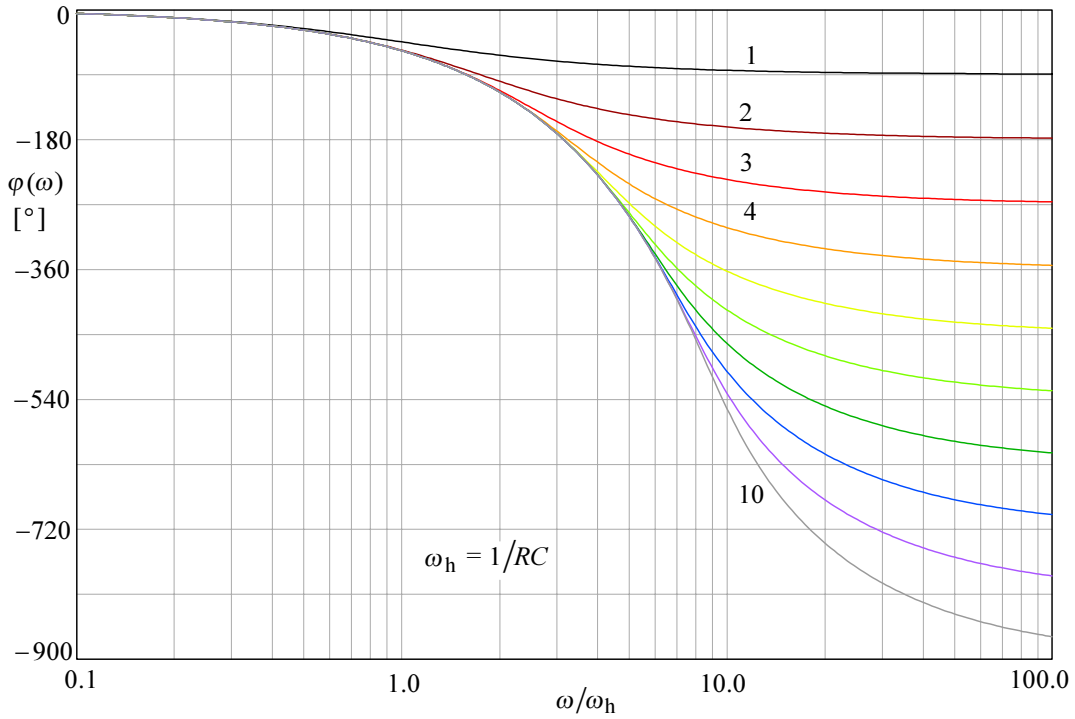


**Fig. 4.4.3:** Phase angle of the systems with Bessel poles of order $n = 1 \ldots 10$.

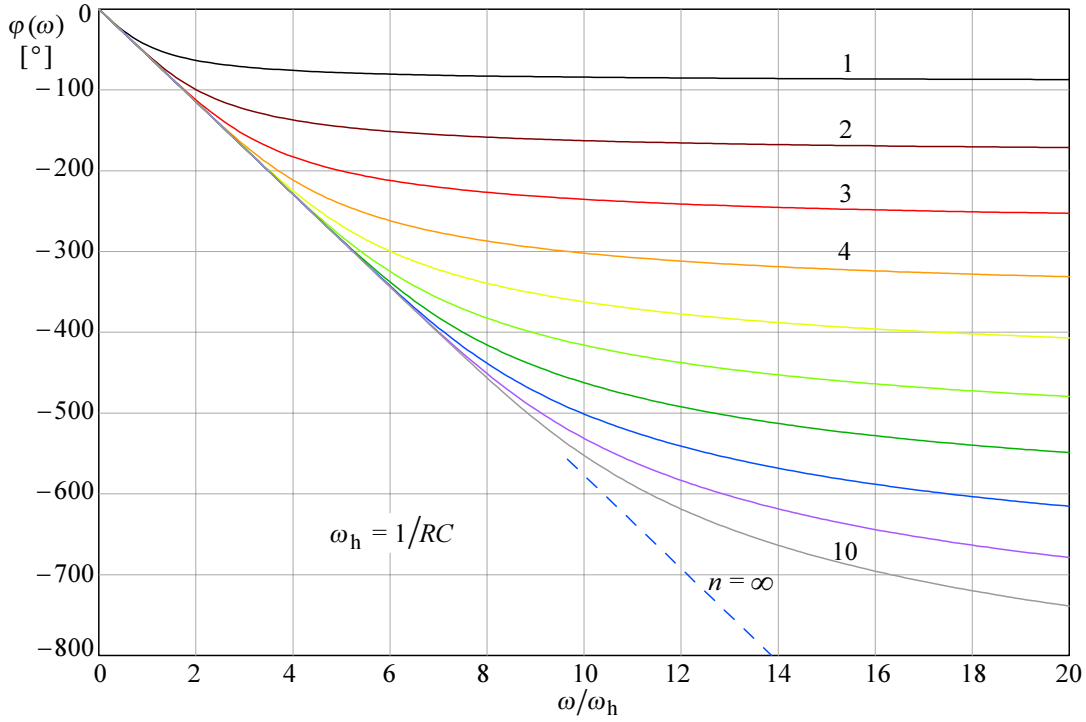


**Fig. 4.4.4:** Phase-angle as in Fig. 4.4.3, but in a linear frequency scale. Note the linear phase frequency-dependence extending from the origin to progressively higher frequencies.

### 4.4.4 Envelope-delay

Here, too, we take the corresponding formula from Butterworth poles and replace the frequency normalization $\omega_H$ by $\omega_h$:

$$\tau_e\,\omega_h = \sum_{i=1}^{n} \frac{\sigma_i}{\sigma_i^2 + \left(\frac{\omega}{\omega_h} + \omega_i\right)^2} \tag{4.4.15}$$

The envelope delay plots are shown in Fig. 4.4.5. The delay is flat up to a certain frequency, which increases with increasing order $n$. This was our goal when we were deriving the Bessel poles, starting with Eq. 4.4.1. Therefore the name MFED (Maximally Flat Envelope Delay) is fully justified by this figure. This property is essential for pulse amplification. Because pulses contain a broad range of frequency components, all of them, (or in practice, the most significant ones, i.e., those which are not attenuated appreciably) should be subject to equal time delay when passing through the amplifier in order to preserve the pulse shape at the output as much as possible.

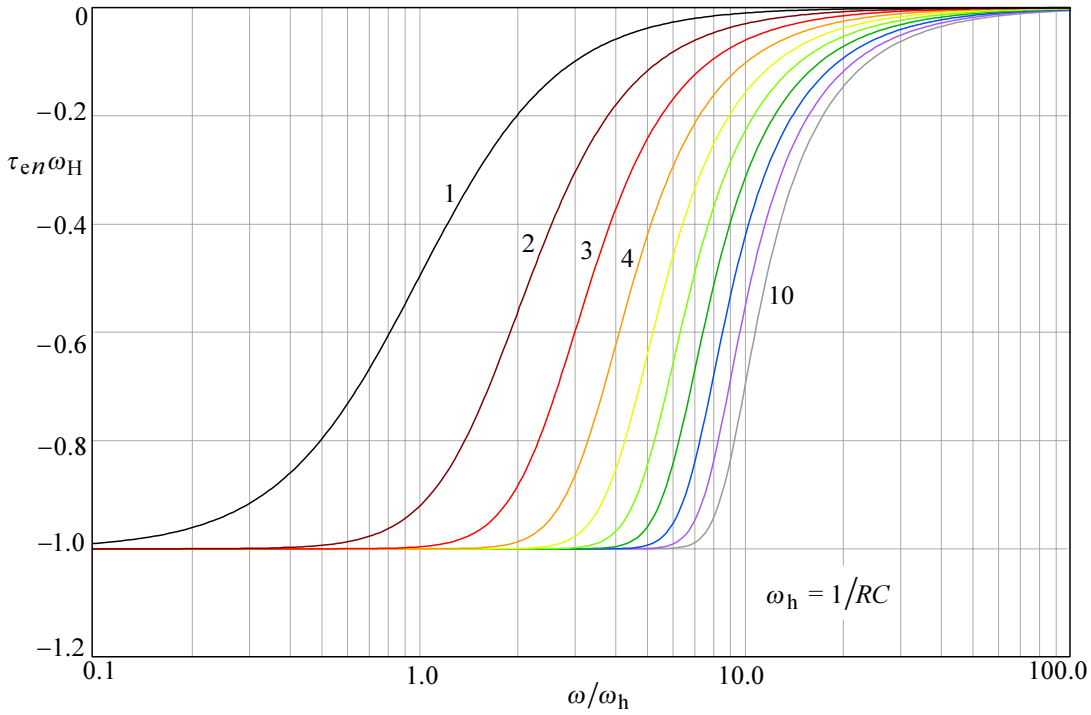


**Fig. 4.4.5:** Envelope delay of the systems with Bessel poles for order $n = 1$–$10$. Note the flat unit delay response increasing with system order. This figure demonstrates the fulfillment of the criterion from which we have started the derivation of MFED.

### 4.4.4 Step Response

We start with Eq. 4.4.12 and multiply it by the unit step operator $1/s$ to obtain:

$$G(s) = \frac{(-1)^n\, s_1\, s_2\, s_3 \cdots s_n}{s\,(s - s_1)(s - s_2)(s - s_3)\cdots(s - s_n)} \tag{4.4.16}$$

By applying the $\mathcal{L}^{-1}$-transform we obtain:

$$g(t) = \mathcal{L}^{-1}\{G(s)\} = \sum_{i=1}^{n} \text{res}_i \frac{(-1)^n\, s_1\, s_2\, s_3 \cdots s_n\, \mathrm{e}^{st}}{s\,(s-s_1)(s-s_2)(s-s_3)\cdots(s-s_n)} \qquad (4.4.17)$$

By inserting the numerical pole values from Table 4.4.3 for the systems of order $n = 1$–10 we can proceed in the same way as in the examples in Appendix 2.3, but it would take too much space. Instead, we shall use the routines developed in Part 6 to generate the plots of Fig. 4.4.6. This diagram is notably different from the step response plots of Butterworth poles in Fig. 4.3.6. Again, the reason is that for normalized Butterworth poles the upper half power frequency $\omega_\text{H}$ is always one, regardless of the order $n$, consequently the step response always has the same maximum slope, but a progressively larger delay. The Bessel poles, on the contrary, have progressively steeper slope, whilst the delay approaches unity. This is also reflected by the improvement in rise time, listed in Table 4.4.2. Of course, the improvement in rise time is even higher for peaking circuits using T-coils.

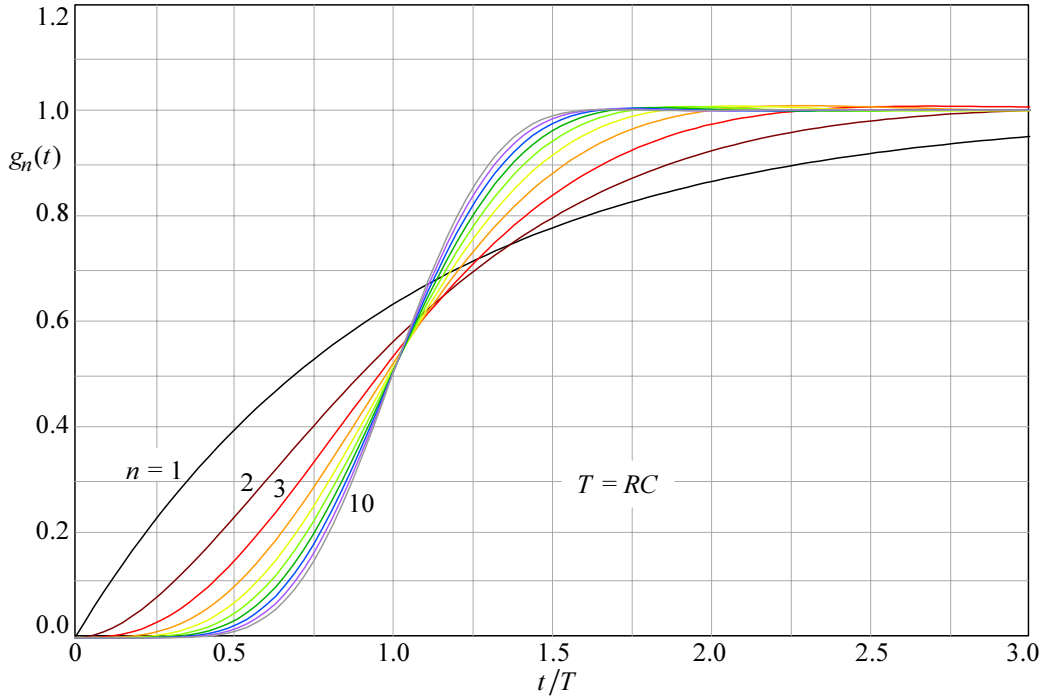


**Fig. 4.4.6:** Step response of systems with Bessel poles of order $n = 1$–10. Note the 50% amplitude delay approaching unity as the system order increases.

**Table 4.4.2:** Relative Rise time Improvement with Bessel Poles

| $n$ | 1 | 2 | 3 | 4 | 5 | 6 | 7 | 8 | 9 | 10 |
|---|---|---|---|---|---|---|---|---|---|---|
| $\eta_\text{r}$ | 1.00 | 1.38 | 1.75 | 2.09 | 2.39 | 2.68 | 2.93 | 3.18 | 3.41 | 3.60 |

From Fig 4.4.2 and 4.4.6 one could make a false conclusion that the upper half power frequency increases and the rise time decreases if more equal amplifier stages are cascaded. This is not true, because all the parameters of systems having Bessel poles are defined with respect to the **single stage non-peaking amplifier**, where $\omega_\text{h} = 1/RC$.

In the case of a system with $n$ Bessel poles this would mean chopping the stray capacitance of a single amplifying stage into smaller capacitances and separating them by coils to create $n$ poles.

Unfortunately there is a limit in practice because each individual amplifier stage input sees two capacitances: the output capacitance of the previous stage and its own input capacitance. Therefore, in a multi-stage amplifier an individual stage can have four poles at most (either Bessel, Butterworth, or of any other pole family). However, a single-stage amplifier can have up to 8 poles (if we apply a T-coil peaking to both input and output).

If we use more than one stage, we can assign a small group of staggered poles from the $n^{\text{th}}$-group (from either Table 4.3.1 or Table 4.4.3) to each stage, so that the system as a whole has the poles as specified by the $n^{\text{th}}$-group chosen. Then **no stage by itself will be optimized, but the amplifier as a whole will be**. More details of this technique are given in Sec. 4.6 and some examples can be found in Part 5 and Part 7.

**Table 4.4.3: Bessel Poles (identical envelope delay)**

| Order $n$ | $\sigma$ [rad/$s$] | $\omega$ [rad/$s$] | $\theta$ [°] |
|---|---|---|---|
| 1 | − 1.0000 | 0.0000 | 180 |
| 2 | − 1.5000 | ± 0.8660 | 180 ∓ 30.0000 |
| 3 | − 2.3222 | 0.0000 | 180 |
| | − 1.8389 | ± 1.7544 | 180 ∓ 43.6525 |
| 4 | − 2.8962 | ± 0.8672 | 180 ∓ 16.6697 |
| | − 2.1038 | ± 2.6574 | 180 ∓ 51.6325 |
| 5 | − 3.6467 | 0.0000 | 180 |
| | − 3.3520 | ± 1.7427 | 180 ∓ 27.4696 |
| | − 2.3247 | ± 3.7510 | 180 ∓ 56.9366 |
| 6 | − 4.2484 | ± 0.8675 | 180 ∓ 11.5411 |
| | − 3.7357 | ± 2.6263 | 180 ∓ 35.1079 |
| | − 2.5159 | ± 4.4927 | 180 ∓ 60.7508 |
| 7 | − 4.9718 | 0.0000 | 180 |
| | − 4.7583 | ± 1.7393 | 180 ∓ 20.0787 |
| | − 4.0701 | ± 3.5172 | 180 ∓ 40.8316 |
| | − 2.6857 | ± 5.4207 | 180 ∓ 63.6439 |
| 8 | − 5.5879 | ± 0.8676 | 180 ∓ 8.8257 |
| | − 5.2048 | ± 2.6162 | 180 ∓ 26.6861 |
| | − 4.3683 | ± 4.4144 | 180 ∓ 45.3011 |
| | − 2.8390 | ± 6.3539 | 180 ∓ 65.9245 |
| 9 | − 6.2970 | 0.0000 | 180 |
| | − 6.1294 | ± 1.7378 | 180 ∓ 15.8295 |
| | − 5.6044 | ± 3.4982 | 180 ∓ 31.9715 |
| | − 4.6384 | ± 5.3173 | 180 ∓ 48.9007 |
| | − 2.9793 | ± 7.2915 | 180 ∓ 67.7753 |
| 10 | − 6.9220 | ± 0.8677 | 180 ∓ 7.1447 |
| | − 6.6153 | ± 2.6116 | 180 ∓ 21.5430 |
| | − 5.9675 | ± 4.3849 | 180 ∓ 36.3085 |
| | − 4.8862 | ± 6.2250 | 180 ∓ 51.8703 |
| | − 3.1089 | ± 8.2327 | 180 ∓ 69.3119 |

### 4.4.5 Ideal Gaussian Frequency Response

Suppose that we have succeeded making an amplifier with zero phase shift and an ideal Gaussian frequency response:

$$G(\omega) = \mathrm{e}^{-\omega^2} \tag{4.4.18}$$

the plot of which is shown in Fig. 4.4.7 for both positive and negative frequencies (and, to acquire a feeling for Bessel systems, compared to the magnitude of a 5th-order system with modified Bessel poles).

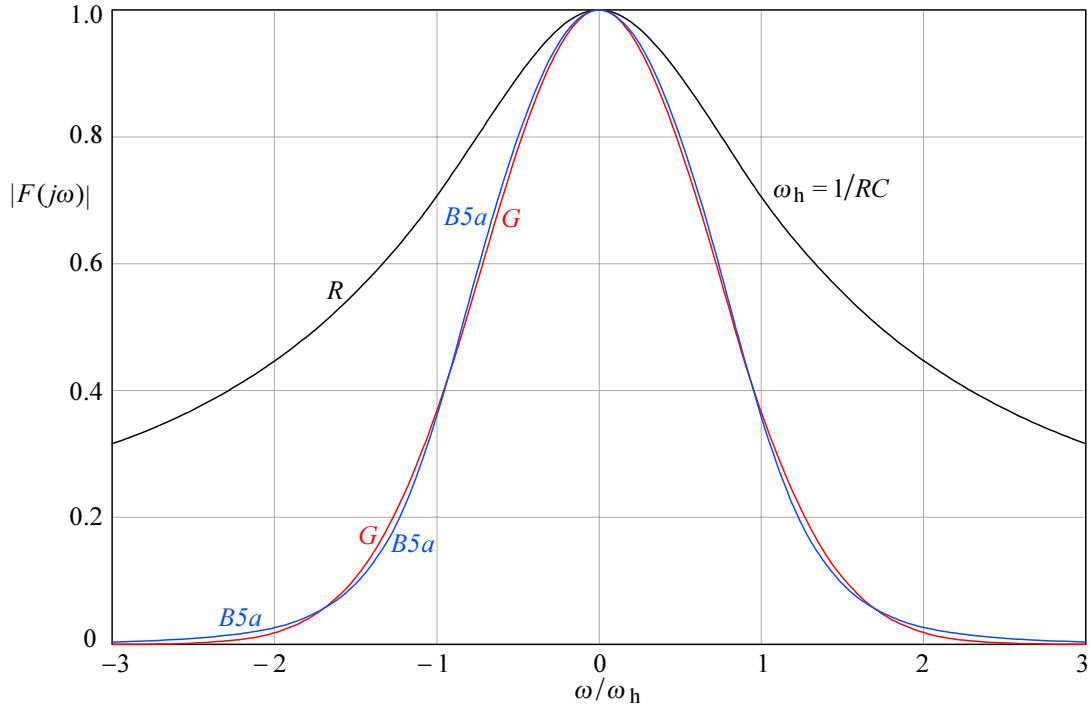


**Fig. 4.4.7:** Ideal Gaussian (MFED) frequency response $G$ (real only, with no phase shift), compared to the magnitude of a 5th-order modified Bessel system $B5a$ (identical cutoff asymptote, Table 4.5.1). The frequency scale is two-sided, linear, and normalized to $\omega_\mathrm{h} = 1/RC$ of the first-order system, which is shown as the reference $R$.

By examining Eq. 4.4.9 and Eq. 4.4.18 we come to the conclusion that it is possible to **approximate** the Gaussian response with any desired accuracy up to a certain frequency. At higher frequencies, the Gaussian response falls faster than the approximated response. This is brought into evidence in Fig. 4.4.8 where the same responses are plotted in log-log scale.

By applying a unit step at the instant $t = 0$ to the input of the hypothetical amplifier having a Gaussian frequency response the resulting step response is equal to the so called *error-function*, which is defined as the time integral of the exponential function of time squared [Ref. 4.2]:

$$g_\mathrm{G}(t) = \mathrm{erf}(t) = \frac{1}{2\sqrt{\pi}} \int_{-\infty}^{t_1} \mathrm{e}^{-t^2/4}\, dt \tag{4.4.19}$$

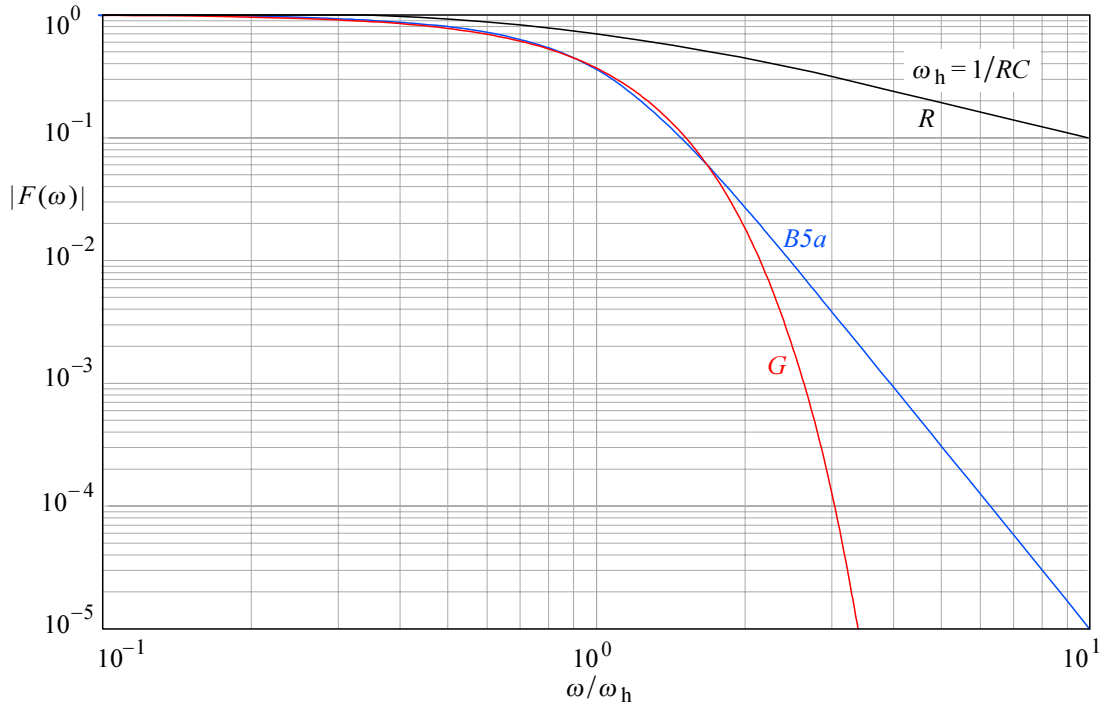


**Fig. 4.4.8:** Frequency response in log-log scale brings into evidence how the ideal Gaussian response $G$ decreases much more steeply with frequency than the 5th-order Bessel response $B5a$. The Bessel system would have to be of infinitely high order to match the Gaussian response.

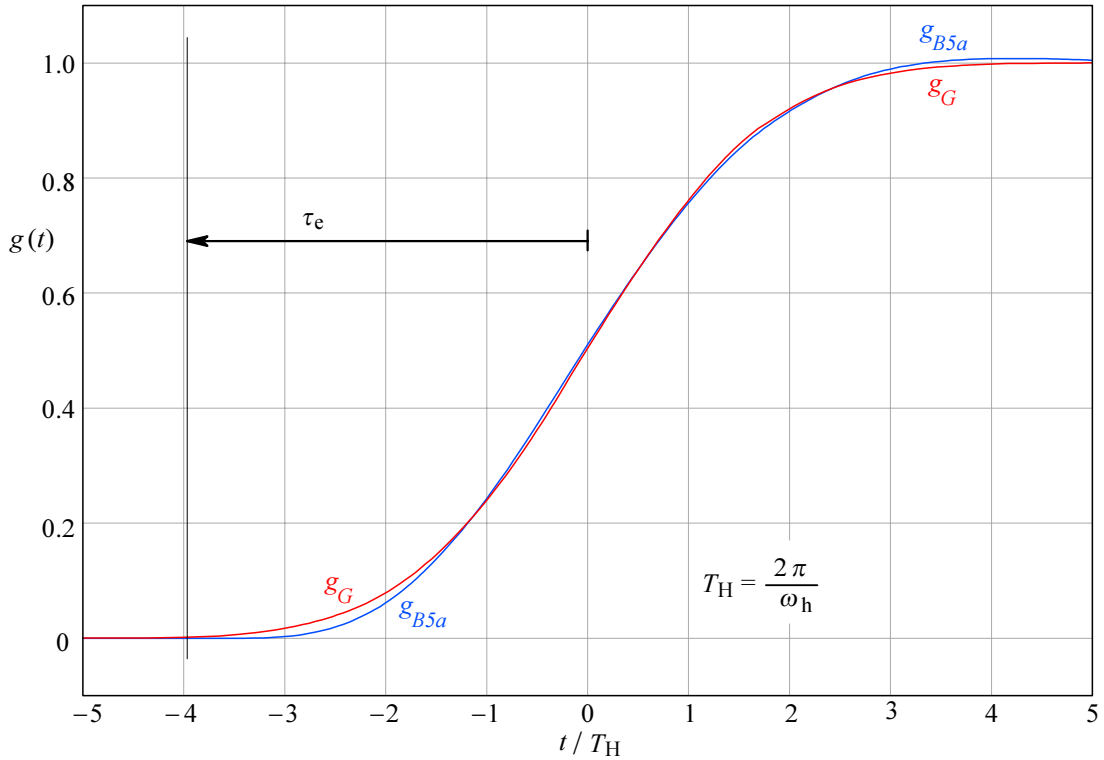


**Fig. 4.4.9:** Step response of a hypothetical system, $g_G$, having the ideal Gaussian frequency response with no phase shift, as the one in Fig. 4.4.7 and 4.4.8. Compare it with the step response of a 5th-order Bessel system, $g_{B5a}$, with modified Bessel poles, Table 4.5.1, and envelope delay compensated ($\tau_e = -3.94\,T_H$) for minimal difference in the half amplitude region.

The plot of Eq. 4.4.19 calculated by the *Simpson method* is shown in Fig. 4.4.9. The step response is symmetrical, without any overshoot. However, here too, we have a response for $t < 0$ as it was in the ideal MFA amplifier.

If our hypothetical amplifier were to have any linear phase delay the curve $g_G$ in Fig. 4.4.9 would be shifted rightwards from the origin, but an infinite phase shift would be required in order to have no response for time $t < 0$ (the same as for Fig. 4.3.8).

By looking back at Eq. 4.4.2–7, we realize that we would need an infinite number of terms in the denominator ( = an infinite number of poles) in order to justify an ' = ' sign instead of an approximation ( ≈ ). This would mean an infinite number of system components and amplifying stages, and therefore the conclusion is that we can not make an amplifier with an ideal Gaussian response (but we can come very close).

A proof, based on the *Paley–Wiener Criterion*, can be carried out in the following way: if we compare the step response in Fig. 4.4.9 with the step response of a non-peaking multi-stage amplifier in Fig. 4.1.7, for $n = 10$, there is a great similarity. Therefore we can ask ourselves if a Gaussian response could be achieved by increasing the number of stages to some arbitrarily large number ($n \to \infty$). By doing so, the phase response diverges when $n \to \infty$ and it becomes infinite if $\omega \to \infty$. Therefore for both reasons (infinite number of stages and divergent phase response) it is not possible to make an amplifier with an ideal Gaussian response.

### 4.4.6 Bessel Poles Normalized to Identical Cutoff Frequency

Because the Bessel poles are derived from the requirement for an identical envelope delay there is no simple way of renormalizing them back to the same cut off frequency. However, such a renormalization would be very useful, not only for comparing the systems with different pole families and equal order, but also for comparing systems of different order within the Bessel family itself.

What is difficult to do analytically is often easily done numerically, especially if the actual number crunching is executed by a machine. The normalization procedure goes by taking the original Bessel poles and finding the system magnitude by Eq. 4.4.13 at the unit frequency ($\omega/\omega_h = 1$). We obtain an attenuation value, say, $|F(1)| = a$ and we want $|F(1)|$ to be $1/\sqrt{2}$. The ratio $q = 1/a\sqrt{2}$ is the correction factor by which we multiply all the poles and insert the new poles again into Eq. 4.4.13. We keep repeating this procedure until $|q - 1/\sqrt{2}| < \varepsilon$, with $\varepsilon$ being an arbitrarily small error; for practical purposes, a value of $\varepsilon = 0.001$ is adequate. In the algorithm presented in Part 6, this tolerance is reached in only 6 to 9 iterations, depending on system order.

The following graphs were made using the computer algorithms presented in Part 6 and show the performance of cut off frequency normalized Bessel systems of order $n = 1$–$10$, as in the previous figures.

Fig. 4.4.10 shows the frequency response magnitude; the plots for $n = 5$–$9$ are missing, since the difference is too small to identify them on such a vertical scale (the difference in high frequency attenuation becomes significant with higher magnitude resolution, say, down to 0.001 or less). Fig. 4.4.11 shows the phase, Fig. 4.4.12 the envelope delay and Fig. 4.4.13 shows the step response. Finally, in Table 4.4.4 we report the values of Bessel poles and their respective angles for systems with equal cut off frequency.

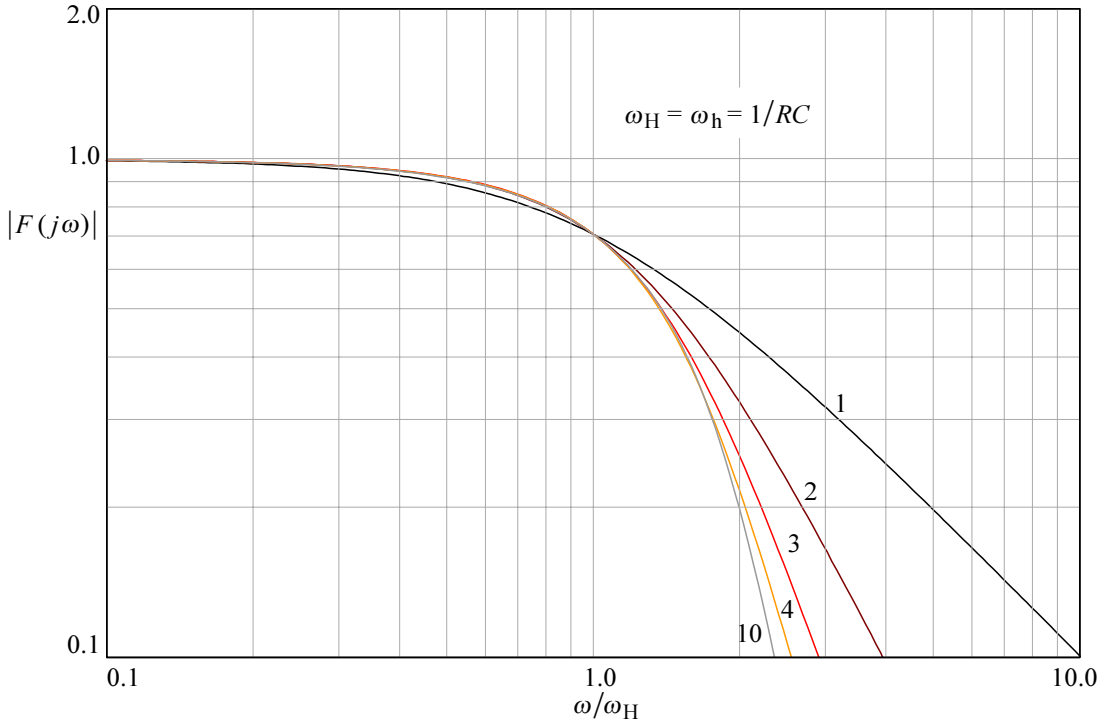


**Fig. 4.4.10:** Frequency response magnitude of systems with normalized Bessel poles of order $n = 1, 2, 3, 4,$ and $10$. Note the nearly identical passband response — this is the reason why we can approximate the oscilloscope (multi-stage) amplifier rise time from the cut off frequency, using the relation for the first-order system: $\tau_r = 0.35/f_T$.

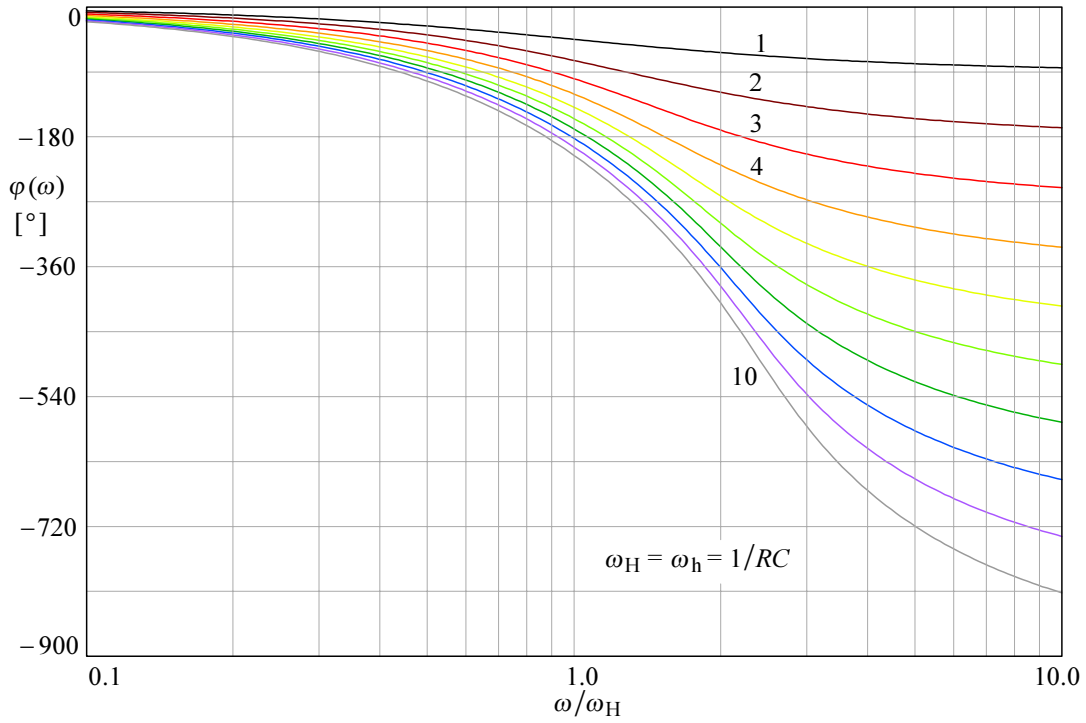


**Fig. 4.4.11:** Phase angle of systems with normalized Bessel poles of order $n = 1$–$10$.

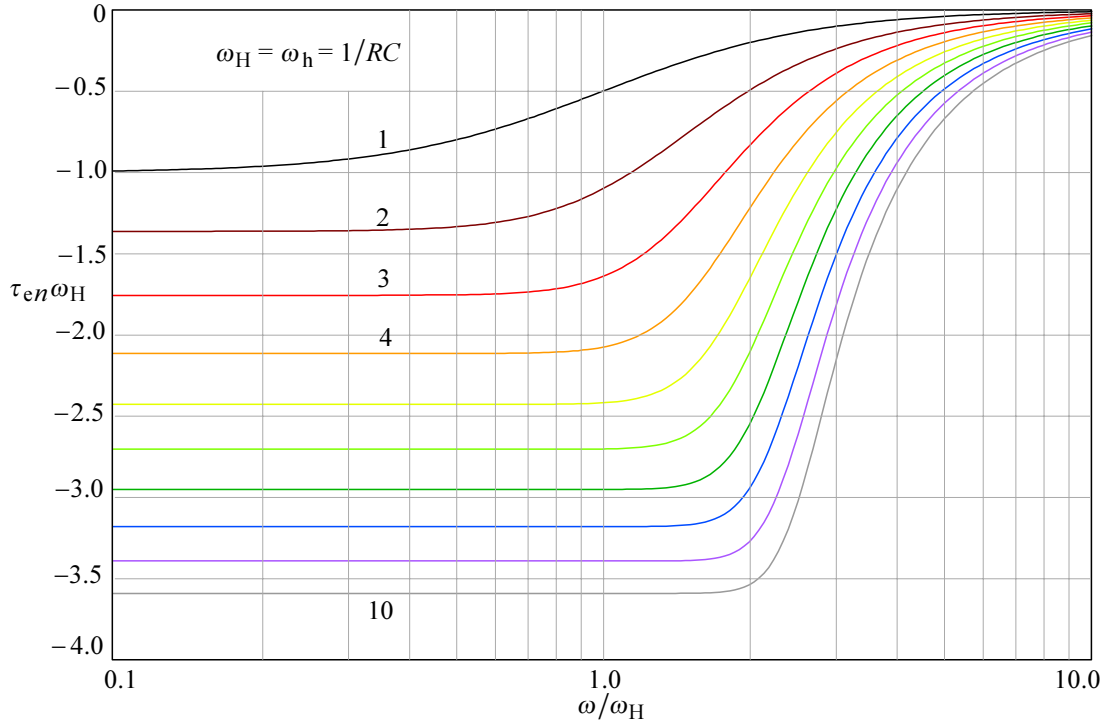


**Fig. 4.4.12:** Envelope delay of systems with normalized Bessel poles of the order $n = 1$–$10$. Although the bandwidth is the same, the delay flatness extends progressively with system order, already reaching beyond the system cut off frequency for $n = 5$.

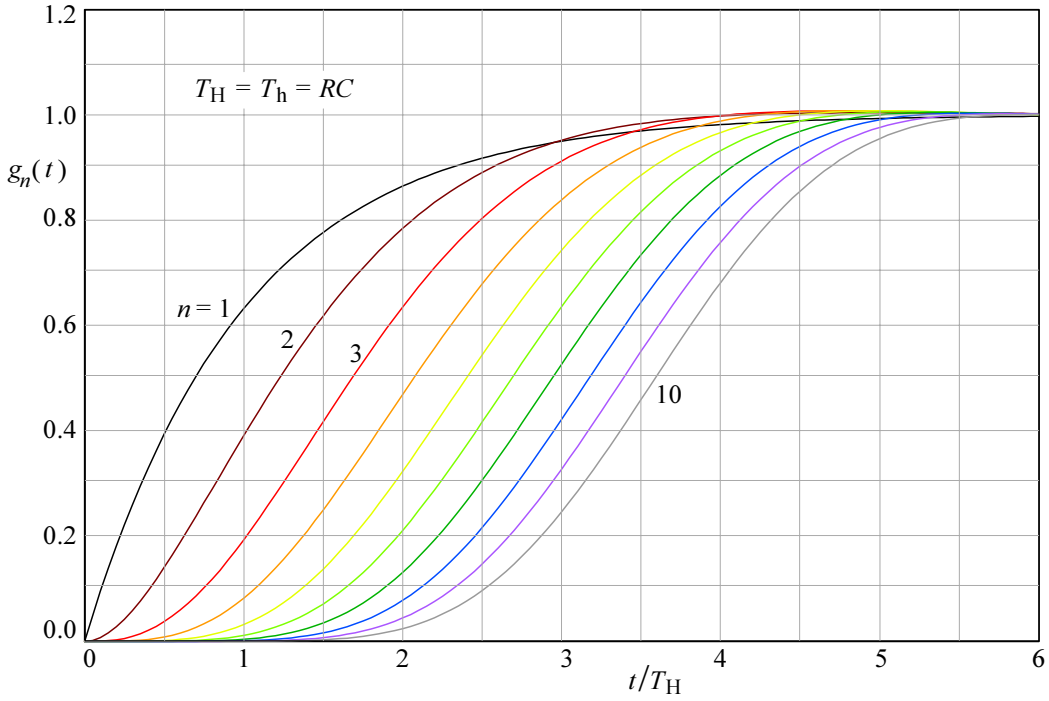


**Fig. 4.4.13:** Step response of systems with normalized Bessel poles of order $n = 1$–$10$. Note the half amplitude slope being almost equal for all systems, indicating an equal system cut off frequency.

**Table 4.4.4: Bessel Poles (equal cut off frequency)**

| Order $n$ | $\sigma$ [rad/$s$] | $\omega$ [rad/$s$] | $\theta$ [°] |
|---|---|---|---|
| 1 | − 1.0000 | 0.0000 | 180 |
| 2 | − 1.1017 | ± 0.6360 | 180 ∓ 30.0000 |
| 3 | − 1.3227 | 0.0000 | 180 |
| | − 1.0475 | ± 0.9993 | 180 ∓ 43.6525 |
| 4 | − 1.3701 | ± 0.4103 | 180 ∓ 16.6697 |
| | − 0.9952 | ± 1.2571 | 180 ∓ 51.6325 |
| 5 | − 1.5024 | 0.0000 | 180 |
| | − 1.3810 | ± 0.7180 | 180 ∓ 27.4696 |
| | − 0.9578 | ± 1.4713 | 180 ∓ 56.9366 |
| 6 | − 1.5716 | ± 0.3209 | 180 ∓ 11.5411 |
| | − 1.3819 | ± 0.9715 | 180 ∓ 35.1079 |
| | − 0.9307 | ± 1.6619 | 180 ∓ 60.7508 |
| 7 | − 1.6845 | 0.0000 | 180 |
| | − 1.6122 | ± 0.5893 | 180 ∓ 20.0787 |
| | − 1.3790 | ± 1.1917 | 180 ∓ 40.8316 |
| | − 0.9099 | ± 1.8366 | 180 ∓ 63.6439 |
| 8 | − 1.7575 | ± 0.2729 | 180 ∓ 8.8257 |
| | − 1.6370 | ± 0.8228 | 180 ∓ 26.6861 |
| | − 1.3739 | ± 1.3884 | 180 ∓ 45.3011 |
| | − 0.8929 | ± 1.9984 | 180 ∓ 65.9245 |
| 9 | − 1.8567 | 0.0000 | 180 |
| | − 1.8072 | ± 0.5124 | 180 ∓ 15.8295 |
| | − 1.6525 | ± 1.0314 | 180 ∓ 31.9715 |
| | − 1.3676 | ± 1.5678 | 180 ∓ 48.9007 |
| | − 0.8784 | ± 2.1499 | 180 ∓ 67.7753 |
| 10 | − 1.9277 | ± 0.2416 | 180 ∓ 7.1447 |
| | − 1.8423 | ± 0.7273 | 180 ∓ 21.5430 |
| | − 1.6619 | ± 1.2212 | 180 ∓ 36.3085 |
| | − 1.3608 | ± 1.7336 | 180 ∓ 51.8703 |
| | − 0.8658 | ± 2.2927 | 180 ∓ 69.3119 |

## 4.5 Pole Interpolation

Sometimes we desire to design an amplifier, or just a single stage, with a performance which is somewhere between the Butterworth and Bessel response. We shall derive the corresponding poles by the pole interpolation procedure which was described by *Y. Peless* and *T. Murakami* [Ref. 4.14].

### 4.5.1 Derivation of Modified Bessel poles

In order to be able to interpolate between Butterworth and Bessel poles, the later must be modified so that, for both systems of equal order, the frequency response magnitude will have the same asymptotes in both passband and stopband. This is achieved if the product of all the poles is equal to one, as in Butterworth systems:

$$(-1)^n \prod_{k=1}^{n} s_k = 1 \tag{4.5.1}$$

A general expression for the frequency response normalized in amplitude is:

$$F(s) = \frac{a_0}{s^n + a_{n-1}\, s^{n-1} + \cdots + a_2\, s^2 + a_1\, s + a_0} \tag{4.5.2}$$

where:

$$a_0 = (-1)^n \prod_{k=1}^{n} s_k \tag{4.5.3}$$

If we divide both the numerator and the denominator by $a_0$ we obtain:

$$F(s) = \frac{1}{\frac{1}{a_0}\, s^n + \frac{a_{n-1}}{a_0}\, s^{n-1} + \cdots + \frac{a_2}{a_0}\, s^2 + \frac{a_1}{a_0}\, s + 1} \tag{4.5.4}$$

Next we introduce another variable $\underline{s}$ such that:

$$\underline{s}^n = \frac{s^n}{a_0} \qquad \text{or} \qquad \underline{s} = \frac{s}{a_0^{1/n}} \tag{4.5.5}$$

Then Eq. 4.5.4 can be written as:

$$F(s) = \frac{1}{\underline{s}^n + b_{n-1}\, \underline{s}^{n-1} + \cdots + b_2\, \underline{s}^2 + b_1\, \underline{s} + 1} \tag{4.5.6}$$

where the coefficients $b_i$ are:

$$\begin{aligned} b_{n-1} &= \frac{a_{n-1}}{a_0^{1/n}} \\ b_{n-2} &= \frac{a_{n-2}}{a_0^{2/n}} \\ &\cdots \\ b_1 &= \frac{a_1}{a_0^{1-1/n}} \end{aligned} \tag{4.5.7}$$

The coefficients $a_k$ for the Bessel polynomials are calculated by Eq. 4.4.10. Then the coefficients $b_k$ are those of the modified Bessel polynomial, from which we can calculate the modified Bessel poles of $F(s)$ for the order $n = 1$–$10$. These poles are listed together with the corresponding pole radii $r$ and pole angles $\theta$ in Table 4.5.1.

### 4.5.2 Pole Interpolation Procedure

At the time of the German mathematician *Friedrich Wilhelm Bessel* (1784–1846), there were no electronic filters and no wideband amplifiers, to which the roots of his polynomials could be applied. *W.A. Thomson* [Ref. 4.9] was the first to use them and he also derived the expressions required for MFED network synthesis. Therefore some engineers use the name *Thomson poles* or, perhaps more correctly, *Bessel–Thomson poles*.

In the following discussion we shall interpolate between Butterworth and the modified Bessel poles. If we were to label the poles by initials only, a confusion would result in the graphs and formulae. Therefore, to label the modified Bessel poles, we shall use the subscript 'T' in honor of W.A. Thomson.

The procedure of pole interpolation can be explained with the aid of Fig. 4.5.1.

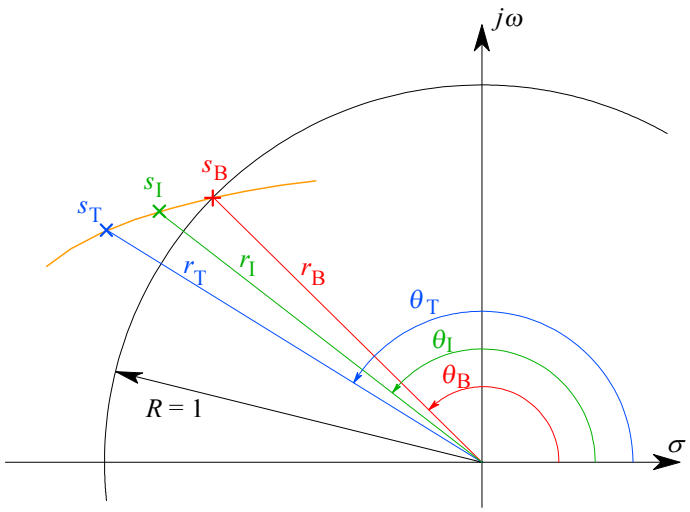


**Fig. 4.5.1**: Pole interpolation procedure. Butterworth (index B) and Bessel poles (index T) are expressed in polar coordinates, $s(r,\theta)$. The trajectory going through both poles is the interpolation path required to obtain the transitional pole $s_I$.

We first express the poles in polar coordinates with the well known conversion:

$$r_k = \sqrt{\sigma_k^2 + \omega_k^2} \tag{4.5.8}$$

and

$$\theta_k = \pi + \arctan\frac{\omega_k}{\sigma_k} \tag{4.5.9}$$

Here the $\pi$ radians added are required because the arctangent function repeats with a period of $\pi$ radians, so it does not distinguish between the poles in quadrant III form those in I, and the same is true for quadrants IV and II.

By using the polar coordinates a pole $s_k$ is expressed as:

$$s_k = \sigma_k + j\omega_k = r_k \, \mathrm{e}^{j\theta_k} \tag{4.5.10}$$

In Eq. 4.5.3 the coefficient $a_0$ is equal to the product of all poles. Because we have divided the polynomial coefficients $a_k$ by $a_0$ to obtain the coefficients $b_k$ we have effectively normalized the product of all poles to one:

$$\left| \prod_{k=1}^{n} s_k \right| = 1 \tag{4.5.11}$$

and this is now true for both Butterworth and the modified Bessel poles. Therefore we can assume that there exists a trajectory going through the $k^{\text{th}}$ Butterworth pole $s_{\mathrm{B}k}$ and the $k^{\text{th}}$ Bessel pole $s_{\mathrm{T}k}$ and each point on this trajectory can represent a pole $s_{\mathrm{I}k}$ which can be expressed as:

$$s_{\mathrm{I}k} = r_{\mathrm{I}k} \, \mathrm{e}^{j\theta_{\mathrm{I}k}} \tag{4.5.12}$$

such that the absolute product of all interpolated poles $s_{\mathrm{I}}$ is kept equal to one. Then:

$$r_{\mathrm{I}k} = r_{\mathrm{T}k}^{m} \tag{4.5.13}$$

and:

$$\theta_{\mathrm{I}k} = \theta_{\mathrm{B}k} + m \, (\theta_{\mathrm{T}k} - \theta_{\mathrm{B}k}) \tag{4.5.14}$$

The parameter $m$ can have any value between $0$ and $1$.

If $m = 0$ we have the Butterworth poles and if $m = 1$ we have the modified Bessel poles. By using, say, $m = 0.5$, the characteristics of such a network would be just half way between the Butterworth and modified Bessel poles.

It is obvious that we need to calculate only one half of the poles, say, those with the positive imaginary value, $\sigma_k + j\,\omega_k$, since the complex conjugate poles $\sigma_k - j\,\omega_k$ have the same magnitude, only the sign of their imaginary component is negative. In the cases with odd $n$ the interpolated real pole remains on the real axis ($\theta_{\mathrm{I}k} = \pi$) between the two real poles belonging to the Buttreworth and the modified Bessel system.

**Table 4.5.1: Modified Bessel Poles**
(with HF asymptote identical as Butterworth)

| Order $n$ | $\sigma$ [rad/$s$] | $\omega$ [rad/$s$] | $r$ | $\theta$ [°] |
|---|---|---|---|---|
| 1 | − 1.0000 | 0.0000 | 1.0000 | 180 |
| 2 | − 0.8660 | ± 0.5000 | 1.0000 | 180 ∓ 30.0000 |
| 3 | − 0.9416 | 0.0000 | 0.9416 | 180 |
| | − 0.7456 | ± 0.7114 | 1.0305 | 180 ∓ 43.6525 |
| 4 | − 0.9048 | ± 0.2709 | 0.9444 | 180 ∓ 16.6697 |
| | − 0.6572 | ± 0.8302 | 1.0588 | 180 ∓ 51.6325 |
| 5 | − 0.9264 | 0.0000 | 0.9246 | 180 |
| | − 0.8516 | ± 0.4427 | 0.9598 | 180 ∓ 27.4696 |
| | − 0.5906 | ± 0.9072 | 1.0825 | 180 ∓ 56.9366 |
| 6 | − 0.9094 | ± 0.1857 | 0.9282 | 180 ∓ 11.5411 |
| | − 0.7997 | ± 0.5622 | 0.9775 | 180 ∓ 35.1079 |
| | − 0.5386 | ± 0.9617 | 1.1022 | 180 ∓ 60.7508 |
| 7 | − 0.9195 | 0.0000 | 0.9195 | 180 |
| | − 0.8800 | ± 0.3217 | 0.9369 | 180 ∓ 20.0787 |
| | − 0.7527 | ± 0.6505 | 0.9948 | 180 ∓ 40.8316 |
| | − 0.4967 | ± 1.0025 | 1.1188 | 180 ∓ 63.6439 |
| 8 | − 0.9097 | ± 0.1412 | 0.9206 | 180 ∓ 8.8257 |
| | − 0.8473 | ± 0.4259 | 0.9483 | 180 ∓ 26.6861 |
| | − 0.7111 | ± 0.7187 | 1.0110 | 180 ∓ 45.3011 |
| | − 0.4622 | ± 1.0344 | 1.1329 | 180 ∓ 65.9245 |
| 9 | − 0.9155 | 0.0000 | 0.9155 | 180 |
| | − 0.8911 | ± 0.2527 | 0.9262 | 180 ∓ 15.8295 |
| | − 0.8148 | ± 0.5086 | 0.9605 | 180 ∓ 31.9715 |
| | − 0.6744 | ± 0.7731 | 1.0259 | 180 ∓ 48.9007 |
| | − 0.4331 | ± 1.0601 | 1.1451 | 180 ∓ 67.7753 |
| 10 | − 0.9091 | ± 0.1140 | 0.9162 | 180 ∓ 7.1447 |
| | − 0.8688 | ± 0.3430 | 0.9341 | 180 ∓ 21.5430 |
| | − 0.7838 | ± 0.5759 | 0.9726 | 180 ∓ 36.3085 |
| | − 0.6418 | ± 0.8176 | 1.0394 | 180 ∓ 51.8703 |
| | − 0.4083 | ± 1.0813 | 1.1558 | 180 ∓ 69.3119 |

### 4.5.3 A Practical Example of Pole Interpolation

Let us calculate the frequency, phase, time delay and step response of a network with three poles. Three poles are just enough to demonstrate the procedure of pole interpolation completely. Let us select $m = 0.5$. From Table 4.3.1 we find the following values for Butterworth poles of order $n = 3$:

$$\begin{aligned} &s_{1B}: && r_{1B} = 1 && \theta_{1B} = \ 180° \\ &s_{2B}: && r_{2B} = 1 && \theta_{2B} = \ +120° \\ &s_{3B}: && r_{3B} = 1 && \theta_{3B} = \ -120° \end{aligned} \tag{4.5.15}$$

and in Table 4.5.1, order $n = 3$, we find these values for modified Bessel poles:

$$\begin{aligned} &s_{1T}: && r_{1T} = 0.9416 && \theta_{1T} = 180° \\ &s_{2T}: && r_{2T} = 1.0305 && \theta_{2T} = \ +136.35° \\ &s_{3T}: && r_{3T} = 1.0305 && \theta_{3T} = \ -136.35° \end{aligned} \tag{4.5.16}$$

Now we interpolate the radii and the pole angles:

$$\begin{aligned} r_1 &= {r_{1T}}^m = 0.9416^{0.5} = 0.9704 \\ r_{2,3} &= {r_{1T}}^m = 1.0305^{0.5} = 1.0151 \\ \theta_{2,3} &= \theta_B + m\,(\theta_T - \theta_B) = 120° + 0.5\,(136.35° - 120°) = 128.175° \end{aligned} \tag{4.5.17}$$

With these values we calculate the real and imaginary components of transitional Butterworth–Bessel poles (TBT):

$$\begin{aligned} s_1 &= -0.9704 = \sigma_1 \\ s_{2,3} &= -r_2 \cos\theta_2 \pm j\, r_2 \sin\theta_2 \\ &= -1.0151 \cos 128.175° \pm j\, 1.0151 \sin 128.175° \\ &= -0.6274 \pm j\, 0.7980 = \sigma_2 \pm j\,\omega_2 \end{aligned} \tag{4.5.18}$$

The relation for the normalized frequency response magnitude is:

$$\left|F(\omega)\right| = \frac{1}{\sqrt{(\sigma_1 + \omega)^2\left[\sigma_2^2 + (\omega + \omega_2)^2\right]\left[\sigma_2^2 + (\omega - \omega_2)^2\right]}} \tag{4.5.19}$$

$$= \frac{1}{\sqrt{(0.9704 + \omega)^2\left[0.6274^2 + (\omega + 0.7980)^2\right]\left[0.6274^2 + (\omega - 0.7980)^2\right]}}$$

The magnitude plot is shown in Fig. 4.5.2 (TBT); for comparison, the magnitude plots with Butterworth poles and modified Bessel poles are also drawn.

The normalized phase response is calculated as:

$$\begin{aligned} \varphi &= \arctan\frac{\omega}{\sigma_1} + \arctan\frac{\omega + \omega_2}{\sigma_2} + \arctan\frac{\omega - \omega_2}{\sigma_2} = \\ &= \arctan\frac{\omega}{-0.9704} + \arctan\frac{\omega + 0.7981}{-0.6275} + \arctan\frac{\omega - 0.7981}{-0.6275} \end{aligned} \tag{4.5.20}$$

In Fig. 4.5.3 the phase plot of the transitional (TBT) system, together with the plots for Butterworth and modified Bessel systems are drawn.

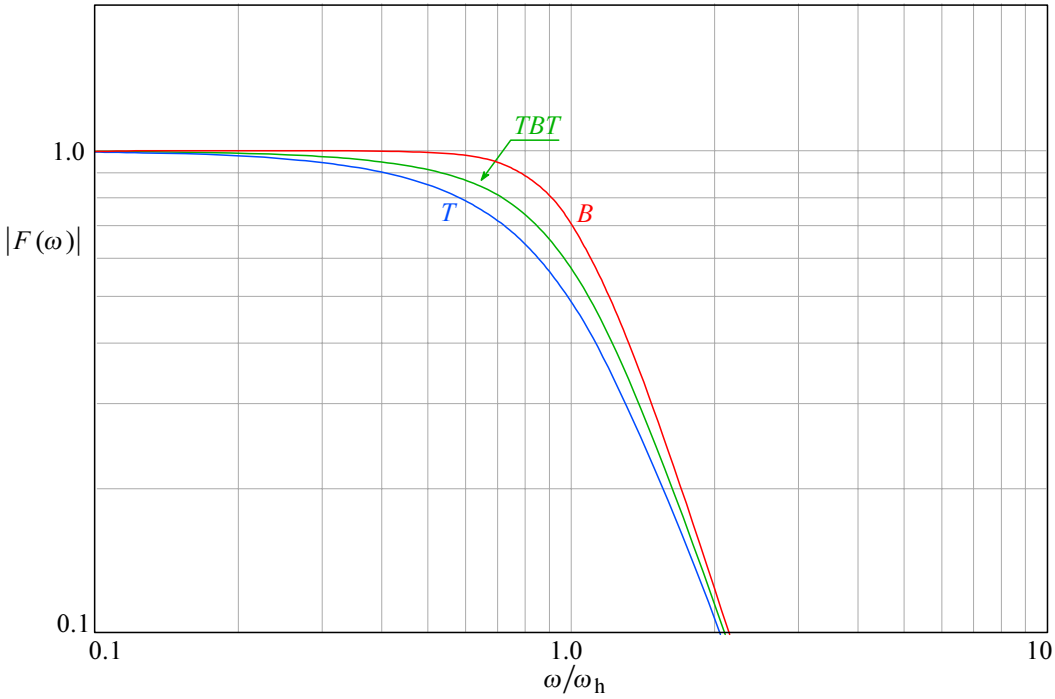


**Fig. 4.5.2**: Frequency response's magnitude of the Transitional Bessel–Butterworth three-pole system (TBT), along with the modified Bessel (T) and Butterworth (B) responses.

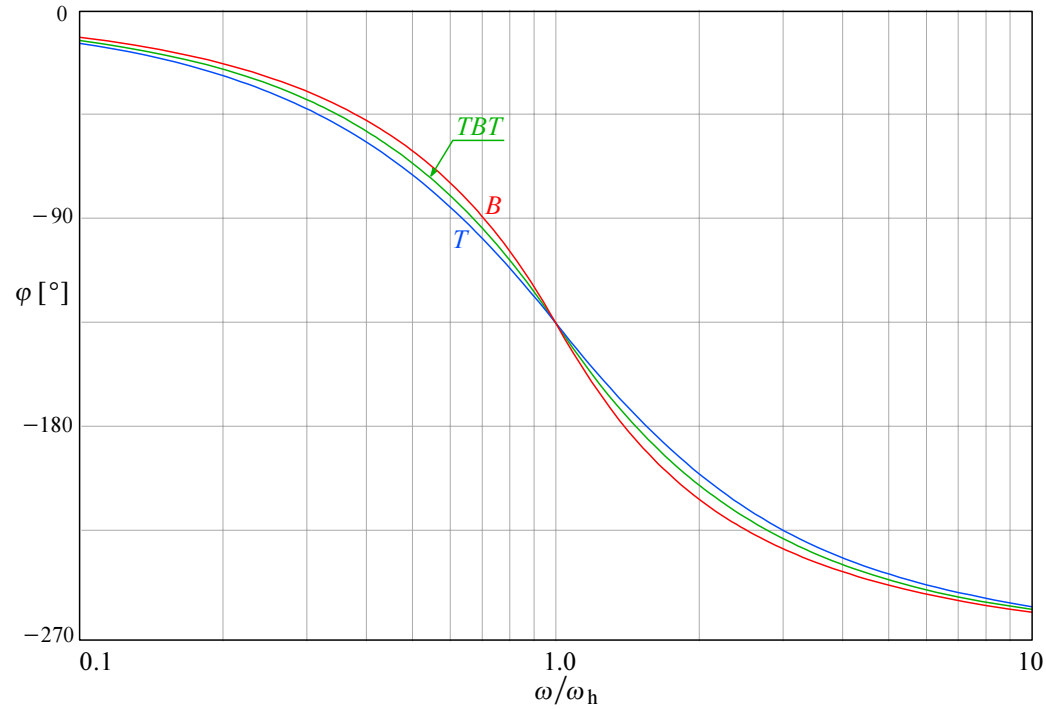


**Fig. 4.5.3**: Phase angle of the Transitional Bessel–Butterworth three-pole system (TBT), along with the Bessel (T) and Butterworth (B) phase.

The normalized envelope delay is calculated as:

$$\tau_e = \frac{\sigma_1}{\sigma_1^2 + \omega^2} + \frac{\sigma_2}{\sigma_2^2 + (\omega + \omega_2)^2} + \frac{\sigma_2}{\sigma_2^2 + (\omega - \omega_2)^2} \tag{4.5.21}$$

$$= -\frac{0.9704}{0.9704^2 + \omega^2} - \frac{0.6275}{0.6275^2 + (\omega + 0.7981)^2} - \frac{0.6275}{0.6275^2 + (\omega - 0.7981)^2}$$

The envelope delay plot is shown in Fig. 4.5.4 (TBT), along with the delays for the Butterworth and the modified Bessel system.

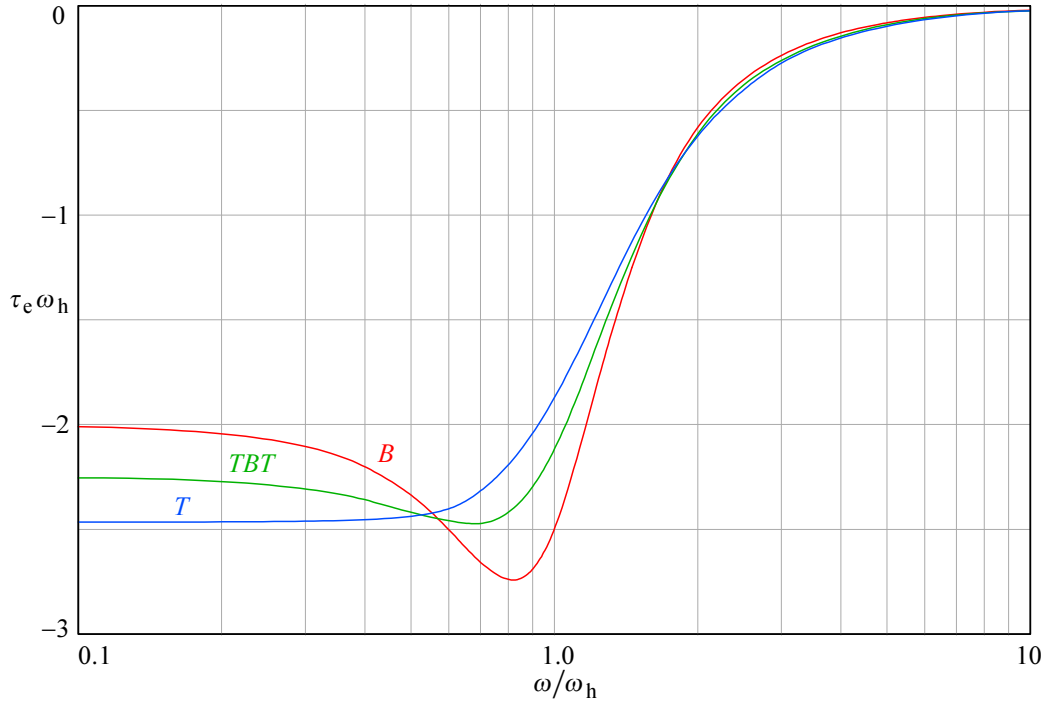


**Fig. 4.5.4**: Envelope delay of the Transitional Bessel–Butterworth three-pole system (TBT), along with the Bessel (T) and Butterworth (B) delays.

The starting point for the step response calculation is the general formula for a three pole function multiplied by the unit step operator $1/s$:

$$G(s) = \frac{-\,s_1\, s_2\, s_3}{s\,(s - s_1)(s - s_2)(s - s_3)} \tag{4.5.22}$$

We calculate the corresponding step response in the time domain by the $\mathcal{L}^{-1}$ transform:

$$g(t) = \mathcal{L}^{-1}\{G(s)\} = \sum_{i=1}^{n} \mathrm{res}_i\, G(s)\, \mathrm{e}^{st}$$

$$= \sum_{i=1}^{3} \mathrm{res}_i \frac{-\,s_1\, s_2\, s_3\, \mathrm{e}^{st}}{s\,(s - s_1)(s - s_2)(s - s_3)} \tag{4.5.23}$$

After the sum of the residues is calculated, we insert the poles $s_1 = \sigma_1$ and $s_{2,3} = \sigma_2 \pm j\,\omega_2$ to obtain (see Appendix 2.3):

$$g(t) = 1 - \frac{\sigma_1 \sqrt{\left[\sigma_2(\sigma_2 - \sigma_1) - \omega_2^2\right]^2 + \omega_2^2(2\sigma_2 - \sigma_1)^2}}{\omega_2\left[(\sigma_2 - \sigma_1)^2 + \omega_2^2\right]}\, \mathrm{e}^{\sigma_2 t} \sin\left(\omega_2\, t + \theta\right)$$

$$- \frac{(\sigma_2^2 + \omega_2^2)}{(\sigma_2 - \sigma_1)^2 + \omega_2^2}\, \mathrm{e}^{\sigma_1 t} \tag{4.5.24}$$

where the angle $\theta$ is:

$$\theta = \pi + \arctan \frac{-\,\omega_2(2\sigma_2 - \sigma_1)}{\sigma_2(\sigma_2 - \sigma_1) - \omega_2^2} \tag{4.5.25}$$

By inserting the numerical values for poles from Eq. 4.5.18, we arrive at the final relation:

$$g(t) = 1 + 1.4211\, \mathrm{e}^{-6275\, t} \sin(0.7981\, t + 2.8811) - 1.3660\, \mathrm{e}^{-0.9704\, t} \tag{4.5.26}$$

The plot based on this formula is shown in Fig. 4.5.5, (TBT). By inserting the appropriate pole values in Eq. 4.5.24 we obtain the plots of Butterworth (B) and modified Bessel (T) system's step responses.

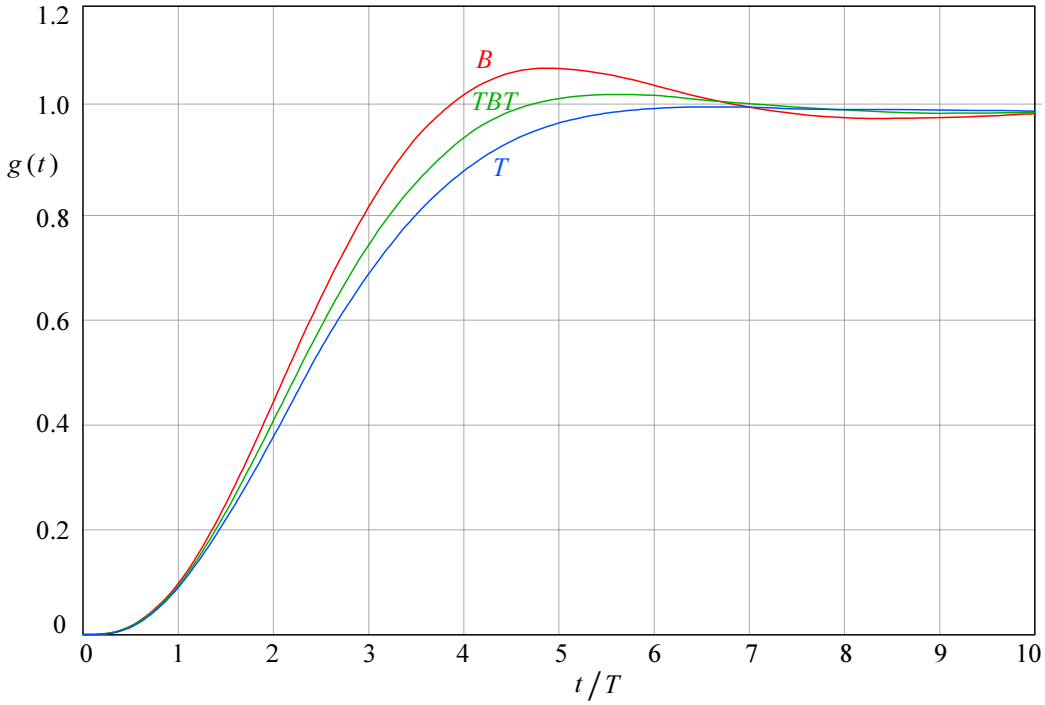


**Fig. 4.5.5**: The step response of the Transitional Bessel–Butterworth three-pole system (TBT), along with the Bessel (T) and Butterworth (B) responses.

## 4.6 Staggered vs. Repeated Bessel Pole Pairs

In order to compare the performance of an amplifier with staggered (index 's') vs. repeated Bessel pole pairs (index 'r') we need to compare the following two frequency response functions:

$$\left|F_{\mathrm{s}}(s)\right| = \left| \frac{s_1 s_2 \cdots s_n}{(s-s_1)(s-s_2)\cdots(s-s_n)} \right| \tag{4.6.1}$$

and:

$$\left|F_{\mathrm{r}}(s)\right| = \left| \frac{(s_1 s_2)^{n/2}}{(s-s_1)^{n/2}\,(s-s_2)^{n/2}} \right| \tag{4.6.2}$$

where $n$ is an even integer (2, 4, 6, ...). For a fair comparison we must use the poles from Table 4.4.4, the Bessel poles normalized to the same cutoff frequency.

The plots in Fig. 4.6.1 of these two functions were made by a computer, using the numerical methods described in Part 6. From this figure it is evident that an amplifier with staggered poles (as reported in the Table 4.4.4 for each $n$) preserves the intended bandwidth. On the other hand, the amplifier with the same total number of poles, but of second-order, repeated $(n/2)$-times, does not — its bandwidth shrinks with each additional second-order stage. Obviously, if $n = 2$ the systems are identical.

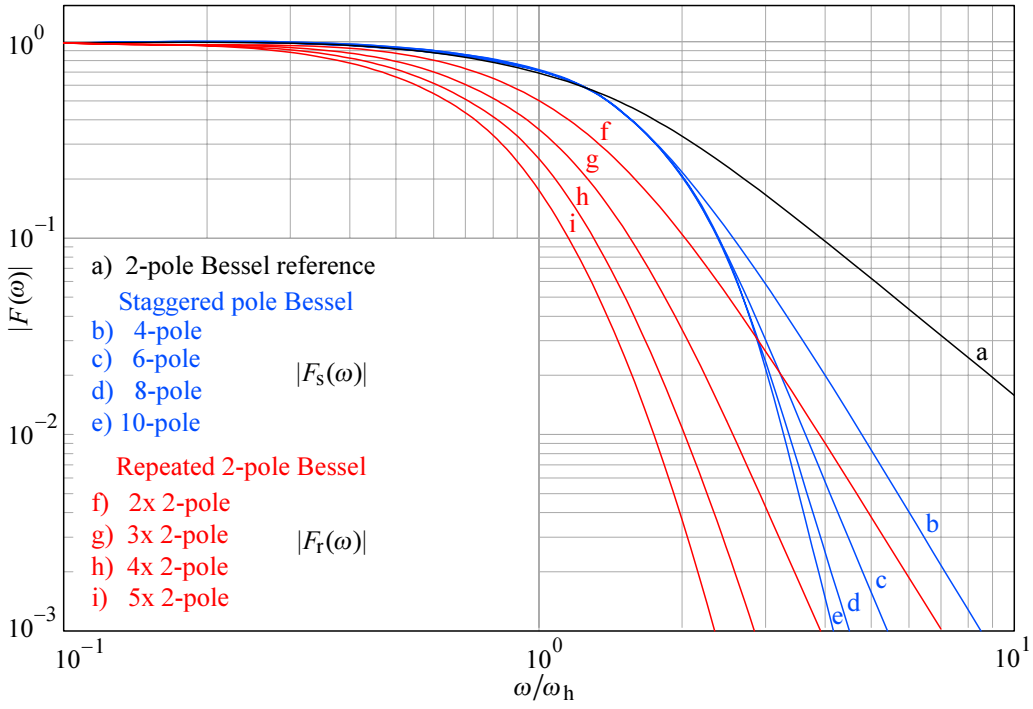


**Fig. 4.6.1**: Frequency response magnitude of systems with staggered poles, compared with systems with repeated second-order pole pairs. By using staggered poles the bandwidth is preserved, whilst for systems with repeated poles it decreases with each additional stage.

Even if the poles were of a different kind, e.g., Butterworth or Chebyshev poles, the staggered poles would also preserve the bandwidth, but the system with repeated second-order pole pairs will not. For the same total number of poles the curves tend to

the same cut off asymptote (from Fig. 4.6.1 this not evident, but it would have been clear if the graphs had been plotted with increased vertical scale, say, down to $10^{-6}$).

In the time domain the decrease of rise times is even more evident. To compare the step responses we take Eq. 4.6.1 and 4.6.2 (without the magnitude sign) and multiply them by the unit-step operator $1/s$, obtaining:

$$G_{\mathrm{s}}(s) = \frac{s_1 s_2 \cdots s_n}{s\,(s-s_1)(s-s_2)\cdots(s-s_n)} \tag{4.6.3}$$

and:

$$G_{\mathrm{r}}(s) = \frac{(s_1 s_2)^{n/2}}{s\,(s-s_1)^{n/2}\,(s-s_2)^{n/2}} \tag{4.6.4}$$

with $n$ being again an even integer.

By using the $\mathcal{L}^{-1}$ transform, we obtain the step responses in the time domain:

$$g_{\mathrm{s}}(t) = \mathcal{L}^{-1}\{G_{\mathrm{s}}(s)\} = \sum \mathrm{res}\, \frac{s_1 s_2 \cdots s_n\, \mathrm{e}^{st}}{s\,(s-s_1)(s-s_2)\cdots(s-s_n)} \tag{4.6.5}$$

and:

$$g_{\mathrm{r}}(t) = \mathcal{L}^{-1}\{G_{\mathrm{r}}(s)\} = \sum \mathrm{res}\, \frac{(s_1 s_2)^{n/2}\, \mathrm{e}^{st}}{s\,(s-s_1)^{n/2}\,(s-s_2)^{n/2}} \tag{4.6.6}$$

The analytical calculation of these two equations, for $n$ equal to 2, 4, 6, 8 and 10, should be a pure routine by now (at least for readers who have followed the calculations in Part 2 and Appendix 2.3; for those who have skipped them, there will be a lot of opportunities to revisit them later, when the need will force them!). Anyway, this can be done more easily by using a computer, employing the numerical methods described in Part 6. The plots obtained are shown in Fig. 4.6.2. The figure is convincing enough and does not need any comment.

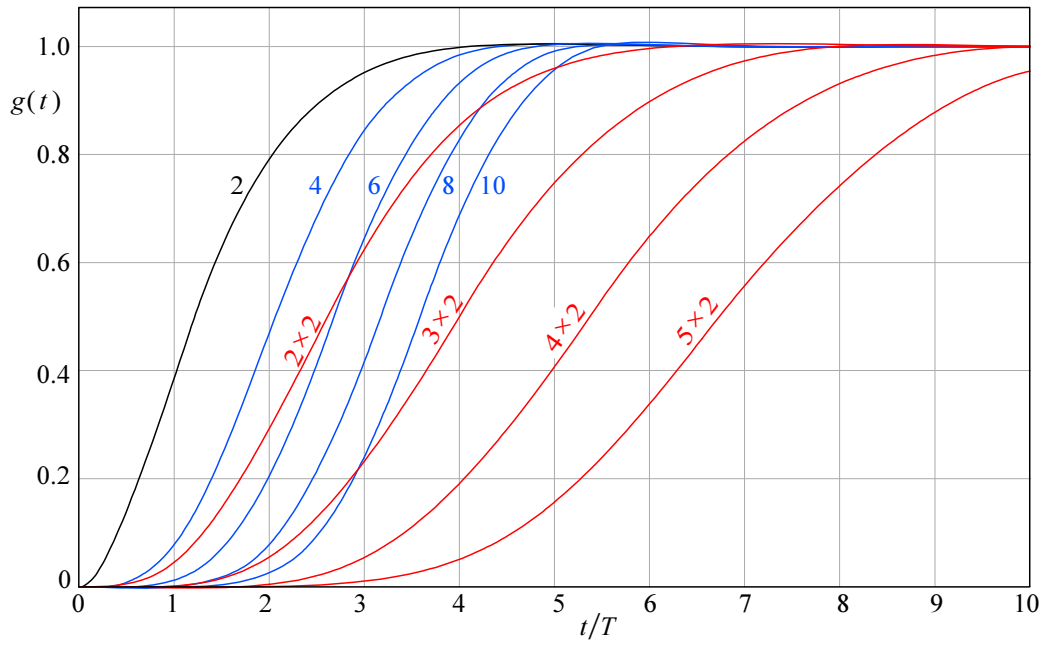


**Fig. 4.6.2**: Step response of systems with staggered poles, compared with systems with repeated second-order pole pairs. The rise times of systems with repeated poles increase with each additional stage, whilst for systems with staggered poles they even decrease slightly!

### 4.6.1 Assigning the Poles For Maximum Dynamic Range

Readers who usually pay attention to details may have noted that we have listed the poles in our tables (and also in figures) in a particular order. We have combined them in complex conjugate pairs and listed them by the increasing of their imaginary part. Yes, there is a reason for this, beyond pure aesthetics.

In general we can choose any number ($m$) of poles from the total number ($n$) of poles in the system, and assign them to any stage of the total number of stages ($k$). Sometimes, a particular choice would be limited by reasons other than gain and bandwidth, e.g., in oscilloscopes, the first stage is a JFET source follower, which provides the high input impedance required and it is usually difficult to design an effective peaking around a unity gain stage, so almost universally this stage has only a single real pole. In most other cases the choice is governed mainly by the gain $\times$ bandwidth product available for a given number of stages.

However, the main reason which dictates the particular pole ordering is the dynamic range. Remember that in wideband amplifiers we are, more often than not, at the limits of a system's realizability. If we want to extract the maximum performance from a system we should limit any overshoot at each stage to a minimum.

If we consider a rather extreme example, by putting the pole pair with the highest imaginary part in the first amplifier stage, the step response of this stage would exhibit a high overshoot. Consequently, the maximum amplitude which the system could handle linearly would be reduced by the amount of that overshoot.

In order to make the argument more clear, let us take a 3-stage 5-pole system with Bessel poles (Table 4.4.3, $n = 5$) and analyze the step response of each stage separately for two different assignments. In the first case we shall use a reversed pole assignment: the pair $s_{4,5}$ will be assigned to the first stage, the pair $s_{2,3}$ to the second stage and the real pole $s_1$ to the last stage. In the second case we shall assign the poles in the preferred order, the real pole first and the pair with the largest imaginary part last.

Our poles have the following numerical values:

$$\begin{aligned} s_1 &= -3.6467 \\ s_{2,3} &= -3.3520 \pm j\,1.7427 \\ s_{4,5} &= -2.3247 \pm j\,3.7510 \end{aligned}$$

We can model the actual amplifier by three voltage driven current generators loaded by appropriate $CR$ or $CLR$ networks. Since the passive components are isolated by the generators, each stage response can be calculated separately. We have thus one first-order function and two second-order functions:

$$g_1(t) = \sum \text{res}\, \frac{s_1\, \mathrm{e}^{st}}{s\,(s - s_1)} = 1 + \frac{1}{s_1}\, \mathrm{e}^{s_1 t}$$

$$g_2(t) = \sum \text{res}\, \frac{s_2 s_3\, \mathrm{e}^{st}}{s\,(s - s_2)(s - s_3)} = 1 + \frac{1}{|\sin\theta_2|}\, \mathrm{e}^{\sigma_2 t} \sin(\omega_2 t + \theta_2)$$

$$g_3(t) = \sum \text{res}\, \frac{s_4 s_5\, \mathrm{e}^{st}}{s\,(s - s_4)(s - s_5)} = 1 + \frac{1}{|\sin\theta_4|}\, \mathrm{e}^{\sigma_4 t} \sin(\omega_4 t + \theta_4)$$

In the reverse pole order case the first stage, with the pole pair $s_{4,5}$, is excited by the unit step input signal. We know that the second-order system from Table 4.4.3 has an optimal step response; since the imaginary to real part ratio of $s_{4,5}$ is larger (greater $\tan\theta_4$) than it is with the poles of the optimal case, we thus expect that the stage with $s_{4,5}$ would exhibit a pronounced overshoot.

In Fig. 4.6.3 we have drawn the response of each stage when it is driven individually by the unit step input signal (the responses are gain-normalized to allow comparison). It is evident that the stage with poles $s_{4,5}$ has a 13% overshoot.

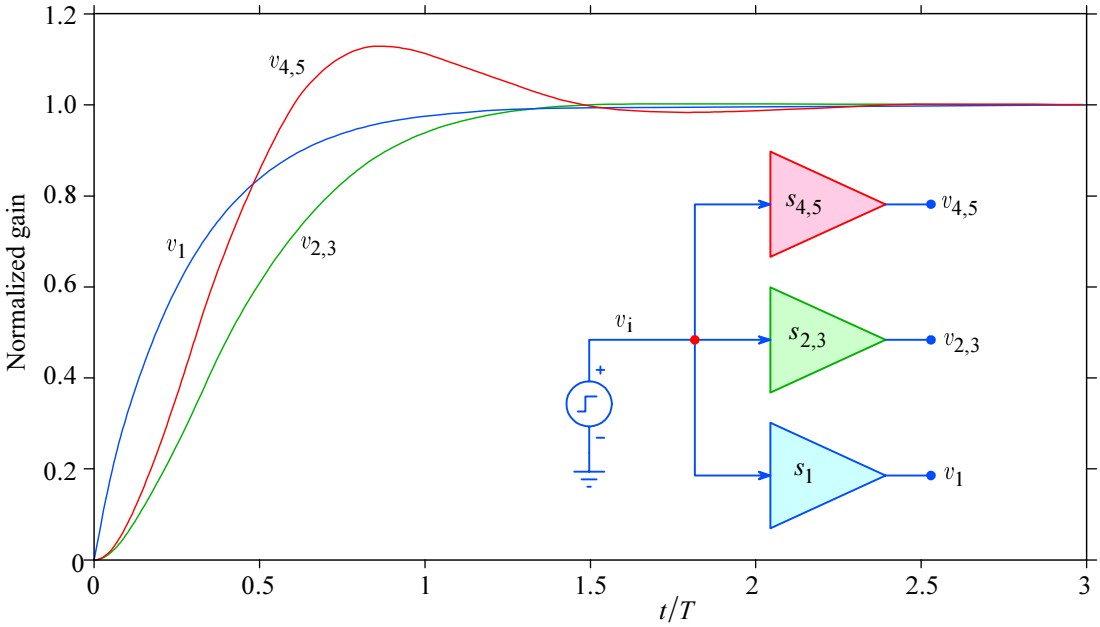


**Fig. 4.6.3**: Step response of each of the three stages taken individually.

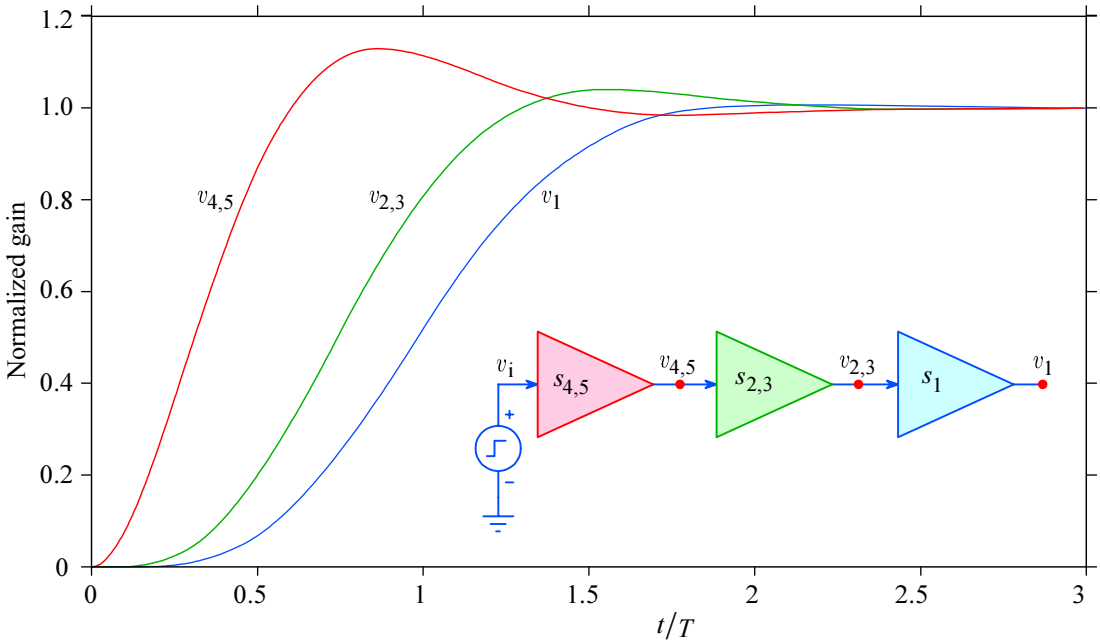


**Fig. 4.6.4**: Step response of the complete amplifier with reverse pole order at each stage. Although the second stage had no overshoot of its own, it overshoots by nearly 5% when processing the $v_{4,5}$ output.

In Fig. 4.6.4 the step response of the complete amplifier is drawn, showing the signal after each stage. Note that although the second stage exhibits no overshoot when driven by the unit step (Fig. 4.6.3), it will overshoot by nearly 5% when driven by the output of the first stage, $v_{4,5}$. And the overshoot would be even higher if the pole $s_1$ had been assigned to the middle stage.

The dynamic range of the input stage will therefore have to be larger by 13% and that of the second stage by 5% in order to handle the signal linearly. Fortunately the maximal input signal is equal to the maximal output, divided by the total gain. If we have followed the rule given by Eq. 4.1.33 and Fig. 4.1.9 the input stage will have only $1/3$ of the total system gain, so its output amplitude will be only a fraction of the supply voltage. On the other hand, the optimal stage gain is rather low, as given by Eq. 4.1.38, so the dynamic range may become a matter of concern after all.

The circuit configuration which is most critical in this respect is the cascode amplifier, since there are two transistors effectively in series with the power supply, so the biasing must be carefully chosen. In traditional discrete circuits, with relatively high supply voltages, the dynamic range was rarely a problem; the major concern was about poor linearity for large signals, since no feedback was used. In modern ICs, with lots of feedback and a supply of only 5V or just 3V, the usable dynamic range can be critical.

We can easily prevent this limitation if we use the correct pole ordering, so that the first stage has the real pole $s_1$ and the last stage the pole pair $s_{4,5}$. As we can see in Fig. 4.6.5, the situation improves considerably, since in this case the two front stages exhibit no overshoot, while the output overshoot is 0.4% only. Note that the final response in all cases is the same, though.

In a real amplifier, the pole assignment chosen can be affected by other factors, e.g., the stage with the largest capacitance will require the poles with the lowest imaginary part; alternatively a lower loading resistor and thus lower gain can be chosen for that stage.

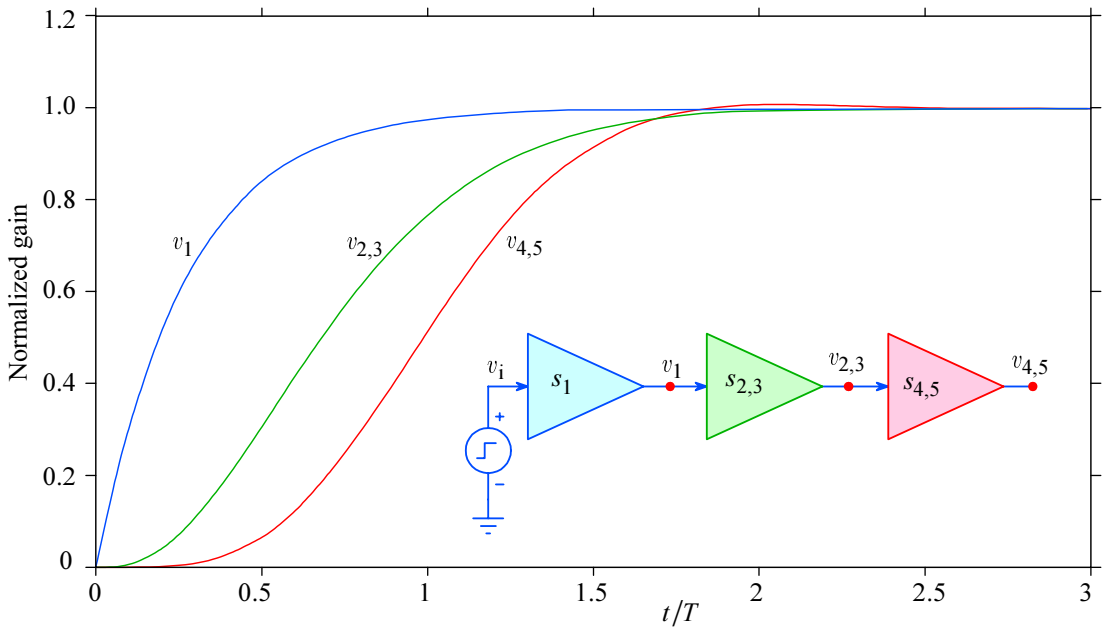


**Fig. 4.6.5**: Step response of the complete amplifier, but with the correct pole assignment.

(blank page)

## Résumé of Part 4

The study of this part should have given the reader enough knowledge to acquire an idea of how multi-stage amplifiers could be optimized by applying inductive peaking circuits, discussed in Part 2, at each stage.

Also, the merit of using DC over AC coupled multi-stage amplifiers should be clearly understood.

A proper pole pattern selection is of fundamental importance for the amplifier's performance. In particular, for a smooth, low overshoot transient response the envelope delay extended flatness offered by the Bessel poles provides a nearly ideal solution, approaching the ideal Gaussian response very quickly: with only 5 poles, the system's frequency and step response conform exceptionally well to the ideal, with a difference of less than 1% throughout most of the transient.

Finally, the advantage of staggered vs. repeated pole pairs should be strictly considered in the design of multi-stage amplifiers when gain × bandwidth efficiency is the primary design goal. We hope that the reader has gained awareness of how the bandwidth, which has been achieved by hard work following the optimizations of each basic amplifying stage given in Part 3, can be easily lost by a large factor if the stages are not coupled correctly.

A few examples of how these principles are used in practice are given in Part 5.

(blank page)

**References:**


[4.1] *P.M. Chirlian*, Electronic Principles and Design,
McGraw-Hill, New York, 1971.

[4.2] *G.E. Valley & H. Wallman*, Vacuum Tube Amplifiers,
MIT Radiation Laboratory Series Vol.18, McGraw-Hill, New York, 1948.

[4.3] *J. Bednařík & J. Daněk*, Obrazové zesilovače pro televisi a měřicí techniku,
Statní nakladatelství technické literatury, Prague, 1957.

[4.4] *L.T. Bruton*, *RC*–Active Circuits, Theory and Design,
Prentice-Hall, 1980.

[4.5] *J.M. Pettit and M. McWhorter*, Electronic Amplifier Circuits,
McGraw-Hill, New York, 1961.

[4.6] *S. Butterworth*, On the Theory of Filter Amplifiers,
Experimental Wireless & Wireless Engineer, Vol.7, 1930, pp. 536–541.

[4.7] *W. Gellert, H. Küstner, M. Hellwich, H. Kästner*, The VNR Concise Encyclopedia of
Mathematics, second edition, Van Nostrand Reinhold Company, New York, 1992.

[4.8] *L. Storch*, Synthesis of Constant Time-Delay Ladder Networks Using Bessel Polynomials,
Proceedings of I.R.E., Vol. 7, 1954, pp. 536–541.

[4.9] *W.E. Thomson*, Networks with Maximally Flat Delay,
Wireless Engineer, Vol. 29, 1952, pp. 253–263.

[4.10] *M.E. Van Valkenburg*, Introduction to Modern Network Synthesis,
John Wiley, New York, 1960.

[4.11] *M. Abramowitz & I.A. Stegun*, Handbook of Mathematical Functions,
Dover Publication, New York, 1970.

[4.12] *J.N. Little & C.B. Moller*, *MATLAB* User's Guide,
The MathWorks, Inc., South Natick, USA, 1990.

[4.13] *P. Starič*, Interpolation Between Butterworth and Thomson Poles (in Slovenian),
Elektrotehniški vestnik, 1987, pp. 133–139.

[4.14] *Y. Peless & T. Murakami*, Analysis and Synthesis of Transitional Butterworth-Thomson Filters
and Bandpass Amplifiers, RCA Review, Vol.18, March, 1957, pp. 60–94.

[4.15] *D.L. Feucht*, Handbook of Analog Circuit Design,
Academic Press, Inc., San Diego, 1990.

[4.16] *A.B. Williams and F.J. Taylor*, Electronic Filter Design Handbook
(LC, Active and Digital Filters), Second Edition, McGraw-Hill, New York, 1988.

[4.17] *A.I. Zverev*, Handbook of Filter Synthesis,
John Wiley and Sons, New York, 1967.